TECHNISCHE UNIVERSITÄT WIEN

institute of telecommunications

DISSERTATION

Operational Mobile Service Quality in Trains and Road Vehicles

ausgeführt zum Zwecke der Erlangung des akademischen Grades eines Doktors der technischen Wissenschaften

Dipl.-Ing. Taulant Berisha

geboren am 21. Dezember 1989

Matrikelnummer: 1528322

Döblinger Hauptstrasse 50/14, 1190 Wien

April 2019

eingereicht an der Technischen Universität Wien
Fakultät für Elektrotechnik und Informationstechnik

Betreuer:

Univ. Prof. Dr.-Ing. Christoph F. Mecklenbräuker

Institute of Telecommunications
Technische Universität Wien
Österreich

Begutachter:

Univ. Prof. Dr.-Ing. Luis Castedo Ribas

Department of Computer Engineering
University of A Coruña
Spain

Univ. Prof. Dipl.-Ing. Dr. Andreas Springer

Institute of Communications Engineering and RF-Systems
Johannes Kepler Universität Linz
Österreich

Abstract

In the past, railway vehicles have been exclusively designed as a land transportation system to serve the society in motion. Later, new generation of low-emissivity windows became integral part of vehicle windows with purpose to ensure comfort and enhance safety of passengers on-board. Nowadays, trains are pivotal elements in railway environments used for commuting people as well as in freight transport. However, low-emissivity coating, multiple window panes, isolating materials deposited between panes as well as metallic materials used to construct the vehicle body itself pose a big impediment to wireless communications. Yet, the problem remains for railway environments, while growing demands for seamless connectivity are not being satisfied from existing solutions owing to high values of Vehicle Penetration Loss and sparse infrastructure deployments. On the other hand, even though dedicated (trackside) cellular networks potentially address the problem of high Vehicle Penetration Loss, poor coverage areas, abrupt changes in signal strengths, high number of handovers, unstable data rates, or high number of retransmissions, yet, they are considered very costly from cellular operators.

While mobile users are on move, they frequently interact to their communication devices, such as smartphones or laptops. Therefore, this dissertation motivates real-world smartphone-based measurement campaigns carried out along large-scale railway tracks with purpose to mimic the quasi-real usage of end-users. Particularly, it investigates RF behaviors of both active and passive architectures that improve the performance of mobile users on-board railway vehicles. However, precise benefits of commercially available solutions on smartphones are unknown in literature. On one hand, key performance indicators are employed to analyze the performance of Universal Mobile Telecommunications System (UMTS)/Long Term Evolution (LTE) mobile users operating at wireless frequencies $800-2600$ MHz, while on the other hand, operational network and measurement limitations challenge the statistical evaluation and as such they require robust statistical approaches.

In general, nonparametric statistical inference and descriptive statistics are applied to make predictions on improvements or impairments for various vehicular use cases. In particular, multiple hypothesis testing is constructed upon rank-based methods which apply to the two-sample problem to infer changes about central tendency. The scope of this dissertation includes the use cases of mobile users on-board inter-city and regional trains equipped with wideband Amplify-and-Forward Repeaters and Frequency Selective Surfaces as well as mobile users on-board road vehicles investigated from the perspective of infotainment applications, voice calls and packet data transfers.

Acknowledgment

This work was carried out at the Institute of Telecommunications at the TU Wien during the years $2016 - 2019$.

First and foremost I want to express my deep gratitude to my advisor Prof. Christoph Mecklenbräuker for motivating my research, sharing his profound scientific and technical knowledge, as well as providing me freedom to pursue topics of interest throughout my doctoral studies. His extensive experience, priceless foresight, and creative ideas provided an indispensable guideline for my dissertation.

I had the opportunity and pleasure to work with a great team of students and researchers at TU Wien. I want to thank my colleagues Gerald Artner, Thomas Blazek and Orlando Trindade, partly involved in my work, for the fruitful discussions as well as their invaluable contributions in publications. Particular thanks go to my colleague Philipp Svoboda whose feedback and constructive criticism enhanced the quality of this work.

Special thanks go to Austrian railway operator, ÖBB Technische Services GmbH, in particular Stephan Ojak and Josef Resch for the excellent cooperation, financial support as well as fruitful support provided before, during, and after the measurement campaigns conducted on-board railway vehicles.

I would like to thank my parents Reshat and Selvije, my sisters Rezarta and Donjeta as well as my brother Leart for their support and love. Finally, I want to thank my love, Fjolla Ademaj, for all the joy she brought to my life.

Contents

1. Introduction **1**

1.1. Motivation and Scope of this Thesis 1
1.2. Outline and Contributions 5
1.3. Notation 6

2. Statistical Methodology **9**

2.1. Hypothesis Testing Approach 9
2.1.1. Fundamental Concepts 10
2.1.2. General Approach 11
2.1.3. Performance Metrics 11
2.2. Parametric Testing 13
2.3. Nonparametric Testing 14
2.3.1. Measurement Scale and Types of Data 15
2.3.2. Rank-based Tests 15
2.3.3. Wilcoxon-Mann-Whitney Test 16
2.3.4. Sign Test 19
2.4. Multiple Comparisons 21
2.4.1. False Discovery Rate 21
2.4.2. Benjamini-Hochberg Procedure 22
2.5. Distributional Clustering 23
2.5.1. Agglomerative Information Bottleneck 23
2.6. Logistic Models 24

3. Mobile Service Quality in Amplify-and-Forward Repeater-aided Railway Vehicles **27**

3.1. System Model 30
3.1.1. Data Outage 30
3.1.2. Service Quality Analysis 31
3.1.3. Spatially-based Analysis 33
3.1.4. Temporally-based Analysis 34
3.1.5. Change Detection 35
3.1.6. Vehicle Penetration Loss 37
3.2. Smartphone-based Measurement Setup 39
3.2.1. Amplify-and-Forward Repeaters 39
3.2.2. Measurement Track 40
3.2.3. Smartphone Placements 41
3.2.4. Smartphone Orientations and Relevant Entities 44
3.2.5. Measurement Configuration 44

3.3. Service Quality Improvements for Train Passengers . . . 45
3.3.1. Coverage Analysis . . . 45
3.3.2. Achievable Throughput . . . 46
3.4. Service Quality Assessment . . . 49
3.4.1. Trip-based Analysis . . . 49
3.4.2. Outage-based Analysis . . . 50
3.4.3. Temporally-based Analysis . . . 53
3.4.4. Change Detection . . . 54
3.4.5. Channel Quality Analysis . . . 54
3.4.6. Vehicle Penetration Loss . . . 56
3.5. Summary . . . 58

4. Mobile Service Quality in Frequency Selective Surface-aided Railway Vehicles 61
4.1. System Model . . . 63
4.1.1. Data Outage . . . 63
4.1.2. Service Quality Analysis . . . 63
4.1.3. Spatially-based Analysis . . . 64
4.2. Smartphone-based Measurement Setup . . . 65
4.2.1. Window Panes with Frequency Selective Properties . . . 65
4.2.2. Measurement Track . . . 66
4.2.3. Smartphone Placements . . . 68
4.2.4. Smartphone Orientations and Relevant Entities . . . 68
4.2.5. Measurement Configuration . . . 68
4.3. Service Quality Improvements for Inter-city Train Passengers . . . 70
4.3.1. Coverage Analysis . . . 70
4.3.2. User Equipment Placement Analysis . . . 70
4.4. Service Quality Assessment . . . 72
4.4.1. Trip-based Analysis . . . 73
4.4.2. Outage-based Analysis . . . 73
4.4.3. Channel Quality Analysis . . . 74
4.5. Summary . . . 75

5. Mobile Service Quality in Road Vehicles 77
5.1. System Model . . . 79
5.1.1. Nominal Environments . . . 79
5.1.2. Service Quality Assessment . . . 80
5.1.3. Small-scale Nominal Environment Measurements . . . 81
5.2. Smartphone-based Measurement Setup . . . 83
5.2.1. Measurement Track . . . 83
5.2.2. Smartphone Placements . . . 84

5.2.3. Smartphone Orientations and Relevant Entities 86
5.2.4. Measurement Configuration 86
5.3. Power Difference Model 87
5.4. Service Quality Impairments for Pickup Truck Passengers 89
5.4.1. Trip-based Analysis 89
5.4.2. Map-based Analysis 91
5.4.3. Environment-based Analysis 94
5.5. Summary 97

6. Conclusions **99**

A. List of Abbreviations **101**

Bibliography **103**

1

Introduction

1.1. Motivation and Scope of this Thesis

Today, whether travelers decide to travel by plane or train does not largely influence their choices when traveling short-haul distances. While on one hand airlines challenge train companies by offering low cost tickets, on the other hand the increase speed and environmental-friendliness of trains promotes companies to challenge airlines with comparable total trip time and even being less polluting. Nowadays, while passengers commute between cities, they acquire access on social media, initiate file transferring, perform video-streaming, and play online games. On business or pleasure, the selection of transportation system from passengers is largely influenced how they can enjoyably use the time before reaching the destination. Yet, there is a big gap between airline and train companies. As of 2019, this fact becomes trains a competitive system not only with the aviation industry but with all other forms of transportation. International Transport Forum of the Organisation for Economic Cooperation and Development (OECD) forecasts $200 - 300\,\%$ increase in passenger mobility and $150 - 250\,\%$ increase in freight activity by 2050 compared to 2010 [1]. Therefore, it is obvious that nowadays railway environments are a pivotal factor of Intelligent Transportation Systems (ITSs) and will continue to be crucial for the future.

Nonetheless, there is significant evidence so far of a few proposed architectures to make Internet access available on trains. Some technologies for access network have been already proposed to provide broadband Internet access to high-speed mobile users. Fig. 1.1 refers to core idea. The first to mention is IEEE 802.11 [2], already a widely used solution on-board the train. IEEE 802.11-based architecture can apply to link a railway vehicle into a computer network and provide Internet access to passengers [3]. For instance, an approach suggests to use a central train server to connect the IEEE 802.11 access points distributed on each carriage. The central train server connects into a cellular-based infrastructure, satellite, radio-over-fiber, or any other technology for access connectivity. As illustrated in [4], T-Mobile in Germany brought Internet access to Intercity Express trains with Wireless Local Area Network (WLAN) and by early 2019 the connection was established on several routes. Few years ago, the railway operator ÖBB [5] in Austria in cooperation with telecommunication providers T-Mobile, A1 Telekom Austria, and Three, introduced Internet on-

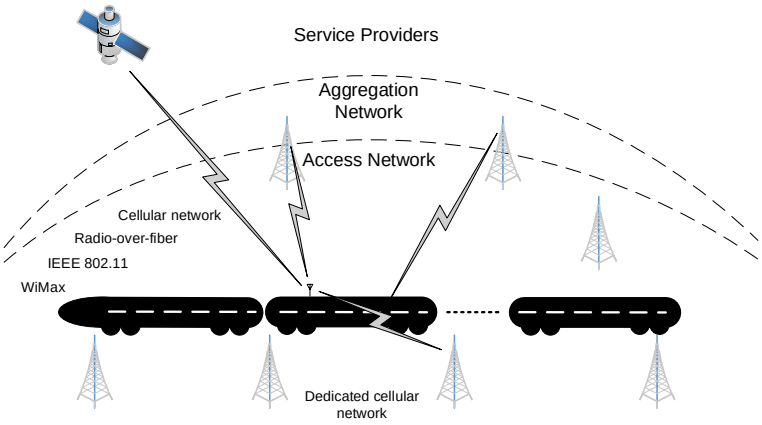

Figure 1.1.: Internet access on trains.

board Railjet trains. Recently, as of 2018, Nomad Digital [6] has announced that Scottish High-Speed and Voyager trains will be equipped with WLAN as well.

On the other hand, railway vehicles can be connected via satellite as well. Satellite-based architecures have been proposed by ACCORDE [7] with a system consisting of communication, distribution and pointing elements. A modem (similar to central train server for WLAN) is the core communication element along with an antenna and a satellite transmitter. Combined with WLAN this approach uses optical fiber links to distribute the signal to IEEE 802.11 access points inside the train. However, satellite has limitations such as a considerable inherent delay (500 to 600 ms) as well as limited bandwidth. On one hand, the delay makes this application less suitable for real time applications, while on the other hand the bandwidth poses a big impediment when a large number of train passengers demand Internet services. Radio-over-fiber is another solution for Internet access to train passengers. This is a dedicated fiber-fed distributed antenna network located along the rail tracks, also called Remote Antenna Units (RAUs). The communication between access network and railway vehicle is established via RAU which converts the optical signals to radio waves. To reduce handoff times for train access terminals, [8] proposed the moving cell concept, i.e., a cell pattern that moves together with the vehicle. Similar dedicated architectures introduce the solution composed of RAUs [9, 10], which still require optimal number of units to achieve performance improvements along track. WiMax is found to operate efficiently in railway environments as well. An architecture of broadband wireless communications in railway environments is presented in [11]. Even though it is observed that the architecture satisfies the requirements for reliable applications, yet, dedicated WiMax nodes need to be deployed along the track to provide connectivity. A study reported that despite this WiMax was being used in the United Kingdom [12]. Furthermore, additional approaches for Internet access exist such as high-altitude platforms [13] as well as internet access through direct connectivity to customer terminals.

Railways, tunnels, subways, mines, and underground represent areas where radio propagation is impossible. To cope with this problem Radiating Cables (RCs) have been widely used to provide coverage along confined areas as well as steady tracks. Practical performance of RC dates back in 1975 [14] while their application in trains was studied in [15]. An RC is used as antenna which is suitable for deployment in areas where radio access is restricted and consequently radio communication is impossible. In the past and still nowadays they are being laid along such environments.

However, each of the proposed methods either fails to satisfy low cost requirements (e.g., dedicated trackside infrastructure); faces installation difficulties (e.g., wiring along train wagons for IEEE 802.11); suffers from weather conditions (e.g., RCs laid along tracks in outdoor environment); or it is limited in capacity as an important demerit when it comes to serve a large number of train passengers. A direct link is very liable to high values of Vehicle Penetration Loss (VPL) due to Faraday cage characteristics of a train wagon. Commercially, available service quality improvements on-board the trains largely vary in achievable gains, complexity, and applicability. Two approaches are viable to provide high quality services to fast moving users. First, *active* improvement-based approach consists of a separate link between the infrastructure and the railway vehicle on the one hand and between the railway vehicle and the users on the other hand. In contrast with existing solutions, this thesis rather investigates a set up where the connection between each train passenger and a base station is instead established via a repeater, termed as *repeater-aided* during the thesis. For evaluation of mobile service improvements, Austrian railway operator ÖBB mounted Amplify-and-Forward Repeaters (AFRs) and laid a couple of RCs on a single side of luggage racks along the entire or partial train length. Second, the bottleneck in direct link caused by VPL can be nearly minimized if the Faraday cage effect is mitigated when the railway vehicle is slightly modified. Additional to the first approach, this thesis investigates a set up with Frequency Selective Surface (FSS) on-board the train, termed as *FSS-aided* during this thesis, which defines a *passive* improvement-based approach. Likewise, ÖBB partially upgraded a single wagon of train with FSSs.

For mobile service providers, monitoring their mobile network is vital to guarantee a dependable and secure network with well-defined Quality of Service (QoS) [16]. It allows the estimation and improvement of service quality which at the end determines the Quality of Experience (QoE) [17]. The Key Performance Indicators (KPIs) are metrics estimated by the network infrastructure and the Mobile Station (MS) based on measurements in physical and logical channels of the mobile communication protocol stack. Advanced statistical analyses and large-scale measurements of KPIs are necessary to deploy, operate and improve mobile cellular networks efficiently. However, KPIs are non-stationary in behavior. On one hand, their statistics of a mobile cellular network vary over space and time, on the other hand they also change as result of improvements, varying loads, and disruptions in mobile networks. To put it another way, it remains a big challenge for analysis when carried out in *operational* networks. Detecting even weak changes in statistical properties of a particular KPI and perceiving such changes by mobile users are two crucial elements. Service quality assessment of mobile users on-board the trains is a good example and, yet, in High Speed Train (HST)

a statistically sufficient characterization of channels is not found [18]. HSTs pose three challenges: (i) they are characterized with high velocity above 250 km/h, (ii) their double-deck structure allows them to accommodate large number of mobile users, (iii) frequency bands in a cellular communication system varies. In order to meet these challenges both network improvements and transceiver design improvements are required. While on one hand, small- and large-scale fading along with frequency- and time-selectivity define the challenges in physical layer [19–21], on the other hand, the large number of mobile users cause the "signaling storm" which overloads the signaling resources [20] in upper layers. The diverse nature of all these challenges motivates measurement campaigns.

Compared to road vehicles, railway vehicles are fundamentally different. First, trains are characterized with substantially higher VPL and frequency of handoffs in cellular networks than cars. Second, railway companies constantly add or remove wagons which imposes the necessity of a network to automatically detect such changes [22]. Third, railway vehicles represent a high vibration environment which requires mechanical isolation of communication devices [23]. Furthermore, they require equipment with minimal maintenance schedules. Yet, both modern railways and highways are constructed along gentle-curved tracks. In context of coverage, mobile network is vastly similar which leads to comparable propagation conditions for mobile users on-board railway and road vehicles. This thesis explicitly proposes and investigates a set up composed of smartphone devices on-board a pickup truck. Commonly, mobile operators are conservative in terms of providing key information such as mobile infrastructure location. This restriction imposes investigation to be carried out in a limited and a controlled environment. On the other hand, environmental details, such as position, shape, size, and density of buildings along with trajectory of roads largely influence the radio propagation. To meet this requirement, deterministic map data aim to simplify the assessment of improvements and impairments on both infrastructure and user side. Open-StreetMap (OSM) [24] represent a convenient source of deterministic map data including comprehensive environment details. When map data are combined with measurement campaigns they convert into a powerful tool for evaluating KPIs.

This thesis relies on real-world data collected in operational networks where no control over the following factors is ensured: (1) Several hundreds of kilometer tracks, varying train velocities, and limited granularity of equipment result in large variation of data sets. While some KPIs are represented with high sample sizes, some other KPIs are represented with small sample sizes which lead to challenges in statistical evaluation. (2) Changes in KPIs do not occur only due to a specific treatment, but they are also conditioned on space, time, propagation effects as well as traffic loads. For these reasons, potential improvements and impairments caused exclusively by a treatment cannot be perfectly isolated. (3) Underlying distributions, data types, and units of KPIs vary largely among each other as well as within a particular KPI. (4) Nature of cellular networks, such as Long Term Evolution (LTE), exhibit strong burstiness behavior along a trajectory, which adds further complexity to establish assessment of service quality. Provided the above challenges, the robustness of any advanced statistical inference is crucial. This motivates the usage of nonparametric methods to detect

changes in KPIs of cellular networks under operational constraints.

1.2. Outline and Contributions

This thesis is structured as follows: Chapter 2 provides the statistical methodology used in this thesis with particular focus on nonparametric inference. The second part of this thesis includes Chapter 3, Chapter 4, and Chapter 5 which represent and outline my contributions. Chapter 3 and Chapter 4 provide descriptive and inferential analysis in context of service quality improvements for mobile users on-board HST. Likewise, Chapter 5 focuses on mobile users on-board a pickup truck. The last three chapters specifically address the problem of assessing improvements and impairments in operational networks. The remainder of this section provides a short abstract for each chapter with focus on my contributions.

Chapter 2

This chapter provides advanced statistical methods employed during this thesis as well as demonstrates their usage with an interface between their application and faced problems. The main focus of the chapter is on using single and multiple binary nonparametric hypotheses motivated by unknown underlying distributions of KPIs. The remainder of this chapter outlines details of distributional clustering as well as logistic models.

Chapter 3

The unknown underlying distributions of KPIs disfavor the application of parametric hypothesis testing. This chapter demonstrates the developed techniques of assessing improvements of service quality for mobile users on-board when a HST or a regional train is equipped with AFRs and RCs. Based on my publications in [25–27], developed detection techniques are proposed, and rank-based methods are employed to exploit statistical properties for extracting improvements in coverage and signal quality.

Chapter 4

While in the past FSSs were classified for military use, nowadays they have found new applications such as railway environments. However, their benefits on smartphone-based mobile users on-board HSTs have been unknown in literature. Based on my publications in [27, 28], this chapter demonstrates a rank-based novel approach to infer improvements in a variety of KPIs and outlines the key findings when a HST is equipped with FSSs.

Chapter 5

Due to structural changes in vehicle body, road vehicles are characterized with much lower VPL than railway vehicles. Yet, both vehicles have many technical challenges in common. For instance,

their outdoor environment is prone to similar infrastructure deployments along both highways and railways. According to my publications in [29, 30], this chapter focuses on LTE investigation as well as characterization of nominal environments in a real-world network. To investigate the network performance, 2D LOS/NLOS maps were implemented and coupled with measurement observations aided by exact location of infrastructure deployments. This was demonstrated in my publication [31].

1.3. Notation

The following notation and commonly used parameters throughout this thesis are listed below.

Tab. 1.1.: Frequently used notations.

Symbol	Annotation
X	Continuous variable
$\dot{X}$	Discrete variable
$F_X(\cdot)$	Empirical cumulative distribution function of X
$p_X(\cdot)$	Probability density function of X
$p_{\dot{X}}(\cdot)$	Marginal probability mass function of $\dot{X}$
$p_{\dot{X}\|\dot{Y}}(\cdot\|\cdot)$	Conditional probability mass function of $\dot{X}$ given $\dot{Y}$
$f_{JS,\pi_2}(\cdot,\cdot)$	Jensen-Shannon divergence between two probability distributions π_2
$I(\cdot;\cdot)$	Mutual information
τ	Rejection ratio
$\mathcal{I}$	Hypothesis operator
$\ddot{\mathcal{I}}$	Multiple hypothesis operator
$\mathbb{E}(\cdot)$	Expectation operator
$\mathbb{V}(\cdot)$	Variance operator
$\mathbb{M}(\cdot)$	Median operator
$\mathbb{S}(\cdot)$	Skewness operator
$\mathbb{P}(\cdot)$	Probability operator
$\mathbb{R}(\cdot)$	Rank operator
λ	Wavelength in $[m]$
f	Frequency in $[Hz]$
f_s	Sampling frequency in $[Hz]$
B_w	Frequency band in $[MHz]$
ℓ_i	Degree of freedom for ith distribution
μ	Mean
σ	Standard deviation
$p_\imath$	Probability of success on an individual trial
$\Gamma(\cdot)$	Gamma function defined as $\Gamma(a) = \int_0^\infty x^{a-1}e^{-x}dx$
N	Number of resource blocks
N_0	White noise power spectral density in $[dBm]$
E_c	Energy per chip of the pilot channel in $[dBm]$
RSRP	Reference signal receive power in $[dBm]$
E-UTRA RSSI	E-UTRA received signal strength indicator in $[dBm]$
RSRQ	Reference signal receive quality in $[dB]$, RSRQ $=$ N $\times$ RSRP/E-UTRA RSSI
SINR	Signal to interference and noise ratio in $[dB]$
R	Physical throughput in $[bit/s]$
RSCP	Received signal code power in $[dBm]$
UTRA RSSI	UTRA received signal strength indicator in $[dBm]$
$\mathrm{E}_c/\mathrm{N}_0$	Signal quality in $[dB]$ defined as $\mathrm{E}_c/\mathrm{N}_0 =$ RSCP/UTRA RSSI
P_T	Transmit power in $[dBm]$
$\mathcal{N}(\mu,\sigma)$	Normal distribution with probability density function $p_X(x) = \frac{1}{\sqrt{2\pi\sigma^2}}e^{-\frac{(x-\mu)^2}{2\sigma^2}}$
$\mathcal{B}(\imath,p_\imath)$	Binomial distribution with probability mass function $p_{\dot{X}}(x) = \binom{\imath}{x}p_\imath^x(1-p_\imath)^{\imath-x}$
$\mathcal{F}(\ell_1,\ell_2)$	F-distribution with probability density function $p_X(x) = \frac{\Gamma(\frac{\ell_1+\ell_2}{2})(\frac{\ell_1}{\ell_2})^{\frac{\ell_1}{2}}x^{\frac{\ell_1}{2}-1}}{\Gamma(\frac{\ell_1}{2})\Gamma(\frac{\ell_2}{2})(1+\frac{\ell_1 x}{\ell_2})^{\frac{\ell_1+\ell_2}{2}}}$

2

Statistical Methodology

One of the purposes of applying inferential statistics in practical problems is to be able to draw inferences (conclusions) based on the usage of collected data. In this regard, hypothesis testing represents a procedure to evaluate a particular statement. While two different approaches are available such as parametric- [32–34] and nonparametric testing [32, 34–37], still a commonly employed approach is to apply the former approach. Yet, the focus of this thesis is on nonparametric hypothesis testing.

In the last decades, descriptive statistics are employed as an important tool in statistics that have gained attention in practical problems, including wireless communication applications. In opposite to hypothesis testing, here however, the data are not employed to make predictions, but are only used for descriptive purposes.

Both statistical approaches, descriptive statistics and hypothesis testing, are applied in this thesis. Furthermore, distributional clustering as well as logistic models are employed as well. Their main application is driven from the aim to classify nominal environments as well as data outage scenarios for currently operating mobile networks defined in 3rd Generation Partnership Project (3GPP) Global System for Mobile Communications (GSM)/Universal Mobile Telecommunications System (UMTS)/Long Term Evolution (LTE) [38–40]. Specifically, they are applied on real-world problems with mobile users consistently moving along trajectories such as highways and railways.

Therefore, this chapter aims to provide an overview of statistical approaches that are applied to solve particular problems, specifically assessment of service quality and mobility-related issues. Moreover, it also provides explanations in context of applications, in order to bridge the gap between theory and practical problems.

2.1. Hypothesis Testing Approach

In statistics, inferential statistics are used for the purpose of drawing inferences about a population distribution. To accomplish this task, it is possible to apply two methods: hypothesis testing and estimation of population parameters. A hypothesis test is a statistical method that uses sample data

to evaluate a hypothesis about a population. Throughout this thesis it is employed the statistical hypothesis. Herein, two statistical hypotheses are termed as: *null*- and the *alternative* hypothesis. On one hand, the null hypothesis is denoted with $\mathcal{I}_0$ and is defined as a statement that there exists no effect (difference) by means of statistics. On the other hand, the alternative hypothesis is denoted with $\mathcal{I}_1$ and is defined as a statement that indicates a presence of an effect. In other words, the null hypothesis acts as baseline from which the alternative hypothesis deviates to greater or less degrees.

2.1.1. Fundamental Concepts

In this section are discussed fundamental statistical concepts that are related to hypothesis testing: null hypothesis, (non)directional alternative hypothesis, significance level, and critical region. To start with, two basic concepts are termed as: *treatment-free* and *treatment-aided*. The treatment-free term is defined to represent the distribution drawn for the null hypothesis, while the treatment-aided term is defined to represent the distribution drawn for the alternative hypothesis. For now, let us assume the problem of central tendency.

Null hypothesis: This kind of hypothesis does make a prediction about central tendency that the means of two distributions statistically do not change. Therefore, let us consider an example for the sake of simplicity. Let us assume that the statistical mean is relevant and denote with $\mu_{\mathcal{I}_0}$ and $\mu_{\mathcal{I}_1}$ statistical means of respective distributions. This statistical location problem is commonly formulated as

$$\mathcal{I}_0 : \ \mu_{\mathcal{I}_1} = \mu_{\mathcal{I}_0} \tag{2.1}$$

which represents no presence of treatment effect.

Nondirectional alternative: This kind of alternative hypothesis does not make any prediction in a particular direction. The nondirectional alternative represents a presence of the treatment effect, e.g., the treatment-aided is either better or worse, this is unknown from the test. This statistical location problem is commonly formulated as

$$\mathcal{I}_1 : \ \mu_{\mathcal{I}_1} \neq \mu_{\mathcal{I}_0} \tag{2.2}$$

which is sensitive only to a statistical change without knowing the direction.

Directional alternative: This kind of alternative hypothesis does make a prediction in a particular direction, e.g., the treatment-aided is better than the treatment-free

$$\mathcal{I}_1 : \ \mu_{\mathcal{I}_1} > \mu_{\mathcal{I}_0} \tag{2.3}$$

or the treatment-aided is worse than the treatment-free

$$\mathcal{I}_1 : \ \mu_{\mathcal{I}_1} < \mu_{\mathcal{I}_0}. \tag{2.4}$$

Significance level: It represents a risk of making an error of incorrectly deciding in favor of $\mathcal{I}_1$ even though the fact is that $\mathcal{I}_0$ is true. In fact, the significance level indicates our reluctance weather to reject or not a null hypothesis. This value is set in advance (even without seeing the observed data) which defines a boundary that separates the high-probability from low-probability samples.

Critical region: It is defined with boundaries specified from the significance level. This region contains extreme low-probability samples, which are very unlikely to occur in case of true null hypothesis.

2.1.2. General Approach

In general, parametric inferential tests are based on assumption that observed data are generated from any particular distribution which is characterized with a population parameter. However, the fundamental problem is that such techniques require stringent assumptions to be drawn, which in practical problems are often unknown. The unknown distributions potentially lead to violate the assumptions. For this reason, the usage of *rank-based* nonparametric inferential tests which ignore the true distribution of observed data is a strong alternative.

Application: In situations of constructing the assessment of service quality, the problem formulates as a binary hypothesis problem denoted with $\mathcal{I}_0$ and $\mathcal{I}_1$ under the assumption that both hypotheses are modeled with respective (un)known probability distributions

$$\mathcal{I}_0 \sim p(x|\mathcal{I}_0) \tag{2.5a}$$

$$\mathcal{I}_1 \sim p(x|\mathcal{I}_1) \tag{2.5b}$$

where x is the parameter. Conditional Probability Density Functions (pdfs) $p(x|\mathcal{I}_0)$ and $p(x|\mathcal{I}_1)$ are illustrated in Fig. 2.1. However, the observed data, e.g., received power, signal quality, or transmit power, potentially do not follow the well-known distributions.

2.1.3. Performance Metrics

In the following are discussed fundamental performance metrics that are crucial for construction of binary hypothesis testing, either single or multiple. The quantification of errors of mistakenly rejecting or failing to reject any hypothesis is established by using the following metrics.

Incorrect decision in favor of $\mathcal{I}_1$: It is the probability of occurrence of rejecting $\mathcal{I}_0$ in favor of $\mathcal{I}_1$ when in fact hypothesis $\mathcal{I}_0$ is in force. It is also called false positive, denoted with $F_{\mathcal{I}_1}$. Under assumption of continuous variable and conditional dependence of hypothesis on observations, it is defined as

$$F_{\mathcal{I}_1} = \mathbb{P}(\text{accept } \mathcal{I}_1|\mathcal{I}_0) = \int \mathbb{P}(\text{accept } \mathcal{I}_1|x, \mathcal{I}_0)p(x|\mathcal{I}_0)dx \tag{2.6}$$

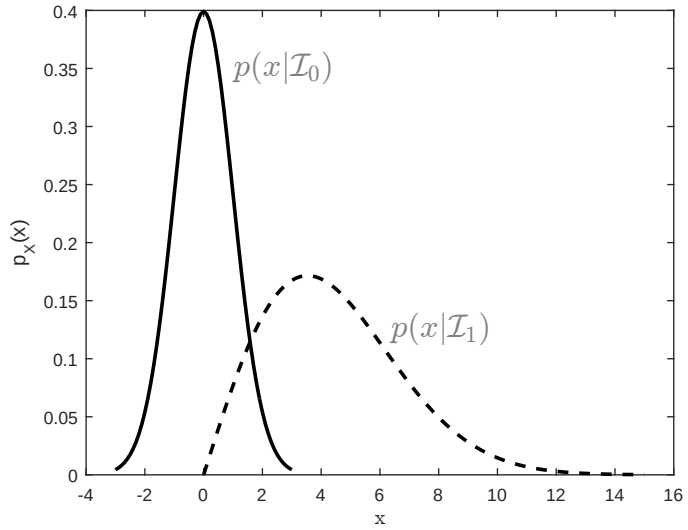

Figure 2.1.: Conditional distributions with sample means $\mu_{\mathcal{I}_0}$ and $\mu_{\mathcal{I}_1}$ for respective null- and alternative hypotheses.

The incorrect decision in favor of $\mathcal{I}_1$ is also known as a type I error and often denoted with α during this thesis.

Incorrect decision in favor of $\mathcal{I}_0$: It is the probability of occurrence of failure to reject $\mathcal{I}_0$ when in fact hypothesis $\mathcal{I}_1$ is in force. It is also called false negative, denoted with $F_{\mathcal{I}_0}$. Under identical conditions as for $F_{\mathcal{I}_1}$, it is defined as

$$F_{\mathcal{I}_0} = \mathbb{P}(\text{accept } \mathcal{I}_0|\mathcal{I}_1) = \int \mathbb{P}(\text{accept } \mathcal{I}_0|x, \mathcal{I}_1)p(x|\mathcal{I}_1)dx \tag{2.7}$$

The incorrect decision in favor of $\mathcal{I}_0$ is also known as a type II error.

Correct decision in favor of $\mathcal{I}_1$: It is the probability of correctly deciding for $\mathcal{I}_1$ as a result from the known fact that $\mathcal{I}_1$ is true. Under identical conditions as for $F_{\mathcal{I}_1}$, it is defined as

$$C_{\mathcal{I}_1} = \mathbb{P}(\text{accept } \mathcal{I}_1|\mathcal{I}_1) = 1 - \mathbb{P}(\text{accept } \mathcal{I}_0|\mathcal{I}_1) = 1 - \int \mathbb{P}(\text{accept } \mathcal{I}_0|x, \mathcal{I}_1)p(x|\mathcal{I}_1)dx \tag{2.8}$$

The correct decision in favor of $\mathcal{I}_1$ is also known as the power.

Correct decision in favor of $\mathcal{I}_0$: It is the probability of correctly deciding for $\mathcal{I}_0$ as a result from the known fact that $\mathcal{I}_0$ is true. Under identical conditions as for $F_{\mathcal{I}_1}$, it is defined as

$$C_{\mathcal{I}_0} = \mathbb{P}(\text{accept } \mathcal{I}_0|\mathcal{I}_0) = 1 - \mathbb{P}(\text{accept } \mathcal{I}_1|\mathcal{I}_0) = 1 - \int \mathbb{P}(\text{accept } \mathcal{I}_1|x, \mathcal{I}_0)p(x|\mathcal{I}_0)dx \tag{2.9}$$

2.2. Parametric Testing

In general, depending on the purpose there exist many tests, which are traditionally discussed in statistics as introductory principles. These kind of tests are based on samples in such a way that they follow a particular assumption. These assumptions are called *parameters*. In the following, are provided some common parametric assumptions: the sample resembles approximately a normal distribution, the sample is randomly drawn from a normal distribution; the sample is large; the sample observations are independent, the samples are drawn from populations of approximately equal variance, or the samples contain values of particular scale. All of them are widely known in literature as *parametric* tests.

Hypothesis testing is commonly constructed based on such tests that have to include a considerable number of assumptions. However, in practice this is not a trivial problem. In such situations, it happens that not all the assumptions hold. Consequently, these rules are broken from a sample distribution which leads to violate the assumptions. Some of the parametric tests are: t-test, z-scores, etc.

Let us assume we are given a two-sample problem to deal with central tendency. Further, let us write both samples from random variables as

$$X_1 = \{x_{11}, x_{12}, ..., x_{1n_1}\},\ \forall x_{1j} \in \mathbb{R} \tag{2.10a}$$

$$X_2 = \{x_{21}, x_{22}, ..., x_{2n_2}\},\ \forall x_{2j} \in \mathbb{R} \tag{2.10b}$$

where n_1 and n_2 are sample sizes of sample distribution X_1 and X_2, respectively. A two-sample t-test is designed to detect a shift in population mean

$$\Delta\mathcal{E}_{12} = \mathcal{E}(X_1) - \mathcal{E}(X_2) \tag{2.11}$$

for a given significance and degree of freedom $\ell = n_1 + n_2 - 2$. The goal of the t-test is to examine whether $\Delta\mathcal{E}_{12} = 0$ or not by calculating the well-known t-statistics denoted with t. The general form of the test statistics for two independent samples with equal or unequal sample sizes formulates as

$$t = \frac{\mathbb{E}(X_1) - \mathbb{E}(X_2)}{\sqrt{\frac{(n_1-1)\mathbb{V}(X_1)+(n_2-1)\mathbb{V}(X_2)}{n_1+n_2-2}}\sqrt{\frac{1}{n_1}+\frac{1}{n_2}}} \tag{2.12}$$

where

$$\mathbb{E}(X_1) = \sum_{a=1}^{n_1} x_{1a} \tag{2.13a}$$

$$\mathbb{E}(X_2) = \sum_{b=1}^{n_2} x_{2b} \tag{2.13b}$$

are the sample means, whereas

$$\mathbb{V}(X_1) = \frac{\sum_{a=1}^{n_1}(x_{1a} - \mathbb{E}(X_1))^2}{n_1 - 1} \tag{2.14a}$$

$$\mathbb{V}(X_2) = \frac{\sum_{b=1}^{n_2}(x_{2b} - \mathbb{E}(X_2))^2}{n_2 - 1} \tag{2.14b}$$

are the sample variances. This test works properly as long as normal distribution is assumed for both samples, i.e., $X_1 \sim \mathcal{N}(\mathbb{E}(X_1), \mathbb{V}(X_1))$ and $X_2 \sim \mathcal{N}(\mathbb{E}(X_2), \mathbb{V}(X_2))$, while their variances are nearly equal (homogeneity test). The homogeneity of variance can be evaluated by using Hartley test [41] defined as

$$F_{MAX} = \frac{\mathbb{V}(X_2)}{\mathbb{V}(X_1)} \tag{2.15}$$

under the assumption that the sample size $n_2 > n_1$. Under these assumptions, the t-statistics follows a distribution in the form of $t \times \ell$. The Hartley test employs F-distribution $F \sim \mathcal{F}(\ell_1, \ell_2)$ for significance testing to estimate the variance homogeneity.

However, the assumption of normality cannot be drawn for the practical problem which this thesis is dealing with. Assumptions denoted with $(\mathcal{A}_i)$: during this thesis are provided as in the following:
$(\mathcal{A}_1)$: Samples X_1 and X_2 are drawn from unknown distributions,
$(\mathcal{A}_2)$: Sample variances are unequal and unknown,
$(\mathcal{A}_3)$: Independence exists among observations of a sample and among both samples.
In this situation, the form $t \times \ell$ followed by t-statistics is no longer ensured. Furthermore, the decision of possible application of the t-test requires careful discussion: First, the t-test is not reliable if $\mathbb{V}(X_1) \neq \mathbb{V}(X_2)$, and higher $\mathbb{V}(X_1) - \mathbb{V}(X_2)$ increases the type I error $F_{\mathcal{I}_1}$. This was demonstrated in [42]. Second, measurement scale and type of data disfavor the usage of the t-test to construct the hypothesis testing. This comes into play when log-transformation applies and the variances of observed data are not equal. The authors in [43] suggest instead to use the median for examination of central tendency.

Therefore, in opposite to parametric tests, there exist another family of tests that demand only few assumptions. This class of tests are called *nonparametric* and will be discussed in the following section.

2.3. Nonparametric Testing

In practice, it is quite common that the observed data x do not follow a normal distribution $X \not\sim \mathcal{N}(\mu, \sigma)$, where μ represents the mean and σ represents the standard deviation. This is the case of nonparametric testing. In fact, these tests are not really assumption-free but instead they have much less assumptions compared to their analogous parametric tests. Typically, the assumptions made

here are that the individual observations are independent for the case of unpaired data or the pairs are independent for the case of paired observations. Nonetheless, exact assumptions will be made according to each test.

Indeed, if the observed data follow a normal distribution, these tests are poorer than parametric ones. This is quantified by analyzing the power of a test. However, the increase in power is found to be surprisingly small [32]. This small increase is even smaller for other distributions. Therefore, this is an indication that appropriate nonparametric tests are plausible to be used in drawing inferences for problems faced in practice. In general, nonparametric tests are more flexible and in some situations even more appropriate than their equivalent parametric tests.

2.3.1. Measurement Scale and Types of Data

The appropriateness to chose a particular class of testing is also dependent on the availability of the measurement scales. For this reason, this section discusses different types of scaling data: nominal, ordinal and interval scale.

Nominal data: They are the kind of data that represent a quantification of number of times for particular events. Group members are categorized according to a particular event or labeling. An exemplary situation is the case of categorizing data usage of mobile users into three categories: low, medium, high. This kind of data fall in the group of nonparametric tests.

Ordinal data: They represent the values based on a rank operator. The ranking is represented by distance between two successive ordinal values which has no special meaning. For example, imagine ranking the values of a particular number of mobile users according to the amount of data usage they use in a particular area. Similarly to nominal data, this group falls in the group of nonparametric tests.

Interval data: Interval data represent the data where the relative distance between any two sequential values is the same. For instance, imagine decibel values used to measure the level of received power. This kind of data falls in the group of parametric tests.

2.3.2. Rank-based Tests

Rank-based tests are a special type of nonparametric testing. The general idea of rank-based tests is to transform the original sample observations into ordinal (rank) data. Thus, these tests establish the comparison based on the transformed sample observations. In the following, let us assume a one-sample problem where the sample observations follow an unknown population. Let us also denote the sample size of the observed data with n and numerical data with $X = \{x_1, x_2, ..., x_n\}$,

i.e., the kth observation is represented by x_k. Mathematically, applying the rank function $\mathbb{R}(\cdot)$ to the kth observation x_k formulates as

$$\mathbb{R}(x_k) = \sum_{1 \leq q \leq n} \mathbb{I}(x_q \leq x_k) \tag{2.16}$$

where $\mathbb{I}(\cdot)$ is an indicator function defined as

$$\mathbb{I}(x) = \begin{cases} 1, & x_q \leq x_k \\ 0, & \text{otherwise} \end{cases} \tag{2.17}$$

where x_q is another observation, where its relative value is lower or equal to x_k, and $q, k \in \mathbb{N}$. Therefore, assuming the observed data are arranged in increasing order such that $X \rightarrow X_{(a)}$, and $X_{(a)} = \{x_{(1)}, x_{(2)}, ..., x_{(n)}\}$, the task of $\mathbb{R}(\cdot)$ is to produce $\{\mathbb{R}(x_{(1)}), \mathbb{R}(x_{(2)}), ..., \mathbb{R}(x_{(n)})\} = \{1, 2, ..., N\}$. As there likely exists the situation of repeated relative values of observed data, it is applied the average of ranks corresponding to respective positions of the set. This is also called the problem of ties or mid-ranks.

The two- or multiple-sample problems follow the same logic. In this cases, the rank function is applied to the pooled sample of the arranged observations. A two-sample problem will be further illustrated in Section 2.3.3.

Application: Let us consider an example where a few Key Performance Indicators (KPIs) are relevant and required in analyzing the network performance. For example, some KPIs such as received power, transmit power, signal-to-noise ratio commonly use their logarithmic units rather than interval units. In general, this thesis approaches the problem of transformation from decibels to ranks followed by a proper hypothesis test for the purpose of assessment.

2.3.3. Wilcoxon-Mann-Whitney Test

In this section, let us consider a problem of univariate two-sample testing. Herein, let us keep the same denotation as for the case of t-test, such as the sample data from the first population with $X_1 = \{x_{11}, x_{12}, ..., x_{1n_1}\}$, and the sample data from the second population with $X_2 = \{x_{21}, x_{22}, ..., x_{2n_2}\}$. For the sake of explanation, let X_1 represent the treatment-free, and let X_2 represent the treatment-aided. The equivalent nonparametric test of t-test is Wilcoxon-Mann-Whitney (WMW) test[1] [32, 36] commonly applied to tackle the two-sample location problem. The general principle of this test is driven by the goal of comparing the central tendencies (medians) of two sample distributions. In other words, often practical problems require to test whether the location of a respective population is greater or lower when compared to the other population (directional alternative), or are required to

[1] For the sake of simplicity, note that this test is also known in literature as Mann-Whitney test which is equivalent to Wilcoxon rank sum test.

test whether the locations of both populations are equal or not (nondirectional alternative). This test requires the following assumptions denoted with $(\mathcal{A}'_i)$:
$(\mathcal{A}'_1)$: Observations $x_{11}, x_{12}, ..., x_{1n_1}$ are a random sample from population $\mathcal{X}_1$. Thus, they are independent and identically distributed. The observations $x_{21}, x_{22}, ..., x_{2n_2}$ are a random sample from pupulation $\mathcal{X}_2$. Thus, they are independent and identically distributed.
$(\mathcal{A}'_2)$: The observations x_{1a} and x_{1b} are mutually independent. This is additional to $(\mathcal{A}'_1)$ (independence within each sample), but now made between samples.
$(\mathcal{A}'_3)$: Populations $\mathcal{X}_1$ and $\mathcal{X}_2$ are continuous populations.

The overall procedure of the WMW test is summarized in six steps:
(1) Chose α, the significance level of the test,
(2) Apply rank operator into the combined observations from both sample distributions, $\mathbb{R}(X_P)$, where X_P is the pooled sample. As a result, the observed data from both sample distributions are ordered according to

$$\{\mathbb{R}(x_{(11)}), \mathbb{R}(x_{(12)}), ..., \mathbb{R}(x_{(1n_1)}), \mathbb{R}(x_{(21)}), \mathbb{R}(x_{(22)}), ..., \mathbb{R}(x_{(2n_2)})\} = \{1, 2, ..., M\} \tag{2.18}$$

(3) Find the sample sizes of respective sample distributions, n_1 and n_2, and calculate their sum

$$n = n_1 + n_2, \tag{2.19}$$

(4) Compute the sum of ranks for the X_2 sample in the pooled distribution, denoted with $\mathcal{T}$ according to

$$\mathcal{T} = \sum_{j=1}^{n_1} \mathbb{R}(X_2). \tag{2.20}$$

(5) If the sample sizes are small enough, exact significance probability can be calculated,
(5.1) If sample sizes are relatively large, the normal approximation by utilizing z-statistics following a normal distribution $z \sim \mathcal{N}(0, 1)$ as

$$\mathcal{T}' = \frac{\mathcal{T} - \mathbb{E}(\mathcal{T})}{\sqrt{\mathbb{V}(\mathcal{T})}} \tag{2.21}$$

is applied where the expectation and variance are derived as

$$\mathbb{E}(\mathcal{T}) = \frac{n_1(n_1 + n_2 + 1)}{2} \tag{2.22a}$$

$$\mathbb{V}(\mathcal{T}) = \frac{n_1 n_2(n_1 + n_2 + 1)}{12}. \tag{2.22b}$$

The correction for continuity for the normal approximation reduces the absolute value of $\mathcal{T}'$ and requires that 0.5 subtracted from Eq. (2.21), which formulates as

$$\mathcal{T}' = \frac{|\mathcal{T} - \mathbb{E}(\mathcal{T})| - \frac{1}{2}}{\sqrt{\mathbb{V}(\mathcal{T})}} = \frac{|\mathcal{T} - \frac{n_1(n_1+n_2+1)}{2}| - \frac{1}{2}}{\sqrt{\frac{n_1 n_2(n_1+n_2+1)}{12}}}. \tag{2.23}$$

On the other hand, when an excessive number of mid-ranks is present in observations, the mid-rank correction based on [44] is applied as

$$\mathcal{T}' = \frac{\mathcal{T} - \mathbb{E}(\mathcal{T})}{\sqrt{\mathbb{V}(\mathcal{T})}} = \frac{\mathcal{T} - \frac{n_1(n_1+n_2+1)}{2}}{\sqrt{\frac{n_1 n_2(n_1+n_2+1)}{12} - \frac{n_1 n_2 \sum_{j=1}^{J}(t_j^3 - t_j)}{12(n_1+n_2)(n_1+n_2-1)}}} \tag{2.24}$$

for a given number of repeated scores J and the number of repetition t_j. The term on the right in denominator results in reducing its value. This results in a slight increase in the absolute value of z. Herein, the significance probability (estimated p-value) can be calculated as

$$\hat{p} = \zeta(z) = \begin{cases} \mathbb{P}(Z \leq z | \mathcal{I}_0 \text{ is true}) & \text{, left-direction} \\ \mathbb{P}(Z \geq z | \mathcal{I}_0 \text{ is true}) & \text{, right-direction} \\ 2 \times \mathbb{P}(Z \geq |z| | \mathcal{I}_0 \text{ is true}) & \text{, nondirectional} \end{cases} \tag{2.25}$$

where function $\zeta(z)$ represents the estimated remaining area under the normal curve,
(6) Make the decision by comparing $\mathcal{T}'$ with z_α (critical value): (1) Median of sample X_2 is larger than median of sample X_1: If $\mathcal{T}' \geq z_\alpha$ holds, it is concluded that there is evidence of significant effect from treatment, otherwise, it is concluded that there is no evidence of significant effect from treatment; (2) Median of sample X_1 is larger than median of sample X_2: If $\mathcal{T}' \leq -z_\alpha$ holds, it is concluded that there is evidence of significant effect from treatment, otherwise, it is concluded that there is no evidence of significant effect from treatment; (3) Median of sample X_1 is not equal to the median of sample X_2: If $|\mathcal{T}'| \geq z_\alpha$ holds, it is concluded that there is evidence of significant effect from treatment, otherwise, it is concluded that there is no evidence of significant effect from treatment.

General approach: Based on the assumptions for WMW test, the problem formulates as a problem of comparing two Cumulative Distribution Functions (CDFs) of X_1 and X_2, denoted with $F_{X_1}(x)$ and $F_{X_2}(x)$, respectively. Therefore, it is possible to construct a null hypothesis testing, which formulates as

$$\mathcal{I}_0 : F_{\mathcal{X}_1}(x) = F_{\mathcal{X}_2}(x) \tag{2.26}$$

with $\forall x \in \mathbb{R}$. It states that the median of population distribution $\mathcal{X}_2$ equals the median of the population distribution $\mathcal{X}_1$. The nondirectional alternative hypothesis defined as

$$\mathcal{I}_1 : F_{\mathcal{X}_1}(x) \neq F_{\mathcal{X}_2}(x) \tag{2.27}$$

states that the median of the population distribution $\mathcal{X}_2$ is not equal to the median of population distribution $\mathcal{X}_1$. The directional alternative hypothesis defined as

$$\mathcal{I}_1 : F_{\mathcal{X}_1}(x) < F_{\mathcal{X}_2}(x) \tag{2.28}$$

states that the median of the population distribution $\mathcal{X}_2$ is larger than the median of population distribution $\mathcal{X}_1$. Eventually, the directional alternative hypothesis defined as

$$\mathcal{I}_1 : F_{\mathcal{X}_1}(x) > F_{\mathcal{X}_2}(x) \tag{2.29}$$

states that the median of the population distribution $\mathcal{X}_1$ is larger than the median of population distribution $\mathcal{X}_2$.

Application: The scope of this thesis aims to investigate whether there is evidence of a presence of a treatment effect to a mobile user. This also supports the assessment of KPIs. Furthermore, both effect models, random and fixed treatment effect.

2.3.4. Sign Test

Frequently in practice is required for an underlying distribution to test whether its observations come from a distribution with a specific median. For this reason, binomial single-sample sign test is a simple test which applies under general conditions. Indeed, in similar conditions Wilcoxon signed-rank test [45] potentially applies, yet it requires the assumption that the underlying distribution is symmetrical. In other words, while Wilcoxon signed-rank test assumes that each κ_i comes from a continuous population (not necessarily the same) that is symmetric about a common median ρ, where $\kappa_i = x_{1a} - x_{1b}$, on the other hand, the paired sign test does not require the stringent assumption about the symmetry in median. This is the main advantage of the sign test over signed-rank test.

In the following, it is specifically discussed the single-sample sign test [46, 47] which is used to determine the likelihood of observing a specified number of observations to be above against below the median of a distribution. In fact, since the median identifies the 50th percentile, it is intuitively expected that one-half of the observations to be larger and the other half to be lower than this value. For this reason, it is crucial to determine both these numbers. Let us recall the same denotations about sample distribution X_1. The sign test requires two assumptions denoted with $(\mathcal{A}''_i)$:
$(\mathcal{A}''_1)$: Observations x_{1a} are mutually independent,
$(\mathcal{A}''_2)$: Each observation x_{1a} comes from the same continuous population with median ρ, so that $\mathbb{P}(x_{1a} > \rho) = \mathbb{P}(x_{1a} < \rho) = 1/2, a = 1, 2, ..., n_1$.
Assumption $(\mathcal{A}''_2)$ can be further weakened by stating that each x_{1a} comes from a population, not necessarily the same. The procedure of the sign test is summarized with below steps:
(1) Choose α, the significance level of the test,
(2) Discard the observations which happen to be equal to ρ, where ρ denotes the hypothesized median
(3) For each observation in X_1, record the sign of the difference

$$\mathcal{Z}_a = \text{sgn}(x_{1a} - \rho),\ a = 1, 2, ..., n_1 \tag{2.30}$$

which imposes the following cases

$$\mathcal{Z}_{a+} = 1 \quad \text{if } x_{1a} - \rho > 0 \tag{2.31a}$$

$$\mathcal{Z}_{a-} = -1 \quad \text{if } x_{1a} - \rho < 0 \tag{2.31b}$$

$$\mathcal{Z}_{a0} = 0 \quad \text{if } x_{1a} - \rho = 0 \tag{2.31c}$$

and thus count the number of plus signs for directional hypothesis to test whether the median of treatment-aided is lower than the median of treatment-free, which formulates as

$$\mathcal{P} = \sum_{a=1}^{f_1} \mathcal{Z}_{a+}, \quad f_1 \leq n_1 \tag{2.32}$$

or count the number of minus signs for directional hypothesis to test whether the median of treatment-aided is larger than the median of treatment-free distribution which formulates as

$$\mathcal{M} = \sum_{a=1}^{f_2} \mathcal{Z}_{a-}, \quad f_2 \leq n_1. \tag{2.33}$$

(4) The significance probability $\hat{p}$ is calculated by utilizing the binomial distribution $\mathcal{B}(\imath, p_\imath)$ where $\imath$ represents the number of trials of an experiment and $p_\imath$ denotes the probability of success on an individual trial. Therefore, for the case of having larger, lower, or unequal median of treatment-aided compared to the treatment-free, respectively, $\hat{p}$ can be calculated as

$$\hat{p} = \binom{n_1}{\mathcal{M}} \left(\frac{1}{2}\right)^{\mathcal{M}} \left(\frac{1}{2}\right)^{(n_1 - \mathcal{M})} \tag{2.34a}$$

$$\hat{p} = \binom{n_1}{\mathcal{P}} \left(\frac{1}{2}\right)^{\mathcal{P}} \left(\frac{1}{2}\right)^{(n_1 - \mathcal{P})} \tag{2.34b}$$

$$\hat{p} = \min(1, B), \quad B = 2\binom{n_1}{\mathcal{C}} \left(\frac{1}{2}\right)^{\mathcal{C}} \left(\frac{1}{2}\right)^{(n_1 - \mathcal{C})}, \quad \mathcal{C} = \min(\mathcal{P}, \mathcal{M}) \tag{2.34c}$$

which is further compared with α to make the decision. On the other hand, for large sample of n_1 the below approximation is used

$$\mathcal{P}' = \frac{\mathcal{P} - \mathbb{E}(\mathcal{P})}{\sqrt{\mathbb{V}(\mathcal{P})}} \tag{2.35}$$

where

$$\mathbb{E}(\mathcal{P}) = \frac{n_1}{2} \tag{2.36a}$$

$$\mathbb{V}(\mathcal{P}) = \frac{n_1}{4} \tag{2.36b}$$

which rejects the null hypothesis if $\mathcal{P}' \geq z_\alpha$ for the case of larger median of treatment-aided against treatment-free, where z_α is the critical value. In another case when the treatment-aided median is asked to be tested for lower median, the null hypothesis is only rejected if $\mathcal{P}' \leq z_\alpha$. Finally, in the case of testing for nondirectionality, the null hypothesis is rejected if $|\mathcal{P}'| \geq z_\alpha$. Normal distribution of z is used as in Eq. (2.25) to estimate the significance probability $\hat{p}$ for large sample approximation.

2.4. Multiple Comparisons

In principle, single testing procedures potentially result in an increased false positive rate, already defined in Eq. (2.6) with $F_{\mathcal{I}_1}$. From the definition of power in Eq. (2.8), it is possible to define the probability of correctly deciding for $\mathcal{I}_1$ when K hypotheses are tested. This formulates as

$$C_{\mathcal{I}_{1,K}} = (1 - \mathbb{P}(\text{accept } \mathcal{I}_0 | \mathcal{I}_1))^K. \tag{2.37}$$

Further, known $C_{\mathcal{I}_{1,K}}$ is is possible to rewrite Eq. (2.6) as

$$F_{\mathcal{I}_{1,K}} = 1 - (1 - \mathbb{P}(\text{accept } \mathcal{I}_0 | \mathcal{I}_1))^K. \tag{2.38}$$

which expresses the probability of incorrectly deciding for $\mathcal{I}_1$ at least once. Consequently, incorrect rejections (false positives) are likely to occur among correct rejections. In general, multiple testing [48–51] are applied to mitigate this issue. Commonly, this is approached as a multiple comparison problem by controlling Family-wise Error Rate (FWER) with Bonferroni or Hochberg procedures [51] as classical approaches for controlling the probability of committing any type I error. However, Bonferroni approach is quite conservative as it rejects all those $\ddot{\mathcal{I}}_{(i)}$ hypotheses for a given K number of hypotheses if the following is satisfied

$$p_{(i)} \leq \frac{\alpha}{K}. \tag{2.39}$$

For instance, for a given $K = 10^3$ and $\alpha = 0.05$, Bonferroni requires $p \leq 5 \times 10^{-5}$ to reject is null hypotheses.

2.4.1. False Discovery Rate

FWER is usually required in a strong sense, i.e., when all hypotheses are true or false. Yet, the problem of increased type I error still remains in FWER procedures. Therefore, this problem is tackled with another approach which is called False Discovery Rate (FDR) [52]. Let us consider a problem with multiple comparisons by simultaneously testing K hypotheses, and assume that k_0 are true, such that $K \geq k_0$. Let us denote with R the number of rejected (null) hypotheses, with R_T the

random variable of truly rejected hypotheses (equivalent to $C_{\mathcal{I}_1}$), and with R_F the random variable of falsely rejected hypotheses (equivalent to $F_{\mathcal{I}_1}$). It is also assumed that variables R_T and R_F are unobservable random variables, while R is an observable variable. The relation between observed and unobserved random variables is as in the following

$$R = R_F + R_T. \tag{2.40}$$

The proportion of falsely rejected hypotheses is investigated from the relationship

$$Z = \frac{R_F}{R} \tag{2.41}$$

where FDR is defined as the expectation of Z as

$$\mathbb{E}(Z) = \mathbb{E}(\frac{R_F}{R}) = \mathbb{E}(\frac{R_F}{R_F + R_T}). \tag{2.42}$$

Indeed, it is impossible to control R at each realization as the case $K = k_0$ holds. However, controlling FDR is possible. In fact, it was proven in [52] that FDR controls the rate of type I errors (as explained in Eq. (2.6)) during multiple testing.

2.4.2. Benjamini-Hochberg Procedure

Benjamini-Hochberg (BH) procedure approaches the multiple significance testing problem by controlling the FDR. Indeed, it also controls the FWER but in the weak sense. In the following, the step-wise procedure of BH is demonstrated.
Procedure: Let us assume the significance problem is approached by testing K number of hypotheses as

$$\ddot{\mathcal{I}}_1, \ddot{\mathcal{I}}_2, ..., \ddot{\mathcal{I}}_K \tag{2.43}$$

which correspond to different p-values

$$p_1, p_2, ..., p_K \tag{2.44}$$

where $\ddot{\mathcal{I}}$ denotes the multiple hypothesis operator. According to procedure, p-values in Eq. (2.44) should be ordered as denoted with $p_{(\cdot)}$

$$p_{(1)}, p_{(2)}, ..., p_{(K)}. \tag{2.45}$$

The ordering in Eq. (2.45) imposes the corresponding hypotheses

$$\ddot{\mathcal{I}}_{(1)}, \ddot{\mathcal{I}}_{(2)}, ..., \ddot{\mathcal{I}}_{(K)}. \tag{2.46}$$

After this step, let L be the largest l, i.e., $l = 1, 2, ..., L$, and according to BH procedure, it rejects all those $\ddot{\mathcal{I}}_{(l)}$ if the following is satisfied

$$p_{(l)} \leq \frac{l}{K}\alpha \tag{2.47}$$

where α is the significance level. The step-wise procedure described here is known as BH procedure [52]. Indeed, other methods such as Bonferroni [50], Hochberg [51] potentially are useful. However, mainly because the BH procedure has the desirable property of increased power with the increased number of constructed hypothesis, it is more convenient to be applied corresponding to the application and the scope of this thesis.

Application: The BH procedure is applied in this thesis on different scenarios for the purpose of assessing possible improvements or impairments to mobile users when a particular treatment effect is considered. The focus here is on analysis of mobile networks for various vehicular use cases. The scope of this thesis covers particular active and passive treatments in proximity of mobile users with purpose to improve the radio link. Therefore, the usage of BH is multifold: It applies by considering each realization as a measurement trip. Herein, hypothesis testing enables the assessment of the overall performance along a trajectory (many realizations) covered from mobile users on-board a vehicle. It also applies to assess the service quality for mimicked short-time experiments, such as voice calls, packet data transferring and so forth. Moreover, combined with different theoretical approaches, it also applies to quantify rejection ratios over mimicked nominal environments.

2.5. Distributional Clustering

Distributional clustering was initially termed in [53] as a problem of self-organization of members of a set S based on the similarity of the conditional distributions of members of another set T, $p(t|s)$. In fact, the authors in [54] showed that such problem is considered as a special case of a more general problem, the task of which is to find only the features of S that are relevant to estimate T. From information theoretical point of view, this is formulated as a problem of finding a compressed version of S, denoted with $\tilde{S}$, such that the mutual information $I(\tilde{S};T)$ is maximized under a constraint $I(S;\tilde{S})$.

Similar problems of distributional clustering are elaborated in [55, 56]. Herein, the problem definition specifically looks at a greedy algorithm as discussed in the following.

2.5.1. Agglomerative Information Bottleneck

Let us assume the observed data are represented by a pair $c_i = (t_i, s_i)$, where variable t is a time variable, whereas variable s is a received power variable. The Agglomerative Information Bottleneck (aIB) [57] finds a quantization $\tilde{t}$ that minimizes the mutual information with the original

time $I(t;\tilde{t})$, while simultaneously maximizing the mutual information $I(s;\tilde{t})$ with the *relevance variable* s. This algorithm is only locally optimal, but allows the greedy computation of the quantizations, resulting in much faster computation speeds. In the following is discussed the procedure.

Procedure: First, as a preparation, t is prequantized in a fine grid, denoted with $\dot{t}$. Thus, every interval contains multiple samples[2] of s and computes the associated empirical conditional Probability Mass Function (pmf) $p(s|\dot{t})$[3]. Then, the costs of merging two adjacent time-intervals is calculated as

$$d_{i,j}(\dot{t}) = (p(\dot{t}_i) + p(\dot{t}_j)) f_{JS,\pi_2}[p(s|\dot{t}_i), p(s|\dot{t}_j)], \tag{2.48}$$

where $f_{JS,\pi_2}(\cdot)$ is the Jensen-Shannon divergence, which is itself a generalized version of the Kullback-Leibler divergence [58] denoted with $f_{KL}(\cdot)$. The Jensen-Shannon divergence is defined as

$$f_{JS,\pi_2}[p(s|\dot{t}_i), p(s|\dot{t}_j)] = \frac{1}{2} f_{KL}(p(s|\dot{t}_i), p_M) + \frac{1}{2} f_{KL}(p(s|\dot{t}_j), p_M) \tag{2.49}$$

which indicates the average Kullback-Leibler divergence of $p(s|\dot{t}_i)$ and $p(s|\dot{t}_j)$ from their mixture distribution p_M. Next, the two time intervals with the smallest merging costs are merged. This corresponds to the two intervals that have the most similar empirical pmfs, $p(s|\dot{t}_i), p(s|\dot{t}_j)$. After that step, new merging costs are calculated, and again the intervals with the lowest costs are merged. In this way, the greedy algorithm always reduces the number of intervals by one in the currently optimal fashion, and intervals are calculated for $|\tilde{t}| = |\dot{t}| \ldots 1$, where $|\cdot|$ is the order of the set. Afterwards, one can pick the most fitting number of intervals.

Application: Throughout this thesis, the aIB is used as a theoretical model for two purposes: First, this supports to find the similarities of statistics of a metric in such manner that statistical dissimilarities correspond to modelling distinct nominal environments, such as urban, sub-urban or rural. For instance, while a mobile user is consistently moving along a trajectory the observed data are collected continuously. Second, the aIB is also applied to statistically classify inter- and intra-technology outage scenarios. As an exemplary situation is a mobile user with access in e.g., UMTS/LTE network.

2.6. Logistic Models

A special type of functions, called logistic functions, are useful in describing particular types of growth in practice. The nature of wireless communications imposes changes in physical layer measurements. This affects radio characteristics on both direction: downlink and uplink. Therefore, it is important to incorporate such models into the analysis. In the following, the Generalized Logistic Function (gLF) and sigmoid function are defined.

[2] This is limited to 1 s in our case due to measurement equipment.

[3] Conditional pmf of S given $\dot{T} = \dot{t}$ is defined as $p_{S|\dot{T}=\dot{t}}(s) = \mathbb{P}(S = s|\dot{T} = \dot{t})$.

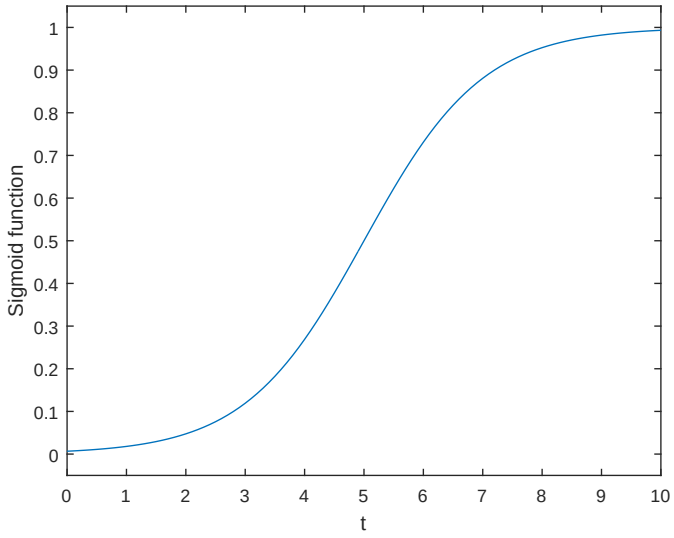

Figure 2.2.: Sigmoid function with $d_1 = 0$, $d_2 = 1$, $k = 1$, $t_0 = 5$.

Generalized logistic function: The gLF function is defined as

$$\mathcal{L}(t) = d_1 + \frac{d_2 - d_1}{c + qe^{-k(t-t_0)}}, \tag{2.50}$$

where d_1 and d_2 are the lower and upper asymptotes, respectively, c and q typically take values of 1, k is the steepness, and t_0 is the midpoint.

Sigmoid function: The sigmoid function is a special case of the gLF, which is defined as

$$\mathcal{S}(t) = d_1 + \frac{d_2 - d_1}{1 + e^{-(t-t_0)}}, \tag{2.51}$$

where $\mathcal{S}(t) = \mathcal{L}(t, c = 1, q = 1, k = 1)$. For the sake of illustration, this is provided in Fig. 2.2, which shows the sigmoid function $\mathcal{S}(t)$ with respect to variable t.

Application: The detection of abrupt changes is an important aspect in mobile networks. The usage of least-squares regression model of $\mathcal{S}(t)$ helps to detect such changes for different paramters such as received power, transmit power, interference levels and other KPIs. An exemplary situation is the case when received power's statistical mean of a mobile user changes abruptly between two time-intervals. Additionally, for a user which is consistently moving, the spatial effect is crucial. For these reasons, logistic models are utilized to compare with nonparametric-based developed detection techniques.

"The emphasis of the carriers has been to market speed, and yet the technology exists today, and it's being adopted slowly ... that would give us really solid coverage and increase the capacity of the system."

Martin Cooper (1928 – present)

3

Mobile Service Quality in Amplify-and-Forward Repeater-aided Railway Vehicles

According to the International Transport Forum of the Organisation for Economic Cooperation and Development (OECD), by 2050, passenger mobility will increase by $200 - 300\,\%$ and freight activity by as much as $150 - 250\,\%$ with respect to 2010 [1]. Today, while passengers commute between cities, they acquire access on social media, play online games, perform video-streaming or initiate file-transferring. That is to say, they demand greater reliability and better quality of experience as two key elements for seamless connectivity. Railway environments are pivotal element of Intelligent Transportation Systems (ITSs) which are modifying current implementations of wireless connectivity to meet mobile user demands. Notably, existing framework of Roll2Rail (R2R) project [59] and European Committee for Standardization EN (ECSEN) [60] aim to identify the needs and technical challenges with current and future mobile communication technologies defined in 3rd Generation Partnership Project (3GPP) as potential solutions to address the communication issues. Yet, existing solutions hardly manage to satisfy the growing costumer demands, since mobile providers traditionally focus to market speed. But at the same time, the existing technologies are being slowly adopted, which weakens the enhancement in quality of experience towards better coverage and increased capacity.

On one hand, despite an increasing interest of improving service quality on-board railway vehicles, there is still a big gap between mobile- and railway operators: While mobile operators aim to slightly deploy the infrastructure beside the railway, railway operators consider the safety and comfort of passengers as a primary consideration by using composite panes of prototype windows that add extra Vehicle Penetration Loss (VPL) [61–64]. Significantly, this design affects resentfully the mobile

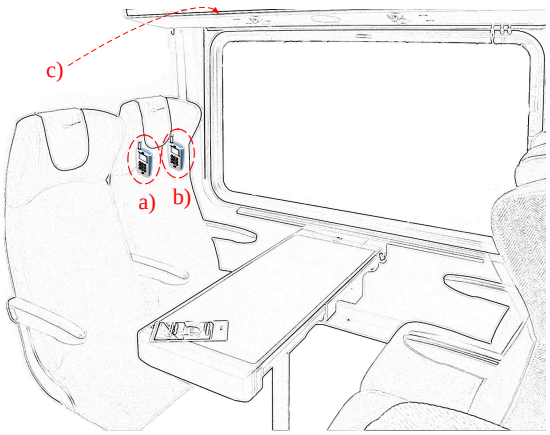

Figure 3.1.: Illustration of smartphone-based measurement setup on-board treatment-aided High Speed Train (HST). Mobile users depicted with a,b) represent end-users, while c) represents the Radiating Cable (RC) laid on luggage racks above the seat.

communication frequencies. On the other hand, while mobile operators have full control on their networks both on infrastructure and user side, here however there is no control on infrastructure's side. Therefore, some crucial factors needs to be taken into consideration: First, the railways are constructed along gentle-curved trajectories, where the varying velocity of railway vehicles challenges the unvarying measurement granularity. This directly impacts the sample sizes of Key Performance Indicators (KPIs). Bursty nature of particular technologies adds further complexity in terms of statistical evaluation. Second, fundamental differences among various KPIs in terms of underlying distribution, data type and unit complicate the investigation and evaluation of a particular treatment in terms of statistical inference. Third, propagation conditions and traffic load in operational networks are unknown which makes the assessment ambitious to draw inferences both spatially and temporally. All the aforementioned challenges require to construct a robust approach in terms of statistical inference. Therefore, railway environments pose a big challenge to wireless connectivity from the point of view of both understanding the treatment benefits and investigating the worst scenarios.

A commercially available solution to boost the performance on-board HST exists. The core scope of the discussion in this chapter aims to demonstrate the benefits and disadvantages of an *active treatment* approach. Repeaters with optimized on-board configuration ensure to bundle the signals via a rooftop antenna that further forward them along the whole length of the vehicle via RCs [14, 65] for coverage extension [66]. Then, the deployed RCs serve the mobile users in proximity as illustrated in Fig. 3.1. The Amplify-and-Forward Repeater (AFR) amplifies all signal and noise at selected signal bands in both uplink and downlink of the Frequency Division Duplex (FDD) mobile network.

Based on [25, 26, 67, 68], the contributions of this chapter outline as in the following:

- Descriptive analysis to investigate the behavior of AFRs and RCs on-board is conducted. The analysis relies on long-time experiments performed in a live network with User Equipment (UE) that mimic the quasi-real usage of end-users. Particular attention is paid to coverage KPIs.

- The novel approach to assess the service quality of vehicular use cases is applied on mobile users on-board a HST. The key idea is to establish a common framework for service quality assessment which classifies particular data-outage scenarios as well as mimics both short- and long-time experiments. The statistical analysis with recursive hypotheses consists of Wilcoxon-Mann-Whitney (WMW) test coupled with nonparametric bootstrap. The proposed design intents to serve as benchmarking baseline to detect KPI improvements and impairments of treatment-aided HST in operational network.

- A spatially-based assessment approach is demonstrated. Estimation of physical throughput in operational traffic potentially leads to high errors. To cope with this, a novel assessment approach to detect the improvements in signal quality is proposed. Key idea is to evaluate Channel Quality Indicators (CQIs) from hypothesis conditions constructed on small chunks of a railway track. The method consists of a combination of nonparametric sign test and sequential hypothesis, which aims to serve as signal quality's detection technique for high mobility scenarios.

- A temporally-based assessment approach is demonstrated. The assessment of service quality over the whole railway track does only represent improvements over a large sample size including all kinds of environments. A new approach to deal particularly with short-time experiments is proposed. Therefore, it mimics specific applications such as average voice call duration, file-transferring, and web-page downloading. Furthermore, as demonstrated, the design deals with the problem of significance among vehicular use cases.

- A technique to characterize VPL is proposed. The approach is compliant to European Telecommunications Standard Institute (ETSI) and is evaluated and applied on experiments conducted in inter-city and regional trains. The overall framework aims to serve not only as an estimation model but also to characterize VPL in operational networks.

3.1. System Model

3.1.1. Data Outage

The target of this section is to provide a statistical evaluation of extreme network conditions on-board railway vehicles. In general, it demonstrates a statistical classification of particular scenarios for users with access in Universal Mobile Telecommunications System (UMTS)/Long Term Evolution (LTE) network. The problem formulates as a problem of finding strong statistical changes occurring in UTRA Received Signal Strength Indicator (RSSI) and E-UTRA RSSI for a AFR-free[1] user. This function is denoted with $\Psi(x,t)$, where x denotes RSSI and t denotes the time. To this end, the problem formulates based on Agglomerative Information Bottleneck (aIB) algorithm [54, 57] as explained in Section 2.5.1.

Therefore, the task of aIB is to distinguish m-intervals, where m is an arbitrary number. The function $\Psi(x,t)$ is equivalent to Eq. (2.49) as

$$\Psi(x,t) \equiv f_{JS,\pi_2}(p(x|\dot{t}_i), p(x|\dot{t}_j)), \quad x \in \mathbb{R}, \quad t \in \mathbb{R}_+ \tag{3.1}$$

where $f_{JS,\pi_2}(\cdot)$ is the Jenson-Shannon divergence and $p(x|\dot{t}_i)$ and $p(x|\dot{t}_j)$ are conditional Probability Mass Functions (pmfs) of RSSI within relevant time intervals $\dot{t}_i$ and $\dot{t}_j$. The ends of m intervals correspond to particular outage scenarios each identified with observed data distribution $X_1^{(o)}(x)$, where $1 \leq o \leq m$, $o \in \mathbb{N}$, and $x \in \mathbb{R}$. In other words, aIB identifies each o-th interval such that its statistics change strongly in RSSI when compared to the rest of $m-1$-intervals. From this are chosen two intervals that satisfy two conditions:
(1) each o-th interval contains samples from both technologies UMTS and LTE, and
(2) any interval among all ms represents the highest RSSI level in average formulated as

$$r_{MAX} = \max_{x \in X_1} \{\mathbb{E}\{X_1^{(1)}\}, \mathbb{E}\{X_1^{(2)}\}, ..., \mathbb{E}\{X_1^{(m-1)}\}, \mathbb{E}\{X_1^{(m)}\}\}, \quad \forall m \in \mathbb{N} \tag{3.2}$$

while any other interval represents the lowest RSSI level in average formulated as

$$r_{MIN} = \min_{x \in X_1} \{\mathbb{E}\{X_1^{(1)}\}, \mathbb{E}\{X_1^{(2)}\}, ..., \mathbb{E}\{X_1^{(m-1)}\}, \mathbb{E}\{X_1^{(m)}\}\}. \tag{3.3}$$

On one hand, condition (1) ensures that at least an inter-technology handover occurs and evaluates both technologies from a joint interval. On the other hand, condition (2) characterizes extreme scenarios of data outages.

For the sake of simplicity, the presented problem is fundamentally different to the problem of nominal environments discussed in Chapter 5. Here, however, the continuity of a particular technology over

[1] It is assumed that this user is incapable of benefiting from a treatment by being located considerably far from the wagon with treatment. Fig. 3.9 provides the details.

the whole railway track is no longer ensured. Instead, each user is served by a technology depending on the network availability. Its major disadvantageous is the disability for evaluating mobile user's performance due to spatial and temporal discontinuity. Despite this, the benefit of this approach is that it allows us to identify data outages based on network conditions.

3.1.2. Service Quality Analysis

The goal is to compare the central tendencies of distributions of two observed data to test whether one distribution is greater or not (to answer e.g., "Is there any improvement in received power if a user is placed under RC?", or "Is there any improvement in received power if a user is placed under the RC but in a different wagon compared to the previous case?"). To do so, the users were placed in suitable positions to enable the assessment of particular vehicular use cases.

Therefore, the assessment problem formulates by constructing binary hypothesis with WMW test as

$$\mathcal{I}_0 : \ F_{X_1}(x) = F_{X_3}(x) \quad \mathcal{I}_1 : \ F_{X_1}(x) < F_{X_3}(x) \tag{3.4a}$$

$$\mathcal{I}_{0'} : \ F_{X_1}(x) = F_{X_2}(x) \quad \mathcal{I}_{1'} : \ F_{X_1}(x) < F_{X_2}(x) \tag{3.4b}$$

where F_{X_1} denotes Cumulative Distribution Function (CDF) of the user placed in a wagon where no impact from treatment is assumed. This user is named *AFR-free* user throughout this chapter. F_{X_2} represents CDF of the user placed within a modified wagon, and F_{X_3} represents CDF of the user placed in the modified wagon other than the previous one. Both of these users are named *AFR-aided* users. Specifically, the former was placed under the RC connected to a different AFR.

The model distinguishes between two cases provided $\mathcal{I}_1$ in Eq. (3.4a) is in force: On one hand, hypothesis imposes a refined model $F_{X_1}(x) = F_{X_3}(x - \tilde{\Delta x})$ under assumption of fixed-effect treatment's model $\tilde{\Delta x} > 0$, $\forall \tilde{\Delta x} \in \mathbb{R}$. In this case, the inference states that F_{X_1} and F_{X_3} differ only in deterministic shift, $\mathbb{E}(X_1) = \mathbb{E}(X_3) - \tilde{\Delta x}$ and their variances are equal $\mathbb{V}(X_1) = \mathbb{V}(X_3)$. In other words, the difference is statistically significant. On the other hand, under assumption of random-effect model, the inference states that F_{X_1} and F_{X_3} differ and their variances are unequal $\mathbb{V}(X_1) \neq \mathbb{V}(X_3)$. Herein, the treatment $\tilde{\Delta x}$ is a random variable. Yet, the difference is statistically significant. The same definition holds for the relationship between X_1 and X_2 in Eq. (3.4b) as well.

Let us now discuss explicitly the problem of assessing the improvements in received power. Transmission losses for AFR-aided and AFR-free users can be estimated as in the following

$$\widehat{L_3} = -10 \log_{10} \Big(\frac{\widehat{P_{R_3}}}{\widehat{P_{T_3}}} \Big) (dB) \tag{3.5a}$$

$$\widehat{L_1} = -10 \log_{10} \Big(\frac{\widehat{P_{R_1}}}{\widehat{P_{T_1}}} \Big) (dB) \tag{3.5b}$$

where $\widehat{P_{R_3}} \in \mathbb{R}$ and $\widehat{P_{R_1}} \in \mathbb{R}$ denote the respective estimated received power and $\widehat{P_{T_3}} \in \mathbb{R}$ and $\widehat{P_{T_1}} \in \mathbb{R}$ denote the respective estimated transmitted power. To arrive at an equivalent representation with $\mathbb{E}(X1)$, Eq. (3.5a) and Eq. (3.5b) are subtracted which implies an estimated difference defined as

$$\widehat{\Delta L_{31}} = \widehat{L_3} - \widehat{L_1}. \tag{3.6}$$

Higher $\widehat{\Delta L_{31}}$ corresponds to higher received power difference. If the below condition

$$\widehat{\Delta L_{31}} > 0 \Leftrightarrow \widehat{L_3} > \widehat{L_1} \tag{3.7}$$

is satisfied, it further indicates improvement which is impacted from the active treatment. This allows us the expression Eq. (3.7) to rewrite as

$$\widehat{P_{R_3}} = \widehat{P_{R_1}} + \tilde{\Delta x} \tag{3.8}$$

which exhibits a representation of the improved signal level, where $\widehat{P_{R_1}}$, $\widehat{P_{R_3}}$, and $\tilde{\Delta x}$ are estimates. An active treatment with AFRs not only decreases the VPL but also during particular amount of time impacts the AFR-aided user to be connected to base stations with better link quality compared to the AFR-free user. This compensates the absence of dedicated deployments. In real-world conditions this is a direct implications to the estimates $\widehat{P_{T_1}}$ and $\widehat{P_{T_3}}$ be not necessarily identical.

Few trips of measurement campaigns impact the limited number of realizations. To estimate the original distribution, the problem formulates using bootstrap with *replacement*. Therefore, let $\forall i = \{1, 2, 3\}$, F_{X_i} be the original distributions and $\widehat{F_{X_{i,j}}}$ be the bootstrap distributions where $j = \{1, 2, ..., M\}$. From this, the procedure follows the construction of multiple hypotheses $\mathcal{I}_{0,M}, \mathcal{I}_{1,M}$, and $\mathcal{I}_{0\prime,M}, \mathcal{I}_{1\prime,M}$, where M is the number of bootstrap distributions. Thus, Eq. (3.4a) now extends and becomes

$$\ddot{\mathcal{I}}_{0,1} : \widehat{F_{X_{1,1}}}(x) = \widehat{F_{X_{3,1}}}(x) \quad \ddot{\mathcal{I}}_{1,1} : \widehat{F_{X_{1,1}}}(x) < \widehat{F_{X_{3,1}}}(x) \tag{3.9a}$$

$$\ddot{\mathcal{I}}_{0,2} : \widehat{F_{X_{1,2}}}(x) = \widehat{F_{X_{3,2}}}(x) \quad \ddot{\mathcal{I}}_{1,2} : \widehat{F_{X_{1,2}}}(x) < \widehat{F_{X_{3,2}}}(x) \tag{3.9b}$$

$$\vdots$$

$$\ddot{\mathcal{I}}_{0,M} : \widehat{F_{X_{1,M}}}(x) = \widehat{F_{X_{3,M}}}(x) \quad \ddot{\mathcal{I}}_{1,M} : \widehat{F_{X_{1,M}}}(x) < \widehat{F_{X_{3,M}}}(x) \tag{3.9c}$$

and similarly Eq. (3.4b) reformulates as

$$\ddot{\mathcal{I}}_{0\prime,1} : \widehat{F_{X_{1,1}}}(x) = \widehat{F_{X_{2,1}}}(x) \quad \ddot{\mathcal{I}}_{1\prime,1} : \widehat{F_{X_{1,1}}}(x) < \widehat{F_{X_{2,1}}}(x) \tag{3.10a}$$

$$\ddot{\mathcal{I}}_{0\prime,2} : \widehat{F_{X_{1,2}}}(x) = \widehat{F_{X_{2,2}}}(x) \quad \ddot{\mathcal{I}}_{1\prime,2} : \widehat{F_{X_{1,2}}}(x) < \widehat{F_{X_{2,2}}}(x) \tag{3.10b}$$

$$\vdots$$

$$\ddot{\mathcal{I}}_{0\prime,M} : \widehat{F_{X_{1,M}}}(x) = \widehat{F_{X_{2,M}}}(x) \quad \ddot{\mathcal{I}}_{1\prime,M} : \widehat{F_{X_{1,M}}}(x) < \widehat{F_{X_{2,M}}}(x) \tag{3.10c}$$

As next step, techniques of False Discovery Rate (FDR) [48, 52] to compensate for type II error are applied. Herein, as a performance metric is defined the rejection ratio as

$$\tau = \frac{\mathbb{P}(\text{accept } \ddot{\mathcal{I}}_{0,j}|x)}{\mathbb{P}(\text{accept } \ddot{\mathcal{I}}_{0,j}|x) + \mathbb{P}(\text{reject } \ddot{\mathcal{I}}_{0,j}|x)}. \tag{3.11}$$

Rejection ratio τ quantifies the proportion of rejected $\ddot{\mathcal{I}}_{0,j}$s in a pool of M multiple hypotheses. The demonstrated framework allows to establish the assessment of KPIs in cellular networks on-board railway vehicles.

3.1.3. Spatially-based Analysis

This section describes a combination of hypothesis testing and spatial segmentation (small chunks). To start with, let us assume composite hypothesis in principle consists of 3-ary hypotheses. Let us also assume the observation set is denoted with Ω, where X variable belongs to. Variable X is chosen to be a link quality parameter, i.e., Reference Signal Received Quality (RSRQ) in LTE and Energy-per-Chip-over-Noise Ratio (EcN0) in UMTS. In this case, the task of hypothesis testing is to find a 3-ary valued decision function $d(x) \in \{0, 1, 2\}$, where a decision rule is a partition of Ω into three disjoint regions $\Omega_0, \Omega_1, \Omega_2$ such that

$$d(x) = i \text{ if } x \in \Omega_i. \tag{3.12}$$

Let each observation set be defined with $\Omega_0 = (-30, -14)$, $\Omega_1 = [-14, -7)$, and $\Omega_2 = [-7, 0]$. Further, this problem reformulates as a one-sample problem with hypothesis that utilizes the *sign test*. Each hypothesis is constructed on observations gathered during equal-sized chunks of $a = 1$km denoted with $s = S_1, S_2, ..., S_A$. Fig. 3.2 illustrates the general problem. Based on this, the evaluation of observations with CQIs takes into account chunks according to a hypothesis decision. This way, each hypothesis detects chunks with best $\sim \Omega_2$, moderate $\sim \Omega_1$ and worst $\sim \Omega_0$ link quality. Nonparametric sign test is applied to detect various link quality to each chunk

$$\ddot{\mathcal{I}}_{0,S_1} : \mathbb{M}\{X_{1,S_1}(x)\} \not> \rho_1 \quad \ddot{\mathcal{I}}_{1,S_1} : \mathbb{M}\{X_{1,S_1}(x)\} > \rho_1 \tag{3.13a}$$

$$\ddot{\mathcal{I}}_{0,S_2} : \mathbb{M}\{X_{1,S_2}(x)\} \not> \rho_1 \quad \ddot{\mathcal{I}}_{1,S_2} : \mathbb{M}\{X_{1,S_2}(x)\} > \rho_1 \tag{3.13b}$$

$$\vdots$$

$$\ddot{\mathcal{I}}_{0,S_A} : \mathbb{M}\{X_{1,S_A}(x)\} \not> \rho_1 \quad \ddot{\mathcal{I}}_{1,S_A} : \mathbb{M}\{X_{1,S_A}(x)\} > \rho_1 \tag{3.13c}$$

where X_{1,S_a} is the observed data of *active* AFR-free user (used as reference) over a chunk where $a \in 1, 2, ..., A$ and $\rho_1 = -7$ dB represents the hypothesized median. The procedure follows

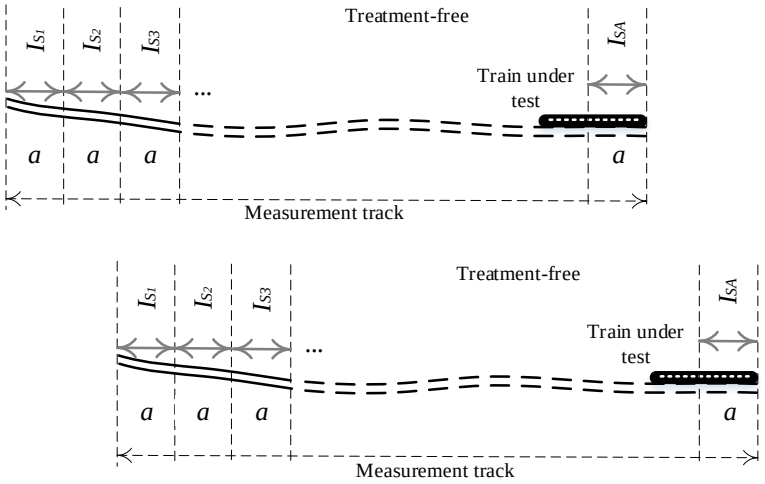

Figure 3.2.: Illustration of spatially-based assessment.

sequentially by selecting those $\ddot{\mathcal{I}}_{0,S_a}$s being in force. This implies the construction of binary hypothesis which formulates as

$$\ddot{\mathcal{I}}_{0,S_1} : \mathbb{M}\{X_{1,S_1}(x)\} \not> \rho_2 \quad \ddot{\mathcal{I}}_{1,S_1} : \mathbb{M}\{X_{1,S_1}(x)\} > \rho_2 \tag{3.14a}$$

$$\ddot{\mathcal{I}}_{0,S_2} : \mathbb{M}\{X_{1,S_2}(x)\} \not> \rho_2 \quad \ddot{\mathcal{I}}_{1,S_2} : \mathbb{M}\{X_{1,S_2}(x)\} > \rho_2 \tag{3.14b}$$

$$\vdots$$

$$\ddot{\mathcal{I}}_{0,S_P} : \mathbb{M}\{X_{1,S_P}(x)\} \not> \rho_2 \quad \ddot{\mathcal{I}}_{1,S_P} : \mathbb{M}\{X_{1,S_P}(x)\} > \rho_2 \tag{3.14c}$$

where $\rho_2 = -14\,\text{dB}$ is the next hypothesized median, X_{1,S_p} denotes the observed data of AFR-free user, where $p \in 1, 2, ..., P$, $P \leq A$, and $P, A \in \mathbb{N}$. Finally, the remaining chunks represent the poor link quality chunks. The same approach is applied for both technologies LTE $800/2600\,\text{MHz}$ and UMTS $2100\,\text{MHz}$.

3.1.4. Temporally-based Analysis

Modelling of statistical significance among use cases requires formulation of simultaneous two-sample hypothesis testing. Therefore, various use cases on-board allow to conduct the significance testing in uniform time interval. An exemplary situation is depicted in Fig. 3.3 which corresponds to comparing a AFR-aided user to a AFR-free user. Although the measurement equipment offer steady continuity of data in time, yet the variability of velocity sacrifices such a property in space. Here, the problem formulates with equal-sized time intervals with on top multiple hypothesis testing.

Let us assume a particular number of independent data sets denoted with l which correspond to the number of vehicular use cases, e.g., mobile users placed in different wagons. Provided a two-sample hypothesis, the problem allows to create $C_2(l)$ combinations without repetitions, based on $C_2(l) = \binom{l}{2}$. The multiple hypothesis formulates on each time interval $t = T_1, T_2, ..., T_Q$ as

$$\ddot{\mathcal{I}}_{0,T_1} : F_{X_{i,T_1}}(x) = F_{X_{j,T_1}}(x) \quad \ddot{\mathcal{I}}_{1,T_1} : F_{X_{i,T_1}}(x) \neq F_{X_{j,T_1}}(x) \tag{3.15a}$$

$$\ddot{\mathcal{I}}_{0,T_2} : F_{X_{i,T_2}}(x) = F_{X_{j,T_2}}(x) \quad \ddot{\mathcal{I}}_{1,T_2} : F_{X_{i,T_2}}(x) \neq F_{X_{j,T_2}}(x) \tag{3.15b}$$

$$\vdots$$

$$\ddot{\mathcal{I}}_{0,T_Q} : F_{X_{i,T_Q}}(x) = F_{X_{j,T_Q}}(x) \quad \ddot{\mathcal{I}}_{1,T_Q} : F_{X_{i,T_Q}}(x) \neq F_{X_{j,T_Q}}(x) \tag{3.15c}$$

where $F_{X_{i,T_q}}$ and $F_{X_{j,T_q}}$ represent CDF of two different use cases, $q = 1, 2, ..., Q$, and $i \neq j$. Each hypothesis produces particular p-value, $p_{T_1}, p_{T_2}, ..., p_{T_Q}$. Note that $Q \in \mathbb{N}$ corresponds to the number of hypotheses. In the following, adjustment of p-values allows to control the FDR. To this end, the model applies Benjamini-Hochberg (BH) procedure which initially arranges p-values in ascending order

$$p_{(1)} \leq p_{(2)} \leq ... \leq p_{(Q-1)} \leq p_{(Q)} \tag{3.16}$$

and then finds χ such that the following condition Eq. (3.17) is satisfied

$$p_{(\chi)} \leq \frac{\chi\alpha}{Q}, \tag{3.17}$$

where $\chi \in \mathbb{R}_+$ is the rank number obtained after arranging p-values. Then, for all $Q \leq \chi$, the respective null hypotheses are rejected.

3.1.5. Change Detection

This section addresses the problem of *change detection* to identify various data outage scenarios. The formulation is performed on top of intervals derived with aIB algorithm as demonstrated in Section 3.1.1. Differently, here the definition of the problem allows to focus on various number of m-intervals rather than limited on extreme cases.

Therein, let m be the number of intervals, i.e., number of quantization levels and n_u the sample size of each subset $\mathcal{S}_u$ where $\mathcal{S}_u \subseteq \mathcal{D}$. Subset $\mathcal{S}_u$ denotes the data set where its intervals are calculated by the algorithm. In other words, the aim is to detect a *changepoint* which occurs in time for a given data set of Reference Signal Received Power (RSRP) and Reference Signal Code Power (RSCP). In general, the approach applies on scenarios from the entire trajectory to smaller tracks. The aim of application is to serve in small tracks though, known that statistical properties do not change significantly. Next, on observations gathered along each track are formulated composite hypotheses

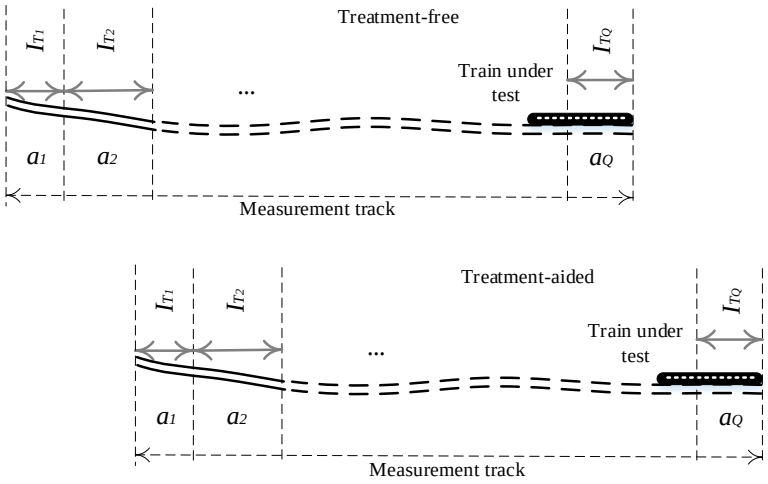

Figure 3.3.: Illustration of temporally-based assessment. The size of each chunk $a_1, a_2, ..., a_Q$ need not to be equal.

by following the logic of sliding window. Fig. 3.4 illustrates this problem. With this intention, non-parametric hypothesis with unpaired two-sample WMW tests applies on each subset $\mathcal{S}_u$ and formulates as below with null $\ddot{\mathcal{I}}_{0,u}$ and alternative $\ddot{\mathcal{I}}_{1,u}$ hypotheses

$$\ddot{\mathcal{I}}_{0,1}: \ F_{X_1}(x) = F_{Y_1}(x) \quad \ddot{\mathcal{I}}_{1,1}: \ F_{X_1}(x) \neq F_{Y_1}(x) \tag{3.18a}$$

$$\ddot{\mathcal{I}}_{0,2}: \ F_{X_2}(x) = F_{Y_2}(x) \quad \ddot{\mathcal{I}}_{1,2}: \ F_{X_2}(x) \neq F_{Y_2}(x) \tag{3.18b}$$

$$\vdots$$

$$\ddot{\mathcal{I}}_{0,h}: \ F_{X_h}(x) = F_{Y_h}(x) \quad \ddot{\mathcal{I}}_{1,h}: \ F_{X_h}(x) \neq F_{Y_h}(x) \tag{3.18c}$$

where $F_{X_u}(\cdot)$ and $F_{Y_u}(\cdot)$ are CDFs created from observed data $X_u \in \mathbb{R}^k$ and $Y_u \in \mathbb{R}^{u-k}$. The sliding window imposes $X_1 \subseteq X_2 \subseteq ... \subseteq X_h \subseteq \mathcal{S}_u$ to hold as illustrated in Fig. 3.4. In other words, X_1 contains measurement data from a starting time t_0 instance to another one t_k, whereas Y_1 contains measurement data from t_{u-k} to t_u and so on. Each hypothesis produces a unique p-value denoted as $p^{(u)}$ for a given significance level. Next, the changepoint detection problem is approached with definition of *effect size* parameter as

$$a^{(u)} = \frac{|Z|}{n_u}, \quad n_{X_1} \leq n_{X_2} \leq, ..., \leq n_{X_h}, \quad u = 1, 2, ..., h, \quad h \in \mathbb{N} \tag{3.19}$$

where $n_u = \sqrt{n_{X_u} + n_{Y_u}}$ and the relationship between $p^{(u)}$ and $a^{(u)}$ is $a^{(u)} \sim \frac{1}{p^{(u)}}$. This allows the detection of a change so the evidence against the null hypothesis is the strongest. Based on asymptotic normality of $p^{(u)}$, maximizing the quantity $a^{(u)}$ provides the largest effect of change

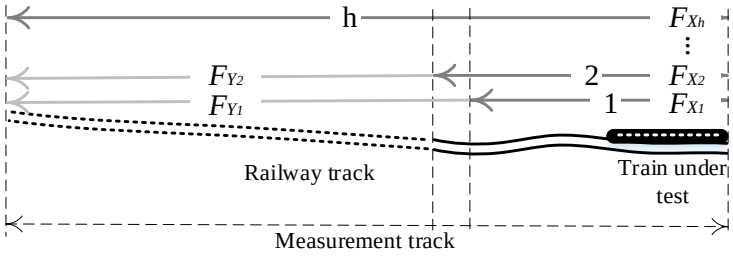

Figure 3.4.: Illustration of applied change detection on a selected track. ©2018 IEEE [26]

which corresponds to characterizing the changepoint detection. Indeed, the effect size does not describe the strength of the treatment, but rather identifies the presence or absence of a significant difference between samples X_u and Y_u [35, 69].

3.1.6. Vehicle Penetration Loss

The estimation of VPL imposes several aspects to consider. First, ideally it is required to estimate the difference of received power of a UE within a railway vehicle to a UE without a vehicle. However, this is not feasible in real-world conditions due to impracticability of walking large distances on foot. As trade-off it is decided to consider the measurement data collected along a rural environment while train is consistently moving. It is first assumed that in a given geographic region and travel direction the changes in the statistical properties of the observed received power within the region are of no statistical significance. This assumption explicitly comprises the difference in mobile network deployment between urban and rural environments. Further, it is also assumed that a rural environment is characterized with low number of unwanted multipaths. Next, under assumption that pathloss on rooftop antenna is lower than the pathloss inside the vehicle, this assumption is particularly stronger for the UE within the railway vehicle. This stems from the fact that outdoor UE is significantly more prone to multipaths than inside UE owing to high penetration loss. Second, in a perfect situation the VPL estimation requires the knowledge of transmitters' locations. The presented model assumes the locations are unknown. This assumption is reasonable considering Angle of Arrivals (AoAs) have random distribution. In this way, the characterization of VPL is possible. Despite this, even if the measurements within an anechoic chamber were possible, yet a full characterization would require a large space to set the vehicle under test, something which is unfeasible. Other solutions may lead to local characterization of VPL. As a solution were considered deterministic trajectories along which train measurements took place. Third, spatial filtering of received power may be limited due to measurement granularity of $f_s = 2\,\text{Hz}$ and high train velocity of 230 km/h.

Therefore, a narrowband signal is considered explicitly in low frequencies to avoid the increased error in VPL estimation. In a controlled environment VPL is defined as

$$\widehat{r} = 10\log_{10}\Big(\frac{P_{R_O}}{P_{R_I}}\Big)(dB) \tag{3.20}$$

where P_{R_O} and P_{R_I} are the received powers of a user without a vehicle and a user inside a vehicle, respectively. However, in an uncontrolled environment it is needed to consider all the aforementioned issues such as, mobility, estimation of RF signals, propagation conditions and so on.

In general, let us consider a volume denoted with $\mathbb{S}$ which characterizes a railway vehicle, i.e., its metallic structure and its windows. Further, let us consider a user placed outside volume $\mathbb{S}$ and another user placed inside this volume. Both users are characterized with estimated received powers denoted with $\widehat{P_{R_{O_\mathbb{S}}}}$ and $\widehat{P_{R_{I_\mathbb{S}}}}$, respectively. Transmission losses for both cases can be estimated as in the following

$$\widehat{L_{O_\mathbb{S}}} = -10\log_{10}\Big(\frac{\widehat{P_{R_{O_\mathbb{S}}}}}{\widehat{P_T}}\Big)(dB) \tag{3.21a}$$

$$\widehat{L_{I_\mathbb{S}}} = -10\log_{10}\Big(\frac{\widehat{P_{R_{I_\mathbb{S}}}}}{\widehat{P_T}}\Big)(dB) \tag{3.21b}$$

where $\widehat{P_T}$ denotes the transmitted power. To arrive at an equivalent representation, Eq. (3.21a) and Eq. (3.21b) are subtracted which implies an estimated difference defined as

$$\widehat{\Delta L} = \widehat{L_{O_\mathbb{S}}} - \widehat{L_{I_\mathbb{S}}} \tag{3.22}$$

The estimated difference $\widehat{\Delta L}$ is expected to be positive, $\widehat{\Delta L} > 0 \Leftrightarrow \widehat{L_{O_\mathbb{S}}} > \widehat{L_{I_\mathbb{S}}}$. This further implies that $\widehat{P_{O_\mathbb{S}}} > \widehat{P_{I_\mathbb{S}}}$ iff $\widehat{P_T}$ is the same for both scenarios.

In the presented system model, Eq. (3.20) is redefined and formulates the VPL estimation over $|\mathcal{J}|$ size of joint Cell IDs (CIDs) as

$$\widetilde{\Delta r} = \frac{1}{\hat{N}}\sum_{c=c_1}^{c_n}\sum_{t=t_s}^{t_e}(\widehat{P_{R_{O_\mathbb{S}},s,t,\hat{\lambda}}} - \widehat{P_{R_{I_\mathbb{S}},s,t,\hat{\lambda}}}) \tag{3.23}$$

where $t_e - t_s$ is the elapsed time of both users at positions $O_\mathbb{S}$ and $I_\mathbb{S}$ being connected to a joint CID denoted with $c_i = \{c_1, c_2, ..., c_n\}$, where $n = |\mathcal{J}| \in \mathbb{N}$. $\widehat{P_{R_{O_\mathbb{S}},s,t,\hat{\lambda}}}$ and $\widehat{P_{R_{I_\mathbb{S}},s,t,\hat{\lambda}}}$ denote the narrowband received powers at positions $O_\mathbb{S}$ and $I_\mathbb{S}$, respectively, which are obtained after being filtered out over distance $\hat{\lambda}\,[\mathrm{m}]$. This filtering is needed to create large-scale fading components. The averaging is performed across the total number of observations denoted with $\hat{N}$. The joint CID is a component of the joint set $\mathcal{J}$, which is defined as

$$\mathcal{J} = \mathcal{C}_{O_\mathbb{S}} \cap \mathcal{C}_{I_\mathbb{S}} \tag{3.24}$$

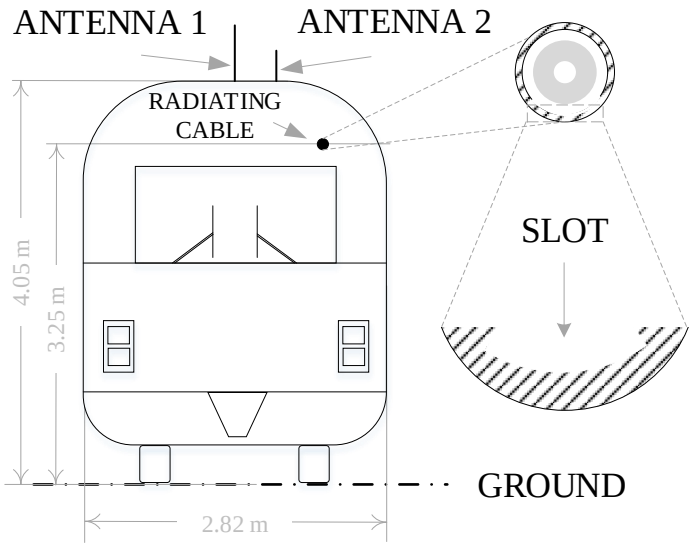

Figure 3.5.: Illustration of AFR-aided Railjet (RJ) train: Antenna 1 is a wideband rooftop antenna and antenna 2 is a multi-band antenna connected to the AFR.

where $\{c_1, c_2, ..., c_n\} \subseteq \mathcal{J}$, while $\mathcal{C}_{O_{\mathbb{S}}}$ and $\mathcal{C}_{I_{\mathbb{S}}}$ are respective sets of served CIDs. This way, the first sum operator characterizes the VPL based on the observations gathered over all joint CIDs given their random locations, while the second sum operator quantifies the observations during a particular amount of time. Nonetheless, the estimate $\widetilde{\Delta r}$ shall neither be directly compared to the isolation of the train nor to the penetration loss caused only by windows (further details are available in [70]).

3.2. Smartphone-based Measurement Setup

3.2.1. Amplify-and-Forward Repeaters

For in-train coverage extension, multi-band AFRs were installed on-board a RJ and a Cityjet (CJ) train. Their principle is described in the following: AFRs are equipped with digital filtering which allows them to operate as channel selective for LTE 800 MHz and 2600 MHz, Global System for Mobile Communications (GSM) 1800 MHz, and UMTS 2100 MHz. The AFR amplifies signal and noise in both uplink and downlink on each frequency band of aforementioned cellular technologies. The parameters of AFR are provided in Table 3.1. The output power P_{out} of AFR depends on input power P_{in} and the gain G. The amplifier operates in two regimes and this is explained as in the following: First, if the input power P_{in} is strong enough the amplifier exhibits nonlinear output-input

Tab. 3.1.: AFR parameters.

Parameter	Value
Noise figure N_F	5 dB
Downlink nominal gain $G_{n,D}$	60 dB (situative)
Downlink maximum output power $P_{max,D}$	25 dBm (situative)
Delay of band/channel selective	1.9 μs/6.2 μs
Number of subbands	maximum 16

behavior and after a specific range of P_{in} it enters a saturation regime. In this regime, the gain starts to decrease, $G \leq G_{n,D}$, and after a particular region it reaches $P_{out} = P_{max,D}$, and as a result P_{out} becomes independent from P_{in}. This regime is characterized with relationship $P_{max,D} < P_{in} + G$. Second, for low input powers the amplifier tends to retain the linear output-input behavior. In this regime, the gain is constant $G = G_{n,D}$ as long as it reaches the nonlinear regime. Therefore, for input powers that do not saturate the amplifier holds the relationship $P_{max,D} \geq P_{in} + G$ and equivalently holds the relationship $P_{out} = P_{in} + G$ as well. The gain strongly depends on the train type and therefore should be carefully configured. As a rule of thumb [66], the gain should be significantly lower than train isolation I to avoid feedback loops, thus $G \leq I - 15\,\text{dB}$.

RCs are connected to a single AFR which feeds them with the signals bundled via a multi-band antenna operating at frequencies $790 - 2700\,\text{MHz}$. Each RC was installed along the whole length of wagons to extend the coverage, while coaxial cables were used for inter-wagon connections (relevant only for a RJ train). The RCs are designed with slotted copper outer conductor with purpose to allow a controlled portion of the internal RF energy to be radiated in a limited area on-board the vehicle. The outer conductor material was made of overlapping copper foil with apertures (group of slots) that are bonded to the jacket as illustrated from RC's cross-sectional representation in Fig. 3.5. The slots are arranged in such a way the radiation direction to be orthogonal to the horizontal axis of RC deployment. This configuration allows the transmitted signal near the cable to couple into the slots and travel along the entire RC's length. Configuration details of AFR will be discussed in Section 3.2.5.

3.2.2. Measurement Track

Smartphone-based measurements were conducted with two trains: RJ and CJ trains [71, 72]. While RJ is an inter-city train that covers long-distances, CJ is an environmental-friendly regional train commuting between urban and sub-urban environments. Both trains were operating non-commercially including only the measurement stuff on-board. Fig. 3.7 illustrates the trains with pictures taken during measurements.

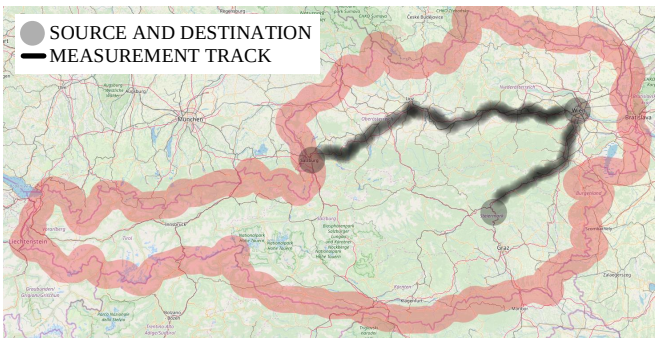

Fig. 3.6.: Measurement tracks under test: Vienna to Salzburg and Vienna to Bruck a.d. Mur.

The measurement campaigns were conducted along the track from Vienna to Salzburg and to Bruck a.d. Mur as highlighted in Fig. 3.6. The former covers a length of 312 km with RJ train commuting along the track, built mainly along rural environments as it is common for inter-city railways, while the latter covers a length of 158 km along which CJ train was tested. Along both railway tracks run operational trains which socially and economically impact the society in motion.

(a) Train type: RJ [71]. **(b)** Train type: CJ [72].

Fig. 3.7.: Railway vehicles under test.

3.2.3. Smartphone Placements

Fig. 3.9 presents two measurement designs of AFR-aided trains. The placements of UEs are denoted with $P_i = \{P_1, P_2, P_3, P_4\}$ to represent distinct vehicular use cases such as a AFR-free user denoted with P_1, AFR-aided users denoted with P_2 and P_3, and an outdoor user denoted with P_4, respectively. In Fig. 3.9a is shown a seven-wagon RJ train equipped with two AFR denoted with $AF = \{AF_1, AF_2\}$. The equipment of RJ with two AFRs ensures the extension of coverage to most of mobile users on-board and still retains the power decay function owing to the RC's length increase. Each AFR

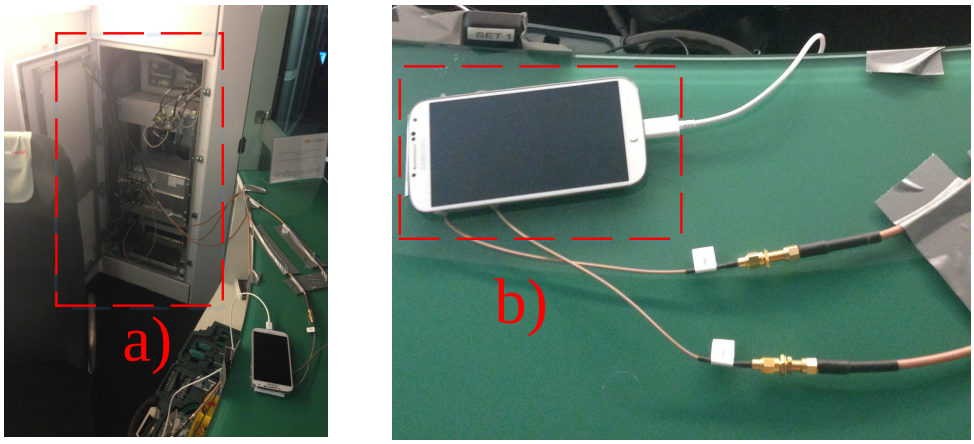

Figure 3.8.: Outdoor measurement setup: b) illustrates a samrtphone attached to a wideband rooftop antenna over the existing TCS a). ©2017 IEEE [26]

feeds two RCs in opposite direction as denoted with $\mathrm{RC} = \{\mathrm{RC}_{11}, \mathrm{RC}_{12}, \mathrm{RC}_{21}, \mathrm{RC}_{22}\}$. On one hand, for the purpose of understanding how much two UE attached to different AFRs benefit, users P_2 and P_3 were placed in similar propagation conditions. On the other hand, the user P_1 does not benefit from AF_2 by not being served from respective RC_{22}. In fact, the observations for this case are gathered from drive tests without AFR on-board.

Since the solution of perfectly neglecting the impact of the train itself is unfeasible, as a compromise a UE was connected to a rooftop wideband antenna operating at frequencies up to 6 GHz. This antenna was mounted[2] on the train roof. This way, this excludes the loss caused from the train wagon, but still considers the propagation effects between infrastructure and the user. Fig. 3.8 illustrates the outdoor measurement setup.

Fig. 3.9b illustrates a three-wagon CJ train. Here, the user placed at P_3 characterizes a user that is expected to benefit the most, while the other user placed at P_2 characterizes a user that is expected to gain less due to power decrease effect impacted from the length increase of the RC. Since CJ is shorter in length than RJ, only a single AFR and a single RC were installed in the middle wagon. Known that the effective surface of the windows of a CJ train is comparable to the overall metallic structure, Frequency Selective Surfaces (FSSs) for this type of train were not taken into consideration due to cost-effectiveness and weight design issues in Chapter 4.

[2]The UE's cover was dismounted to connect two ports of antennas via SMA cables to the existing Train Communication System (TCS). The TCS was intended for WiFi access on-board.

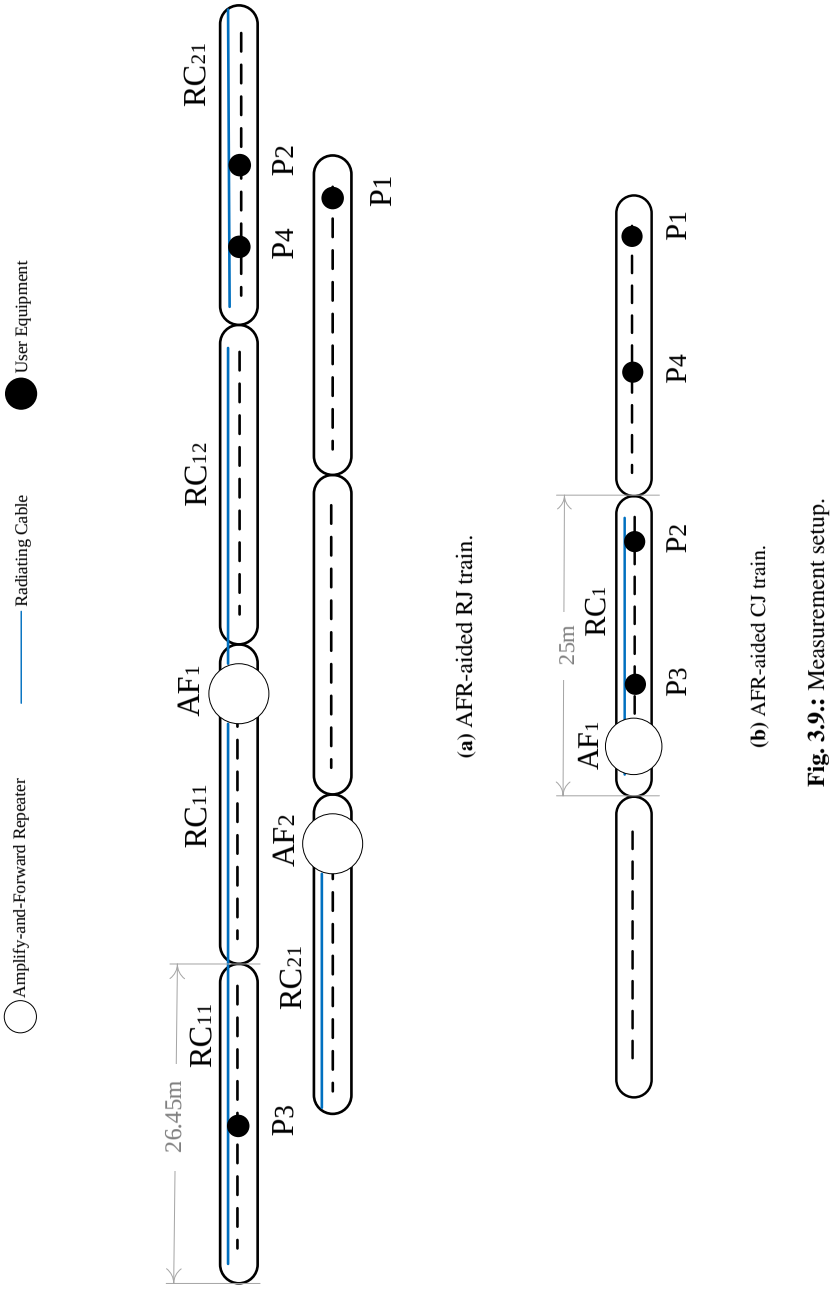

(a) AFR-aided RJ train.

(b) AFR-aided CJ train.

Fig. 3.9.: Measurement setup.

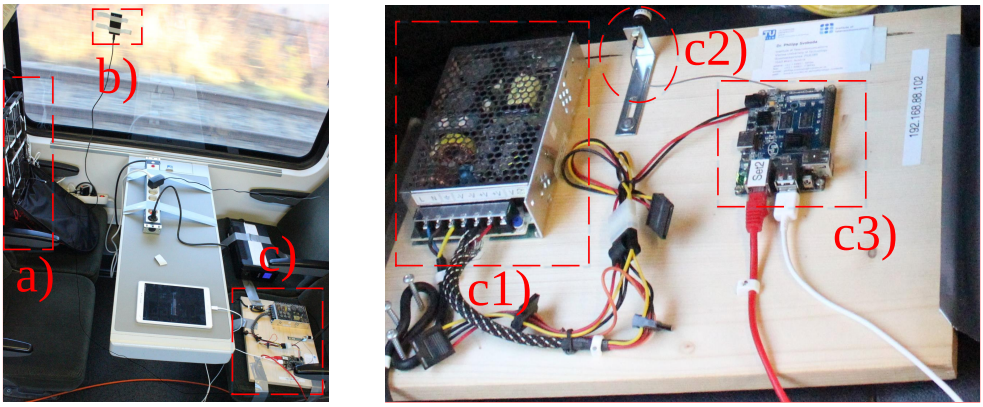

Figure 3.10.: Indoor measurement setup: a) represents the UE; b) represents a GPS antenna connected to one of the UE; c) illustrates the mini PC setup containing an attached antenna c2) to Banana Pi c3) and its power supply c1). ©2016 IEEE [67]

3.2.4. Smartphone Orientations and Relevant Entities

NEMO benchmarking system [73] was utilized to represent a UE on-board the train. Each UE was adjusted on vertical orientation tilted at roughly 90°. This way it represents a person holding a smartphone to his ear on voice mode or e.g., streaming a video on data mode. This adjustment characterizes the *non-handsfree* usage of end-users. In this manner, several UE with identical configuration were placed in different positions on-board as discussed in Section 3.2.3.

Fig. 3.10 demonstrates the indoor measurement setup. The entity depicted with c) shows an installed mini PC which was connected to a master tablet being able to transfer the monitoring window to a central PC. This PC connects all the smartphone placements located in different measurement points via Ethernet and was only used for monitoring purposes. The right hand side of Fig. 3.10 demonstrates the main table of mini PC together with an antenna and its own power supply. The power supplies were integrated into the measurement setup in case of power outage.

3.2.5. Measurement Configuration

The UE were configured with sequential tasks of voice and data as common end-user interactions that mimic *quasi-real* usage. UE operating in UMTS and LTE used the same script. Voice and data sessions were concomitant events carefully configured to approach a true usage scenario. Telephone calls, started at fixed time, were designed to phone a dedicated fixed automatic telephone system. Both voice sessions and data sessions were scripted. During data sessions, UE operating in UMTS and LTE transferred 10 MB File Transfer Protocol (FTP) data packets and downloaded 10 MB HyperText Transfer Protocol (HTTP) file from a webpage in each sequential session. Those sessions had

previously determined parameters for telephony (e.g. call duration and attempt) and data connection parameters (e.g. connection attempts and connection timeout).

3.3. Service Quality Improvements for Train Passengers

3.3.1. Coverage Analysis

Descriptive statistics are used to illustrate the behavior of AFRs and RCs in KPIs, RSSI, RSRP, and RSCP. Explicitly, empirical Quantile-Quantile (Q-Q) provide a graphical inspection to perform rigorous investigation on whether the probability distribution of X_i plausibly reproduces the underlying distribution of X_j. They particularly provide information on skewness, scale, and location. For this reason, empirical Q-Q are widely used during this thesis. In the experiments, the observed data X_i and X_j may come from different directions. Yet, they adhere to the same railway vehicle and railway track. For instance, data X_i represent the AFR-aided user's distribution, while data X_j represent the AFR-free user's distribution.

Figs. 3.11 and 3.12 show the AFR-aided user quantile - AFR-free user quantile in UMTS 2100, LTE 800, and LTE 2600. Each Q-Q consists of a 45° straight line $f(x) = x$ which is artificially graphed to simplify the graphical inspection. This is further named as *reference line*. Therefore, even if the points do not lie above the reference line but they are offset whose line is still parallel to the reference line, such linearity suggests that the data come from the same distribution and differ only in location.

Fig. 3.11 demonstrates the Q-Qs for the case of RJ train. From here it is obvious that AFR-aided distributions do not come from the same distribution as AFR-free. The points follow a strongly nonlinear behavior and this is valid for all parameters, RSCP, RSSI, and RSRP. This behavior suggests that there is difference in variance and particularly skewness. Indeed, both AFR-aided users follow the same behavior, which is impacted from users P_2 and P_3 being located under very similar conditions. Therefore, AFR-aided users P_2 and P_3 outperform the AFR-free user P_1 with 17 dB difference in mean in both UTRA RSSI and RSCP UMTS 2100. Significant improvement of $8 - 15$ dB is observed in E-UTRA RSSI and RSRP in both LTE 800 and LTE 2600 as well. Table 3.2 shows the details about mean, median, variance and skewness.

Fig. 3.12 illustrates the AFR-aided user quantile - AFR-free user quantile in UMTS 2100, LTE 800, and LTE 2600, all being subject to a CJ train. From here it is similarly obvious that AFR-aided distributions mainly do not come from the same distribution as AFR-free. Likewise, the points follow a nonlinear behavior and this is particularly valid for all parameters in LTE 800 and LTE 2600. This can also be verified from skewness shown in Table 3.2. Overall, the AFR-aided users P_3 and P_2 outperform the AFR-free user P_1 with 20 dB difference in mean in UMTS 2100 RSCP and UTRA RSSI as well as 17 dB in LTE 800 RSRP and E-UTRA RSSI. LTE 2600 shows even

Tab. 3.2.: Descriptive statistics: sample mean, median, variance and skewness are denoted with $\mathbb{E}(\cdot)$, $\mathbb{M}(\cdot)$, $\mathbb{V}(\cdot)$ and $\mathbb{S}(\cdot)$, respectively.

	LTE 800						LTE 2600						UMTS 2100					
	E-UTRA RSSI			RSRP			E-UTRA RSSI			RSRP			UTRA RSSI			RSCP		
	$\{X_1\}$	$\{X_2\}$	$\{X_3\}$	$\{X_1\}$	$\{X_2\}$	$\{X_3\}$	$\{X_1\}$	$\{X_2\}$	$\{X_3\}$	$\{X_1\}$	$\{X_2\}$	$\{X_3\}$	$\{X_1\}$	$\{X_2\}$	$\{X_3\}$	$\{X_1\}$	$\{X_2\}$	$\{X_3\}$
AF repeater-aided Railjet																		
$\mathbb{E}(\cdot)$	-75	-60.2	-62.7	-106.3	-91.3	-93.4	-73	-60.5	-65.2	-101.7	-89.6	-94	-80.9	-63.8	-63.9	-89.2	-72.2	-72.1
$\mathbb{M}(\cdot)$	-74.2	-56.6	-61.8	-106.5	-87.4	-92.3	-72	-59.6	-64.1	-101.1	-88.3	-92.5	-81.8	-61.1	-60.7	-90.3	-69.5	-69
$\mathbb{V}(\cdot)$	79.4	113.9	59.9	123	165	94.2	112.6	32.1	36.3	130.6	42	49.9	114.4	94.9	97.9	155.9	138.4	136
$\mathbb{S}(\cdot)$	0.2	-0.9	-0.9	0.1	-0.8	-0.9	0	-1.3	-1.2	0	-1	-1.3	0.2	-1.3	-1.2	0.2	-0.9	-1
AF repeater-aided Cityjet																		
$\mathbb{E}(\cdot)$	-68.5	-56.9	-51.7	-98.5	-87.1	-81.2	-68.3	-53.9	-47.7	-97.9	-83.5	-76.4	-73.7	-58.7	-52.6	-84.4	-69.2	-63.1
$\mathbb{M}(\cdot)$	-69	-54.8	-49.1	-100.9	-84.3	-79.1	-67.3	-53.3	-44.9	-97.1	-83.1	-73.7	-72.8	-57.1	-50.3	-83.7	-67.7	-61.4
$\mathbb{V}(\cdot)$	120	117.6	125.6	148.6	142	146	53.5	21.8	89.8	69.5	31.6	108.1	91.2	54.5	90.1	118.1	80.9	122.2
$\mathbb{S}(\cdot)$	0.2	-0.7	-0.9	0.1	-1	-1.1	-0.3	-1.8	-2.3	-0.4	-1.1	-2	-0.6	-1.8	-1.6	-0.2	-0.5	-1.2

more improvement, however, this frequency is typical for urban environments which is quite bursty overall.

Overall, an AFR is a device with nonlinear behavior because there is a maximum output power level due to RF circuit constraints and power transmission limits.

3.3.2. Achievable Throughput

Indeed, railway environments pose a big challenge to performance of mobile users inside a HST. Consequently, this strongly impacts achievable throughput. The model distinguishes between two key limiting factors: (1) the achievable throughput are limited by poor coverage over distances of several hundred kilometers, (2) the achievable throughput are limited due to several tens of VPL. In this regard, it is feasible to investigate the differences in achievable throughput [bit/s] for an AFR-free user compared to an outdoor environment. This approach enables to take into account both factors in estimating this difference which corresponds to the loss in throughput. The achievable throughput is estimated during FTP and HTTP sessions in LTE and UMTS.

It is observed that the maximum loss in achievable throughput evaluated with Empirical Cumulative Distribution Function (ECDF) ranges to 5 Mbit/s and 24 Mbit/s in UMTS and LTE, respectively. It is also observed that during Multiple-Input Multiple-Output (MIMO) transmission, outdoor user outperforms the AFR-free user with 20% in Physical Downlink Shared Channel (PDSCH) bit rates for both codewords 0 and 1. To this end, the achievable throughput by a user connected to the outdoor rooftop antenna shows that there is room for improvement for the indoor telecommunication services.

The solution is a system composed of rooftop mounted antennas, AFRs, and RCs. A single omnidirectional antenna is used as donor antenna for the AFR, i.e., a Single-Input Single-Output (SISO) system. This fundamentally influences the MIMO achievable throughput for HST services though. Yet, it significantly improves the achievable throughput in low regime, as demonstrated in Fig. 3.13.

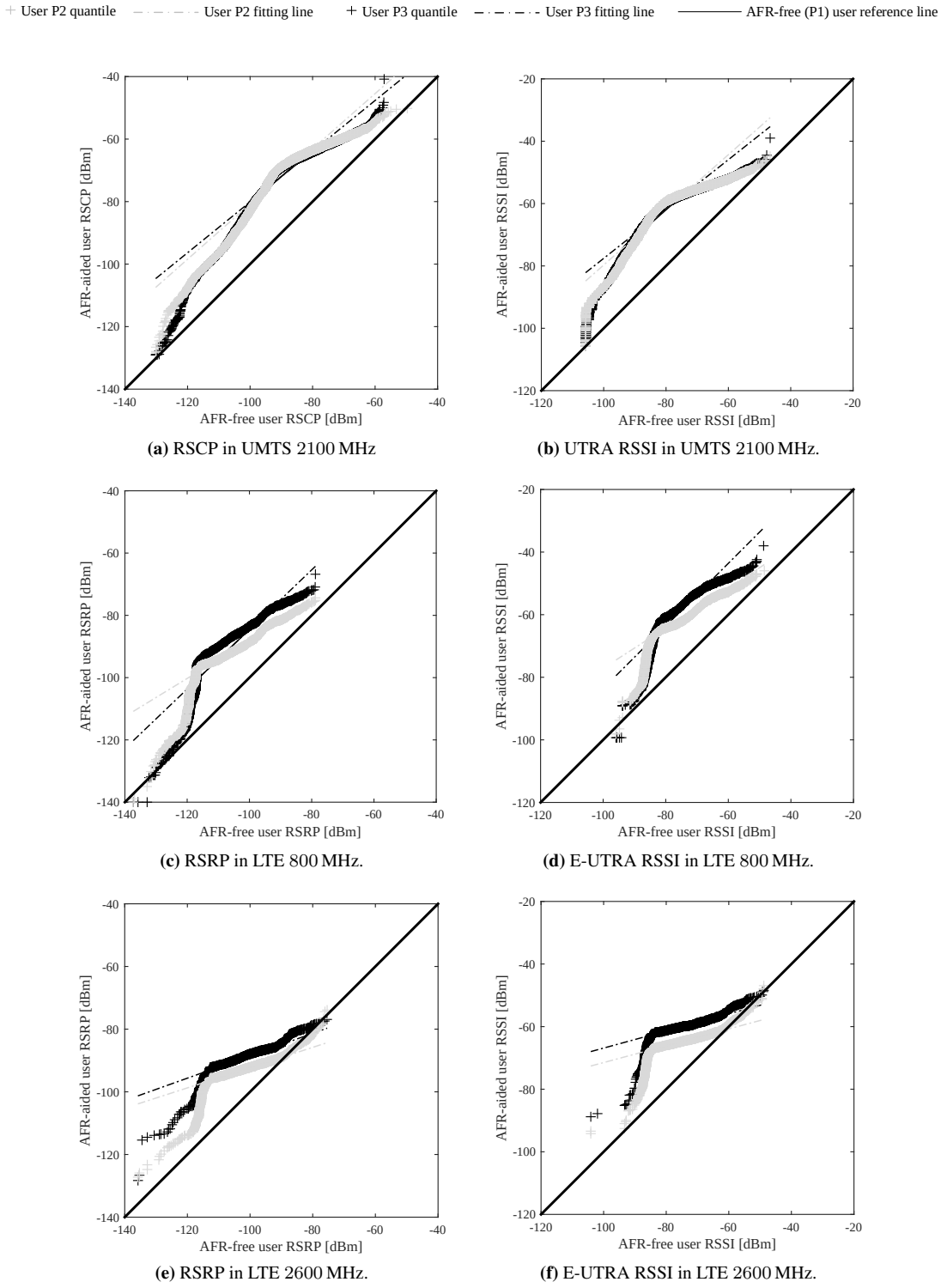

(a) RSCP in UMTS 2100 MHz

(b) UTRA RSSI in UMTS 2100 MHz.

(c) RSRP in LTE 800 MHz.

(d) E-UTRA RSSI in LTE 800 MHz.

(e) RSRP in LTE 2600 MHz.

(f) E-UTRA RSSI in LTE 2600 MHz.

Fig. 3.11.: AFR-aided user quantile - AFR-free user quantile: RJ train case study.

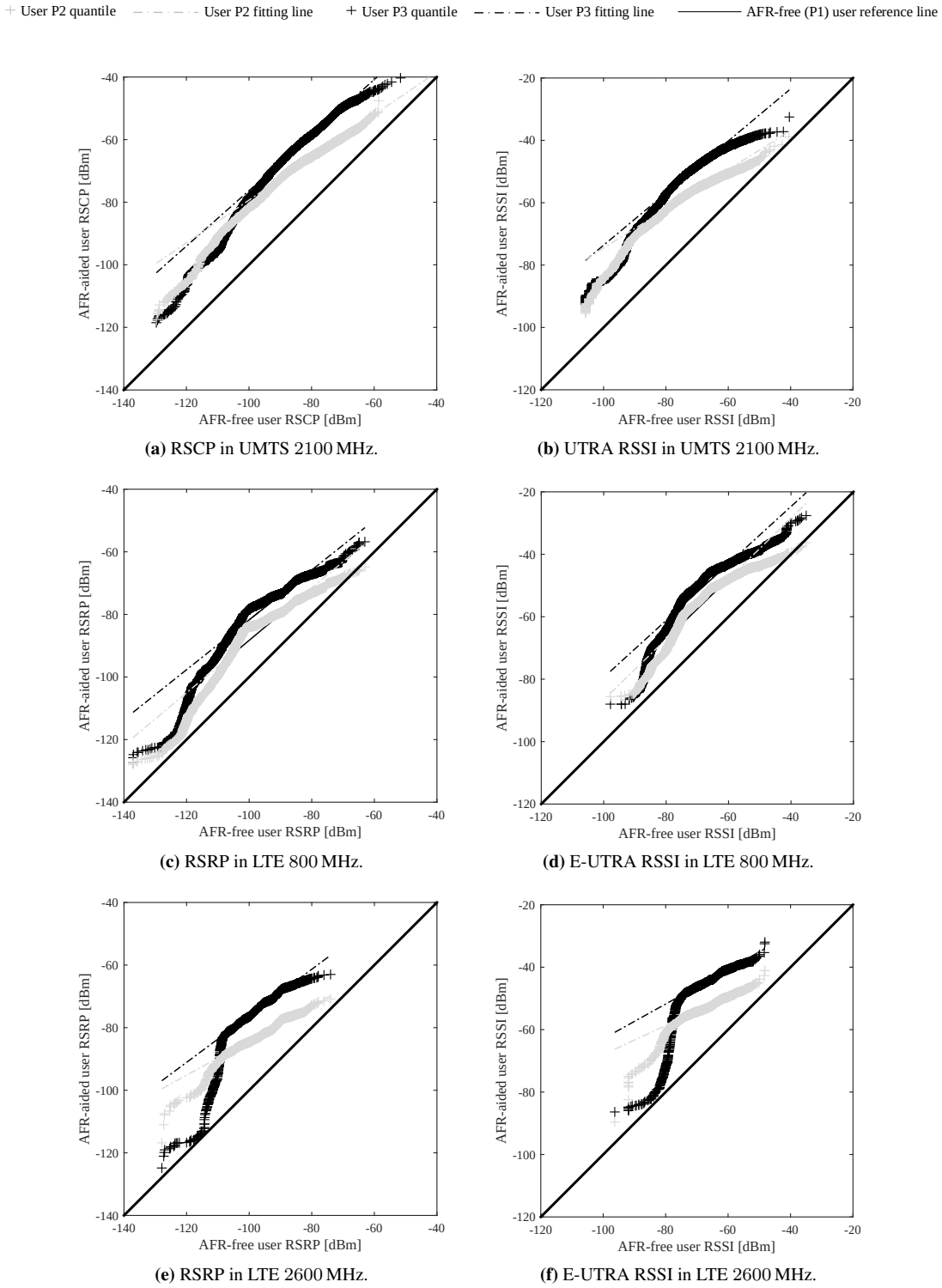

(a) RSCP in UMTS 2100 MHz.

(b) UTRA RSSI in UMTS 2100 MHz.

(c) RSRP in LTE 800 MHz.

(d) E-UTRA RSSI in LTE 800 MHz.

(e) RSRP in LTE 2600 MHz.

(f) E-UTRA RSSI in LTE 2600 MHz.

Fig. 3.12.: AFR-aided user quantile - AFR-free user quantile: CJ train case study.

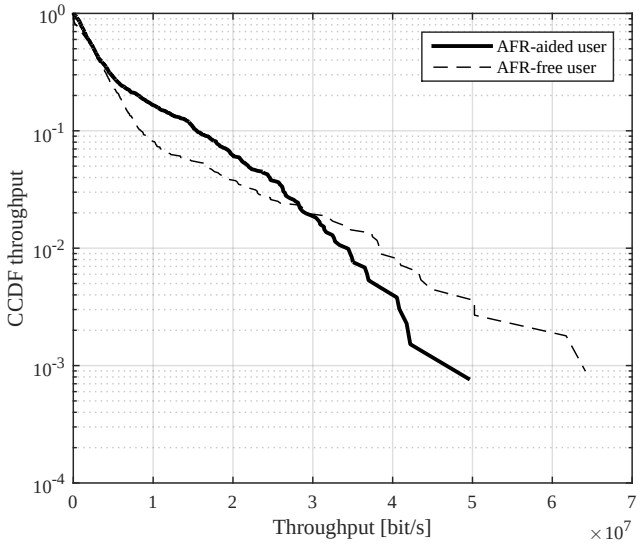

Figure 3.13.: Illustration of improvement in low regime of achievable throughput in LTE : AFR-aided RJ train case study.

The Complementary Cumulative Distribution Function (CCDF) achievable throughput shows that the AFR-aided user outperforms the AFR-free user in the achievable throughput range as far as it reaches 30 Mbit/s. Above this value, the CCDF achievable throughput of AFR-aided user slightly deteriorates, because the AFR improves signal levels only and limits the diversity order of the propagation channel to the number of rooftop donor antennas connected to the AFR. Nevertheless, this solution is still efficient particularly on poor coverage conditions which strongly characterize the railway environments.

3.4. Service Quality Assessment

3.4.1. Trip-based Analysis

This section demonstrates and discusses the assessment improvements and impairments of KPIs as explained and presented in Section 3.1.2. The trip-based assessment enables the assessment of true improvements, as it contains the data collected during the entire track under test. In other words, the developed procedure assesses *overall* improvements on mobile users impacted from AFRs and RCs in real-world conditions. Table 3.3 provides the rejection ratios denoted with $\tau_{i,j}$ at type I error $\alpha = 0.05$. This is denoted with *overall* to represent the entire railway track. The purpose of applying bootstrap is to mimic the realizations of experiments in order to avoid the problem of small-scale measurements. For this reason, it was chosen a high M number of hypotheses with each

bootstrap distribution represented with comparable sub-sample size to the original sample size. The obtained results are discussed in the following and are subject to particular train configurations and user placements.

AFR-aided RJ - This train configuration adheres to the details illustrated in Fig. 3.9a. Herein, the assessment exhibits significant improvement in LTE and UMTS when a RJ train is equipped with two AFRs. This is particularly valid for parameters E-UTRA RSSI, UTRA RSSI, RSRP and RSCP. Furthermore, such result impacts directly the uplink direction as well. The procedure combined with multiple hypothesis results in uplink improvement for AFRs-aided users that significantly transmit less power. This mainly comes due to substantial higher received power of AFR-aided users P_2 and P_3 compared to AFR-free user P_1. However, no improvement is observed in signal quality, i.e., RSRQ and EcN0. This is likely to be a consequence of AFR-aided user being located 35 m apart from the AFR as well as the group-delay problem. Despite this result, the service quality improvement is approached differently later on to verify this problem statistically.

AFR-aided CJ - This train configuration adheres to the details illustrated in Fig. 3.9b. The CJ train equipped with a single AFR is the most convenient in terms of overall improvements in KPIs under investigation. The assessed improvement is again valid for parameters E-UTRA RSSI, UTRA RSSI, RSRP and RSCP. However, on contrary to the AFR-aided RJ case, here the signal quality shows improvement in both LTE and UMTS. The assessed improvement in RSRQ and EcN0 is particularly true for the pair of users (X_3, X_1) which mainly comes from the fact of the AFR-aided user being located in proximity of AFR. Therefore, the closer to the AFR, the higher the signal quality. On the other hand, in all cases holds the relationship $\tau_{X_3,X_1} \geq \tau_{X_3,X_2}$ which stems from the fact of AFR-aided user P_3 being closer than AFR-aided user P_2 in relation to AFR. The result indicates the effect of AFR-aided users under the same RC being served in different conditions. Moreover, such an indication is in agreement with Section 3.4.3 which revels the position-dependence effect. Despite this, no direct pairing between both approaches shall be established. The trend of rejection ratios to the remaining KPIs are followed as in the case of AFR-aided RJ.

3.4.2. Outage-based Analysis

In this section, the focus of assessment is on service quality improvements in terms of distinct scenarios. Herein, the procedure applies the classification of distinct scenarios by using aIB algorithm as elaborated in Section 3.1.1. This classification is therefore named as: *best*- and *worst* scenario. The best scenario is characterized with highest received power of AFR-free user in terms of RSSI, whereas the worst scenario is characterized with the lowest received power as defined in Eq. (3.2) and Eq. (3.3). The number of m-intervals is arbitrarily set to eight and this number does not depend on the train configuration. Fig. 3.14 illustrates this.

The developed procedure constructs $M = 10^4$ binary hypotheses to consider M number of bootstrap distributions to each scenario. Each hypothesis is performed under the assumption of asymptotic normality of p-values at type I error $\alpha = 0.05$. Depending on the scenario, the sub-sample n_s of each bootstrap distribution is chosen to mimic short-time experiments, e.g., a voice call, a file-transferring session, a webpage downloading session. To mimic M number of voice calls, we set the sample size $n_s = 240$ which corresponds to testing $2\,\mathrm{min}$ voice call duration. While the sub-sample size for voice is kept the same over technologies and scenarios, for data sessions various sub-sample sizes are applied as provided in Table 3.3. Afterwards, the rejection ratio is calculated based on the adjusted p-values with BH procedure. Known that the target of the developed procedure aims to assess improvements in terms of KPIs, for this reason it is built upon multiple unpaired binary hypothesis consisting of an AFR-free user P_1 and an AFR-aided user P_2 or P_3. Since it is expected that AFR-aided users to gain in received power, signal quality levels, as well as transmit power, it makes more sense to apply either right or left directional hypothesis than non-directional testing, correspondingly. In Table 3.3 are shown rejection rates $\tau_{i,j}$ derived from multiple hypotheses over both train configurations considering the pair of users (i, j). The obtained results are discussed in the following and are subject to the train configurations and user placements.

AFR-aided RJ - As expected, the obtained rejection ratios strongly support the hypothesis that AFRs improve the coverage. This is valid for both cases under investigation best and worst, both technologies LTE 800/2600 and UMTS 2100, as well as voice and data sessions. The rejection ratios quantify this improvement in E-UTRA RSSI and UTRA RSSI at $\tau_{X_3,X_1} \approx \tau_{X_2,X_1} \approx 1$. The assessment of transmit power also shows similar behavior in most of the scenarios. On the other hand, the assessment of RSRQ does not support the hypothesis that for best scenario the AFRs-aided users experience better service quality than the AFR-free user. On contrary, the assessment of EcN0 strongly supports the hypothesis that for worst scenario both AFR-aided users experience improvement. This holds in UMTS 2100 and is in compromise with findings in Section 3.4.5, although no direct pairing between two approaches shall be established.

AFR-aided CJ - The obtained rejection ratios fully support the hypothesis of coverage improvement in RSSI, RSRP, and RSCP. This is true for both voice calls and data sessions at rejection ratios $\tau_{X_3,X_1} = \tau_{X_2,X_1} = 1$. Indeed, transmit power is directly impacted as well due to higher received power for AFR-aided users than for AFR-free user. On the other hand, the rejection ratios suggest that there is improvement in signal quality in LTE 800/2600 and UMTS 2100 AFR-aided user P_3 in worst scenario, yet such improvement is not noticed for AFR-aided user P_2 in best scenario. All things considered, the closer to the AFR the better signal quality is observed.

The developed assessment procedure reveals its strong property of detecting changes in coverage parameters. Yet, the service quality parameters such as RSRQ and EcN0 do not support such property as consistently as for coverage parameters. This accounts for the problem of detecting weak changes in decibels ranging from $1 - 2\,\mathrm{dB}$. Therefore, a different approach of assessment is required.

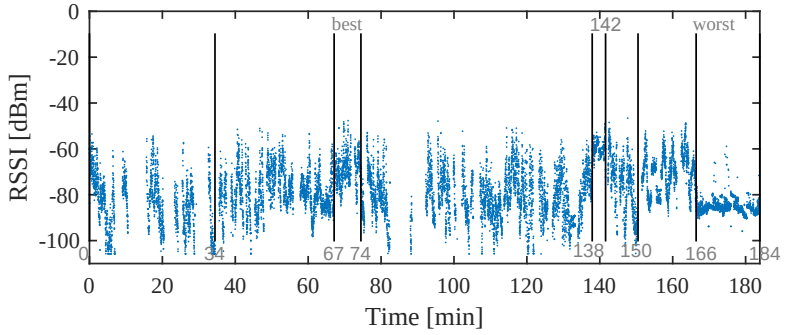

(a) Case study: RJ train

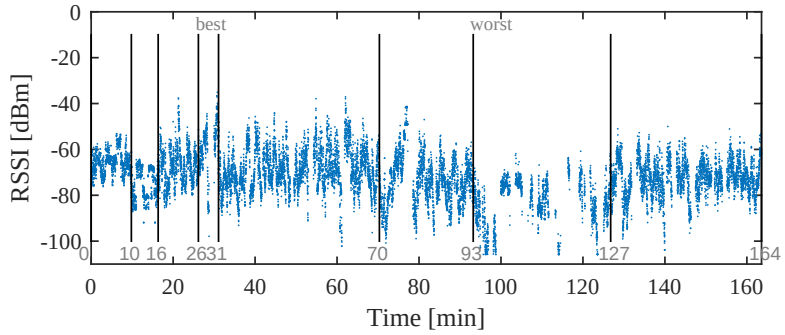

(b) Case study: CJ train

Fig. 3.14.: Illustration of outage-based assessment with RSSI. Vertical black lines represent intervals obtained with aIB. Note that the data contain UMTS as well as LTE connections on served cells.

Tab. 3.3.: Rejection ratios obtained from significance probability with adjustment at type I error $\alpha = 0.05$ and the number of hypotheses $M = 10^4$. The rejection ratio is denoted with $\tau_{i,j}$ which stands for pair of the users (i, j). While for voice the sub-sample size is kept the same over technologies and scenarios, to mimic the data sessions the following sub-sample sizes are applied: $n_{s,best}^{(UMTS)} = 75$, $n_{s,best}^{(LTE)} = 35$, $n_{s,worst}^{(UMTS)} = 320$, $n_{s,worst}^{(LTE)} = 160$.

	LTE 800/2600								UMTS 2100							
	E-UTRA RSSI		RSRP		RSRQ		T_x		UTRA RSSI		RSCP		E_c/N_0		T_x	
	τ_{X_2,X_1}	τ_{X_3,X_1}	τ_{X_2,X_1}	τ_{X_3,X_1}	τ_{X_2,X_1}	τ_{X_3,X_1}	τ_{X_2,X_1}	τ_{X_3,X_1}	τ_{X_2,X_1}	τ_{X_3,X_1}	τ_{X_2,X_1}	τ_{X_3,X_1}	τ_{X_2,X_1}	τ_{X_3,X_1}	τ_{X_2,X_1}	τ_{X_3,X_1}
AF repeater-aided Railjet																
best (voice)	1	1	1	0.99	0	0	1	0.74	1	1	1	1	0	10^{-4}	1	1
best (data)	0.99	0.83	0.98	0.36	0	0	0.91	0.01	1	1	1	1	0	0	0.91	1
worst (voice)	1	1	1	1	0	0	1	1	1	1	1	1	0.74	0.67	1	1
worst (data)	1	1	1	1	0	0	0.99	1	1	1	1	1	0.84	0.81	1	1
overall	1	1	1	1	0	0	1	1	1	1	1	1	0	0	1	1
AF repeater-aided Cityjet																
best (voice)	1	1	1	1	0	0	1	1	1	1	1	1	0	0	1	1
best (data)	1	1	1	1	0	0	1	1	1	1	1	1	0	0	0.99	1
worst (voice)	1	1	1	1	0	0.65	1	1	1	1	1	1	0.1	0.66	1	1
worst (data)	1	1	1	1	0	0.45	1	1	1	1	1	1	0.19	0.78	1	1
overall	1	1	1	1	0	1	1	1	1	1	1	1	0	1	1	1

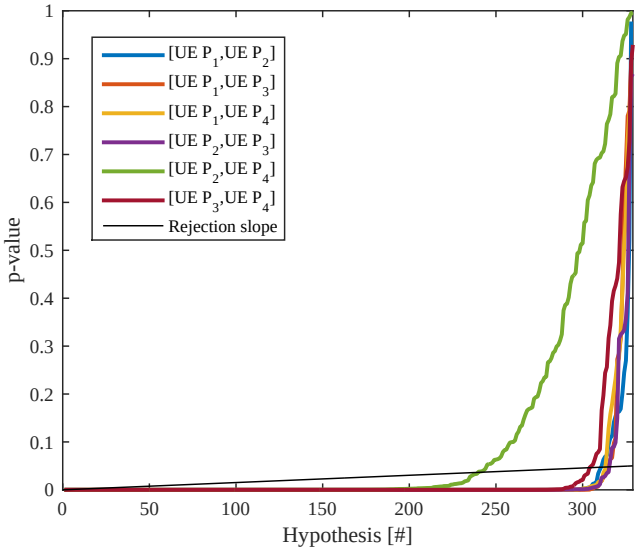

Figure 3.15.: Illustration of rejection ratio τ with temporally-based assessment: CJ train case study. ©2018 IEEE [26]

3.4.3. Temporally-based Analysis

The developed temporally-based assessment allows to detect the impact of AFR on-board the train evaluated within an arbitrarily time interval. This time interval was chosen to be 30 s, which ensures to detect a change within, e.g., a short duration of a file transfer, webpage download, or a short voice call. Combined with multiple hypothesis testing, the technique produces a quantity which is expressed with rejection ratio τ_{X_i,X_j}. The problem targets the change detection in RSRP/RSCP to all vehicular use cases on-board the train , i.e., $\{i \neq j : \forall i, j \in \mathbb{R}_+\}$. For this reason, it was decided to establish two-sample testing of sample distributions X_{i,T_q} and X_{j,T_q}. Provided four mobile users represent distinct vehicular use cases, the problem involves $C_2(4) = 6$ pairs of combinations without repetitions.

Fig. 3.15 shows the ordered p-values in terms of multiple hypotheses as explained in Section 3.1.4. The lowest $\tau_{X_2,X_4} = 0.72$ is obtained for the pair of users (X_2, X_4) which is then followed by other pairs of users with obtained rejection ratios of $\tau_{X_i,X_j} \geq 0.92$. This result suggests that AFR-aided user which is located in the end of the RC (P_2) will experience data outages such that it is significantly less different to a mobile user outside the train (P_4) compared to any other combination of use cases. Another crucial issue for the case of CJ train is the isolation. The RF gain of the AFR must not exceed the lowest isolation on-board in any train configuration. This implicates two aspects as in the following: On one hand, this severely limits the range of possible gains of AFR. On the other hand, a high gain of the AFR allows for a CJ solution with only a single AFR on-board.

3.4.4. Change Detection

Change detection is a pivotal factor that aims to serve as benchmarking baseline for infrastructure deployments. The overall procedure is subject to aIB algorithm which enables the classification of data outage scenarios. Despite this, the target of this section is to investigate different approaches of change detection techniques rather than to perform an investigation on whether the obtained time-intervals with aIB approximate to the output of the developed change detection technique. Because of this, it was decided to observe the output of the developed change detection technique as illustrated in Section 3.1.5. For comparison reasons, the evaluation considers the change detection approached with Logistic Function (LF) as well. Therefore, the approach presented in [74, 75] is used here as reference.

The Generalized Logistic Function (gLF) defined in Eq. (2.50) was utilized to derive a restricted sigmoid function $\mathcal{L}(t)$ as a special case which was used to detect a change. According to the procedure in [74, 75], parameters of $\mathcal{L}(t)$, (d_1, d_2, x_0), were fitted by generating uniformly distributed mid-point values x_0 where each of them is used to perform a unique run. This was carried out to avoid the risk of becoming stuck at local minima while using non-linear least-squares regression. Yet, another quantity named *changepoint coefficient* was formulated to determine the candidate number of regressions.

Fig. 3.16 illustrates the obtained results for distinct vehicular use cases as well as arbitrary number of m-intervals. On one hand, the developed nonparametric approach shows the global maxima on each time interval specified with a unique m. On the other hand, the sigmoid regressions with the highest number of regressions converge to a particular time value within the specified interval with a unique m. The overall evaluation indicates that the developed change detection technique tends to converge to the regressions obtained according to the changepoint coefficient definition. Therefore, the developed change detection technique aims to serve as a benchamarking baseline to mobile operators with purpose of detecting the performance improvements as well as detecting the scarcity of infrastructure deployments along a railway track.

3.4.5. Channel Quality Analysis

CQI is a vital parameter to estimate the performance of mobile users in operational networks. As such, they disregard the necessity of cell load information or infrastructure location which are unknown in this context. To answer the unanswered questions from Section 3.4.2, this section demonstrates the proposed assessment approach explained in Section 3.1.3 and proves its applicability on real-world conditions. As it was stressed, identifying and understanding the mobile user benefits and possible (dis)advantages of the AFR-aided RJ train with respect to signal quality is not a straightforward task. The developed assessment techniques are not so sensitive to be able to detect weak changes in the order of $1 - 2\,\mathrm{dB}$. Thus, a well-built micro-analysis of the entire track is necessary. In this section, the discussion focuses on CQIs for AFR-aided- and AFR-free user on-board the RJ train. The

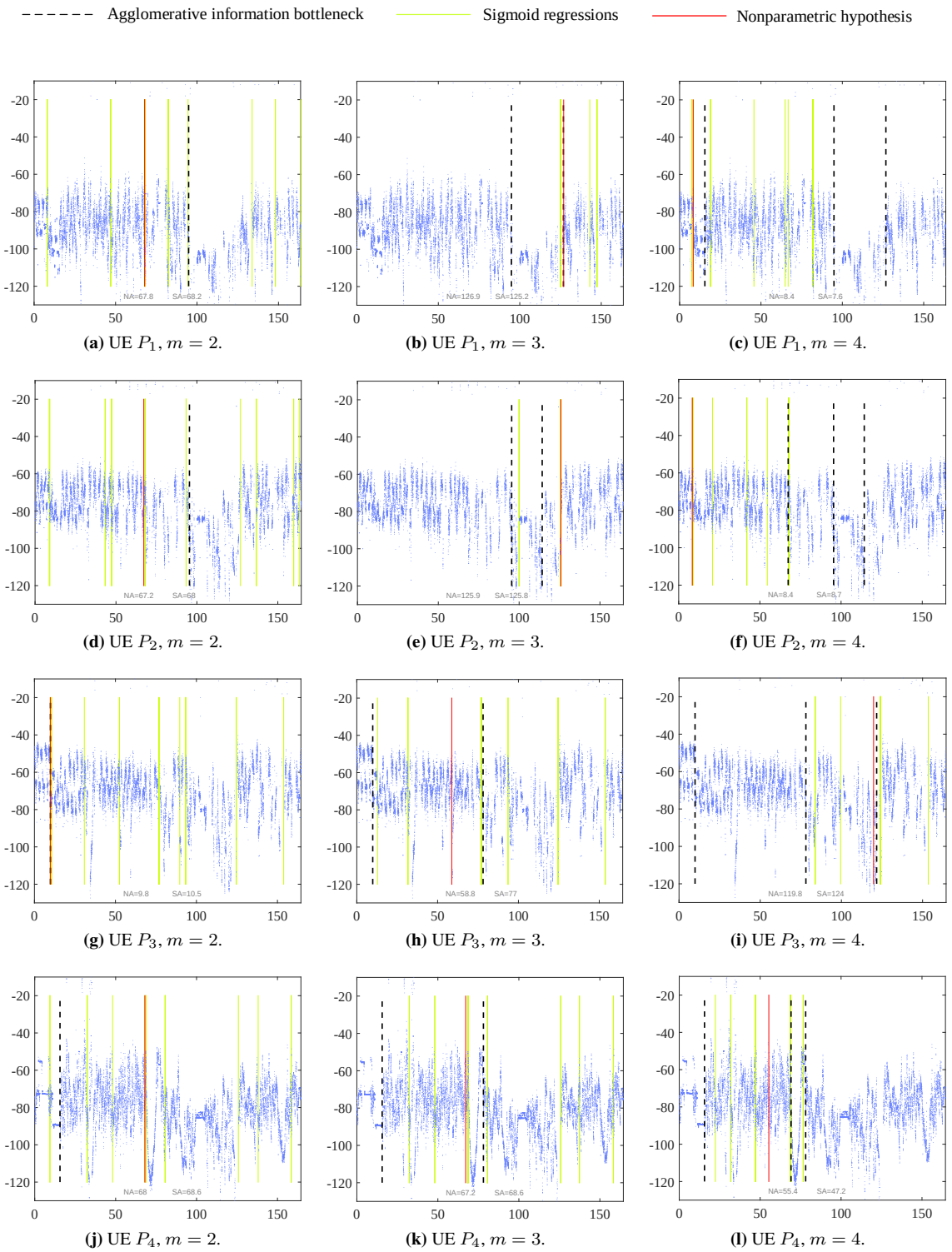

(a) UE P_1, $m = 2$. **(b)** UE P_1, $m = 3$. **(c)** UE P_1, $m = 4$.

(d) UE P_2, $m = 2$. **(e)** UE P_2, $m = 3$. **(f)** UE P_2, $m = 4$.

(g) UE P_3, $m = 2$. **(h)** UE P_3, $m = 3$. **(i)** UE P_3, $m = 4$.

(j) UE P_4, $m = 2$. **(k)** UE P_4, $m = 3$. **(l)** UE P_4, $m = 4$.

Fig. 3.16.: Change detection for vehicular use cases: CJ train case study. ©2018 IEEE [26]

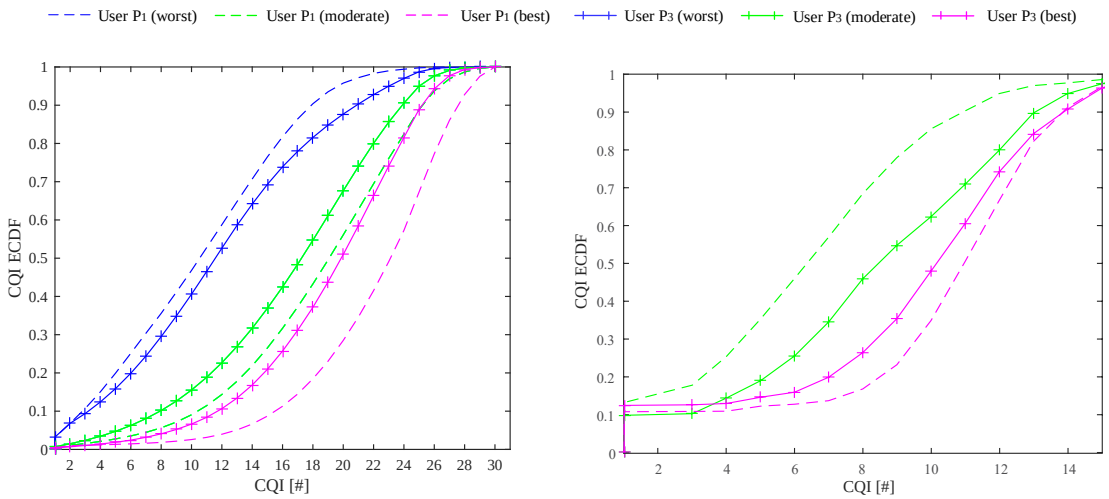

(a) UMTS 2100 MHz.

(b) LTE 800/2600 MHz.

Fig. 3.17.: Aggregate segmentation-based CQI assessment. ©2017 IEEE [25]

ultimate objective is to assess improvements and impairments of achievable data rates in UMTS/LTE networks. The procedure evaluates the aggregate distribution of all the chunks which are grouped based on a particular hypothesis condition. Each hypothesis condition is a result of a decision rule $d(x)$ and corresponds to partition of three disjoint regions $\Omega_0, \Omega_1, \Omega_2$. Each region is further named as *worst*, *moderate*, and *best* according to RSRQ and EcN0 values.

Fig. 3.17 demonstrates the ECDF CQIs classified based on the aforementioned conditions. Therefore, it can be observed as in the following: Firstly, the AFR-aided user shows substantial improvement in the *worst* case scenario, i.e., up to two indexes of CQIs. This reflects the main target to improve bit rates in low regime. Note, this scenario dominates the statistics and as such is a direct implication of true performance improvement known that rural environments predominate railway tracks. Secondly, the other two scenarios named as *moderate* and *best* cases exhibit impairment in terms of ECDF CQI. Herein, the AFR-free user outperforms the AFR-aided user. This comes from the fact of AFR having installed a single antenna in the outside environment. Consequently, UMTS and LTE users are limited to gain in performance due to the effect of keyhole channels [76]. Therefore, the single rooftop antenna and a single RC lead to reduce the rank even when AFR-aided users are in rich scattering environment.

3.4.6. Vehicle Penetration Loss

Having demonstrated the model of VPL estimation and characterization in Section 3.1.6, this section demonstrates its applicability on RJ and CJ trains. Nevertheless, before moving forward, let us discuss the challenges taken into consideration as in the following: First, the model applies RSRP as

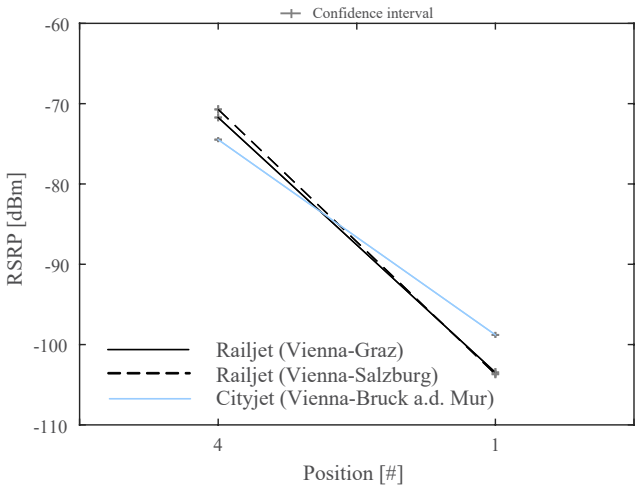

Figure 3.18.: VPL estimation: RJ and CJ case studies.

a parameter which by its definition is the power linearly averaged over the narrowband. Moreover, it does not include the noise and interference from other sectors. This way, the unwanted signals likely to increase the estimation error are disregarded. Second, the model targets frequency $800\,\text{MHz}$ to obtain an accurate VPL estimation, since higher frequencies require higher spatial sampling which may result in higher error. This is solely a limitation of the measurement equipment owing to the granularity. Thus, the large-scale fading samples are calculated by averaging out small-scale fading over distance, i.e., wavelengths. This is calculated based on relationship $\overline{v_t}/f_s$ at average velocity $\overline{v_t}[\,km/h] = \{80, 120\}$ and sampling frequency $f_s = 2\,\text{Hz}$ for a CJ and RJ train, respectively. This results in average spatial filtering $S_d[\,m] = \{29\lambda, 44\lambda\}$ for respective trains. Third, the samples are gathered according to the same amount of elapsed time over joint Confidence Intervals (CIs) when the outdoor and inside UE are in connected mode. Several CIDs yield to obtain samples from dominant paths of rays coming from random directions. This property explicitly helps to characterize the penetration loss for the whole train, i.e., including standard windows, metallic body, and other materials involved in structure of the train.

The VPL evaluates at user positions P_1 and P_4 as illustrated in Fig. 3.9, while the observations were gathered along three different tracks as illustrated in Fig. 3.6 and Fig. 4.3. As a result, estimated values of $24\,\text{dB}$ and $32 - 33\,\text{dB}$ for CJ and RJ train are obtained, respectively. It is observed a difference of $1.3\,\text{dB}$ when the estimates are compared among different tracks along with RJ operation. Fig. 3.18 remarks the findings.

On one hand, the obtained results reveal the scalability property of railway tracks over rural environments. Furthermore, the presented model implies the flexibility of small-scale measurements to provide satisfying statistical results. On the other hand, the good fit among different railway tracks indicates the same policy applied from the mobile operator to deploy the infrastructure.

3.5. Summary

In this chapter, descriptive and inferential statistics are applied to evaluate the improvements in coverage parameters for UMTS 2100 MHz and LTE $800/2600$ MHz on-board AFR-aided RJ and CJ trains. Being in similar propagation conditions, the results indicate that a difference in mean of 17 dB coverage improvement in UMTS 2100 is achievable when a RJ is equipped with AFRs. Similar finding is observed in both LTE 800 and 2600 in E-UTRA RSSI and RSRP showing $8 - 15$ dB improvement. Additionally, it is observed that the shape of empirical Q-Qs which describe the observations of AFR-aided and AFR-free users is nonlinear in behavior. On the other hand, a CJ train equipped with a single AFRs and a single RC shows comparable behavior. Coverage parameters exhibit maximum improvements in UMTS 2100 achieving 20 dB as well as 17 dB in LTE 800. However, a slightly linear behavior is noticed when an AFR-aided user is placed in the beginning of the RC. Above all, the AFR reveals a nonlinear behavior due to RF circuit constraints and power transmission limits owing to maximum output power level.

The achieved throughput by the single user connected to the outdoor rooftop antenna shows that there is room for improvement for indoor telecommunication services. Indeed, the solution with equipped AFR on-board fundamentally influences MIMO achievable data rates. It is observed that the AFR significantly improves the data rates in low regime at the expense of deteriorating them in high regime. Furthermore, a combination of nonparametric hypothesis and segmentation of railway track is introduced. Sequential and composite hypotheses were applied to assess the improvement in link quality parameters in operational network. The evidence supports the hypothesis for link quality improvement in low regime.

Supported by the fact of mobile users being dependent on network availability conditions an approach that utilizes information bottleneck algorithm characterizes extreme coverage conditions. Coupled with the multiple hypothesis and bootstrap, this approach mimics short-time experiments such as voice calls, file transferring sessions, or web-page downloads, and quantifies the improvements based on definition of the statistical performance metric. The applied approach strongly supports the hypothesis that the equipment of RJ/CJ with AFRs improves the observed UTRA RSSI, E-UTRA RSSI, RSCP, and RSRP. The approach aims to serve as benchmarking baseline to assess the service quality improvements and impairments in operational networks.

A nonparametric-based approach to detect the scarcity of infrastructure deployments as well as possible performance improvements is presented. The technique detects changes on observations gathered over distances of several hundred kilometers. It is observed that the approach is very similar compared to a machine-learning based approach. Additionally, a developed temporally-based assessment technique allows to detect the impact of AFR within a particular time interval. The time interval utilizes small sample-sizes that represents short-time experiments.

VPL is a crucial factor in the world of railway environments. For this motivation, VPL was estimated and evaluated for both trains under investigation along distinct rural railway tracks. The presented technique considers the outdoor environment which is compliant to ETSI and good agreement between railway tracks is found. It is observed that a RJ train and a CJ train exhibit VPL estimates of $33\,\mathrm{dB}$ and $24\,\mathrm{dB}$, respectively. Furthermore, the technique supports the characterization of VPL in real-world conditions.

Self-critically considering the contributions of this chapter, further ideas may be considered. First, the existing measurement configuration allows to assess the improvements and impairments for users under the effect of single a RC. It would be worth considering more than a single RC being connected via more than a single rooftop antennas. This would potentially boost multiplexing gains in wireless MIMO transmission and could be considered a flexible long term solution for future wireless technologies. Second, the existing analysis considers UE operating in a real-world cellular network while persistently being part of the operational traffic. It would be worth testing out the treatment effect in a more controlled environment, e.g., static measurements in a rural environment. Even though this solution does not truly mimic real-world scenarios, yet it would be a robust solution to dynamic changes of channel conditions, mobility as well as fast changes due to relatively heavy-traffic. Third, the nonparametric approach combined with bootstrap allows to mimic small-scale measurements and short-time experiments. While on one hand it uses the sample median as a central tendency, on the other hand it barely helps to draw inferences about quantiles. Therefore, it would be worth applying the same combination as proposed in this thesis. This would provide an estimate of confidence intervals of quantiles, e.g., Harrell-Davis weighted average [77] combined with Wilcox test. Forth, a long RJ train with $210\,\mathrm{m}$ length restricts the distribution of users due to limited number of measurement equipment. It would be worth distributing the users in a way to represent more use cases, a solution which would allow to verify the uniformity in terms of isolation on-board.

"No longer classified for military use, Frequency Selective Surfaces (FSSs) technology is finding new applications ..."

Ben A. Munk (1929 – 2009)

4

Mobile Service Quality in Frequency Selective Surface-aided Railway Vehicles

With enhanced developlement of railways is increased the demand of users in railway applications [60] as well. Customer-oriented services on-board railway vehicles are of primar consideration in R2R project [59] which aims to develop key technologies such as 3rd Generation Partnership Project (3GPP) Long Term Evolution (LTE) and IEEE 802.11 WiFi. Therefore, it is obvious that railway environments are gaining interest due to their social and economical impact. Promising forecasts exist [1], but existing technical solutions, such as WiFi in High Speed Train (HST), are insufficient despite this.

Commonly, vehicle manufacturers construct the HSTs with metallic structures. Additionally, vehicle's windows are designed with composite panes capable to reduce the heat loss which comes in form of Infrared (IR) as well as to decrease the insulating value U-factor which controls thermal insulation that comes in form of Ultraviolet (UV) rays. Yet, such composite panes affect lower frequencies too, i.e., mobile communication's frequencies. In this situation, Vehicle Penetration Loss (VPL) increases above 30 dB and affects the performance of radio communications such as Global System for Mobile Communications (GSM)/Universal Mobile Telecommunications System (UMTS)/LTE. To give an illustration of the general problem Fig. 4.1 covers the key idea.

To cope with this, Frequency Selective Surfaces (FSSs) are a promising solution and International Telecommunications Union (ITU) in [78] reports technical recommendations with theoretical and practical elaborations. On the other hand, various geometrical structures are utilized to build FSS structures with desirable RF filter characteristics. Square, rectangular, circular, or their combinations [79, 80] apply on window panes. While design of FSSs is out of scope of this thesis, this chapter

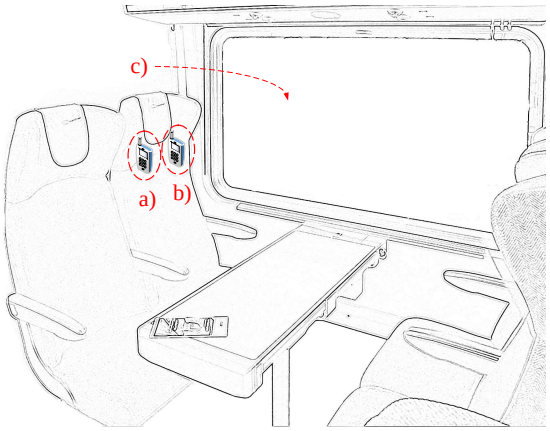

Fig. 4.1.: Illustration of smartphone-based measurement setup on-board treatment-aided HST. Mobile users depicted with a,b) represent end-users, while window depicted with c) can be either FSS or FSS-free structure. ©2019 IEEE [28]

focuses on a FSS structure [81] which was designed particularly for railway applications as shown in Fig. 4.2.

Based on [25, 27, 28], the contributions of this chapter outline as in the following:

- Both descriptive- and inferential-based analysis to a proposed prototype of windows on-board is conducted. The analysis relies on experiments performed in a live network with User Equipment (UE) that mimic the quasi-real usage of end-users.

- The novel approach to assess the service quality of vehicular use cases is applied on mobile users on-board a HST. The key idea is to establish a common framework for service quality assessment which deals with particular data-outage scenarios. The proposed model serves as a benchmarking baseline to railway vehicle's manufacturers and cellular operators.

- A segmentation-based micro-analysis assessment approach is proposed. Evaluation of physical throughput during active times with traffic leads to miss-estimation. However, the approach proposed here to deal with this problem is differently. The key idea is to evaluate Channel Quality Indicators (CQIs) from hypothesis conditions constructed on smaller chunks of a railway track. The benefit of the proposed approach leads to evaluate Multiple-Input Multiple-Output (MIMO) transmission for various vehicular use cases.

4.1. System Model

4.1.1. Data Outage

As emphasized in Section 3.1.1, the identification of extreme data outage scenarios is of vast importance in evaluating performance of on-board mobile users. Therefore, the objective of this section is to establish a theoretical approach which performs this classification.

To accomplish this evaluation, it is needed to let all the mobile users on-board to be connected on a particular technology based purely on network conditions. Similarly to Section 3.1.1, a treatment-free[1] user is used as reference. The reference user is further termed as *FSS-free user* throughout this chapter.

Herein, let us denote with m the number of intervals which correspond to unique outage scenarios, each of them identified with observed data distribution $Y_1^{(o)}(y)$, where $1 \leq o \leq m$, $o \in \mathbb{N}$ and $y \in \mathbb{R}$. The procedure follows as in Section 3.1.1, where the function $\Psi(y,t) \equiv f_{JS,\pi_2}(p(y|\dot{t}_i), p(y|\dot{t}_j))$ enables the identification of the best scenario which formulates as

$$r_{MAX} = \max_{y \in Y_1} \{\mathbb{E}\{Y_1^{(1)}\}, \mathbb{E}\{Y_1^{(2)}\}, ..., \mathbb{E}\{Y_1^{(m-1)}\}, \mathbb{E}\{Y_1^{(m)}\}\}, \quad \forall m \in \mathbb{N} \tag{4.1}$$

and the worst scenario which formulates as

$$r_{MIN} = \min_{y \in Y_1} \{\mathbb{E}\{Y_1^{(1)}\}, \mathbb{E}\{Y_1^{(2)}\}, ..., \mathbb{E}\{Y_1^{(m-1)}\}, \mathbb{E}\{Y_1^{(m)}\}\}. \tag{4.2}$$

Further relevant details are provided in Section 3.1.1.

4.1.2. Service Quality Analysis

Similarly to Section 3.1.2, the key idea is to construct a rigorous investigation on central tendencies of FSS-aided- and FSS-free users' distributions. Known this goal, the distributions of two observed data are assumed to be unknown and so are assumed to be their variances too. The general problem tends to test whether the central tendency of a distribution is greater or not (to answer e.g., "Is there any improvement in received power if a mobile user is placed next to FSS structure?", or "Is there any improvement in received power if a mobile user is placed next to FSS-free structure but within the same wagon with few FSS structures?"). To do so, the UE were placed in such positions to enable the assessment of particular vehicular use cases.

[1] This user is assumed to be incapable of benefiting from a treatment being located far enough from the modified wagon. Fig. 4.5 reveals the details.

Indeed, the nonparametric significance testing tests whether the median of two distributions F_{Y_1} and F_{Y_3} are equal or not. Therefore, mathematically the assessment problem formulates by constructing binary hypothesis with Wilcoxon-Mann-Whitney (WMW) test as

$$\mathcal{I}_0 : \; F_{Y_1}(y) = F_{Y_3}(y) \quad \mathcal{I}_1 : \; F_{Y_1}(y) < F_{Y_3}(y) \tag{4.3a}$$

$$\mathcal{I}_{0'} : \; F_{Y_1}(y) = F_{Y_2}(y) \quad \mathcal{I}_{1'} : \; F_{Y_1}(y) < F_{Y_2}(y) \tag{4.3b}$$

where F_{Y_1} denotes the Cumulative Distribution Function (CDF) of user placed within an adjacent wagon (FSS-free user). F_{Y_2} represents the CDF of user placed within a modified wagon, and F_{Y_3} represents the CDF of user placed in the modified wagon but in better conditions than the previous one. Specifically, the former was placed next to a FSS structure. Both F_{Y_2} and F_{Y_3} are named as *FSS-aided users* throughout this chapter. Therein, similarly as in Section 3.1.2 the model distinguishes between two ways of specifying directional testing.

The procedure follows the construction of multiple hypotheses $\mathcal{I}_{0,M}, \mathcal{I}_{1,M}$, and $\mathcal{I}_{0\prime,M}, \mathcal{I}_{1\prime,M}$, where M is the number of bootstrap distributions. Thus, Eq. (4.3a) now becomes

$$\ddot{\mathcal{I}}_{0,1} : \; \widehat{F_{Y_{1,1}}}(y) = \widehat{F_{Y_{3,1}}}(y) \quad \ddot{\mathcal{I}}_{1,1} : \; \widehat{F_{Y_{1,1}}}(y) < \widehat{F_{Y_{3,1}}}(y) \tag{4.4a}$$

$$\ddot{\mathcal{I}}_{0,2} : \; \widehat{F_{Y_{1,2}}}(y) = \widehat{F_{Y_{3,2}}}(y) \quad \ddot{\mathcal{I}}_{1,2} : \; \widehat{F_{Y_{1,2}}}(y) < \widehat{F_{Y_{3,2}}}(y) \tag{4.4b}$$

$$\vdots$$

$$\ddot{\mathcal{I}}_{0,M} : \; \widehat{F_{Y_{1,M}}}(y) = \widehat{F_{Y_{3,M}}}(y) \quad \ddot{\mathcal{I}}_{1,M} : \; \widehat{F_{Y_{1,M}}}(y) < \widehat{F_{Y_{3,M}}}(y) \tag{4.4c}$$

and similarly Eq. (4.3b) reformulates as

$$\ddot{\mathcal{I}}_{0\prime,1} : \; \widehat{F_{Y_{1,1}}}(y) = \widehat{F_{Y_{2,1}}}(y) \quad \ddot{\mathcal{I}}_{1\prime,1} : \; \widehat{F_{Y_{1,1}}}(y) < \widehat{F_{Y_{2,1}}}(y) \tag{4.5a}$$

$$\ddot{\mathcal{I}}_{0\prime,2} : \; \widehat{F_{Y_{1,2}}}(y) = \widehat{F_{Y_{2,2}}}(y) \quad \ddot{\mathcal{I}}_{1\prime,2} : \; \widehat{F_{Y_{1,2}}}(y) < \widehat{F_{Y_{2,2}}}(y) \tag{4.5b}$$

$$\vdots$$

$$\ddot{\mathcal{I}}_{0\prime,M} : \; \widehat{F_{Y_{1,M}}}(y) = \widehat{F_{Y_{2,M}}}(y) \quad \ddot{\mathcal{I}}_{1\prime,M} : \; \widehat{F_{Y_{1,M}}}(y) < \widehat{F_{Y_{2,M}}}(y) \tag{4.5c}$$

Similarly to Section 3.1.2 are applied the procedures of False Discovery Rate (FDR) [48, 52].

4.1.3. Spatially-based Analysis

High speed mobility as well as low granularity of observations are two key limiting factors. However, it is expected that statistical properties do not change quickly when the observations are gathered on

a limited space. This section describes a combination of hypothesis testing and spatial segmentation (small chunks). The size of each chunk is denoted with $a = 1\,\text{km}$ which ensures that statistical properties within a chunk do not change abruptly in context of distinct environments. This is particularly true for nominal environments, urban, sub-urban and rural. For example, the distribution of a sub-urban environment within a chunk is expected to follow the same distribution from another chunk that characterizes the same environment. The procedure follows as explained in Section 3.1.3 and further details are available there.

Therefore, each hypothesis is constructed on observations gathered during 1km size chunks. Based on this, the evaluation of observations with CQIs takes into account chunks according to a hypothesis decision. In other words, each hypothesis detects chunks with best-, moderate- and worst link quality. Therefore, nonparametric sign test is applied to detect various link quality to each chunk sequentially by starting with

$$\ddot{\mathcal{I}}_{0,s} : \mathbb{M}\{Y_{1,s}(y)\} \not> \rho_1 \quad \ddot{\mathcal{I}}_{1,s} : \mathbb{M}\{Y_{1,s}(y)\} > \rho_1 \tag{4.6}$$

where $Y_{1,s}$ represent the variable of *passive* treatment-free user with observations collected over each chunk $s = S_1, S_2, ..., S_A$ and $\rho_1 = -7\,\text{dB}$ represents the hypothesized median. When $\ddot{\mathcal{I}}_{0,s}$s are in force the following binary hypothesis formulates as

$$\ddot{\mathcal{I}}_{0,p} : \mathbb{M}\{Y_{1,p}(y)\} \not> \rho_2 \quad \ddot{\mathcal{I}}_{1,p} : \mathbb{M}\{Y_{1,p}(y)\} > \rho_2 \tag{4.7}$$

where $\rho_2 = -14\,\text{dB}$, and $p = S_1, S_2, ..., S_P$ such that $P \leq A$. The same approach is applied for both technologies LTE $800/2600\,\text{MHz}$ and UMTS $2100\,\text{MHz}$.

4.2. Smartphone-based Measurement Setup

4.2.1. Window Panes with Frequency Selective Properties

FSS-free prototype windows are proven to negatively influence RF propagation by impacting the wavelengths from $300 - 1300\,\text{nm}$ and lower frequencies too. The FSS-free structures reduce the thermal heat loss to leak outside the environment and reflect the sunlight rays. This is enabled by composite structure of panes. However, they also degrade RF propagation of mobile communications such as GSM/UMTS/LTE. For this reason, FSS structures with IR and UV protection properties can be considered a proper and competitive solution. ITU has released a technical report [78] with theoretical analysis and experimental results on effects of composite structures on radiowave propagation. As a matter of fact, the FSS structures can be designed with high-shielding effectiveness utilized to save energy [82–84], or can be used as band-pass filter for a particular frequency range [62], e.g. mobile communications.

In general, a FSS consists of a two-dimensional periodic geometric structure composed of metallic and dielectric materials [85, 86]. The geometric structure defines the effective EM characteristics,

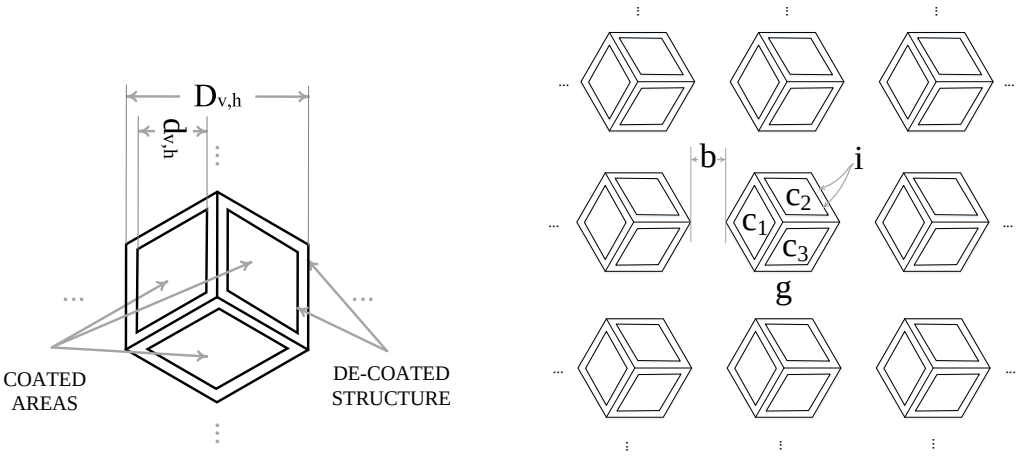

(a) Illustration of a single hexagonal element. ©2019 IEEE ACCESS [27]

(b) Illustration of FSS structure. ©2019 IEEE [28]

Fig. 4.2.: FSS transparent structure with conductive periodic grating proposed in [81].

i.e. permittivity, conductivity, and magnetic permeability. The authors in [81] have developed a FSS structure particularly for railway vehicles. Fig. 4.2 illustrates this design. As can be seen, the structure is organized with horizontal and vertical periodic hexagonal grating denoted with g. The size of g is approximately $D_{v,h} = \lambda/4$, where λ is the effective wavelength of the minimum frequency, $f_{MIN} = 700\,\text{MHz}$. Each structure g contains embedded diamond-shaped coated areas denoted with c_1, c_2, c_3. Their purpose is to operate as band-stop filter for WiFi frequencies, i.e., stop the propagation out of the vehicle in the range $5200 - 5800\,\text{MHz}$. Their size is $d_{v,h} = \lambda/2$ and designed to resonate at WiFi frequency of $f_{MAX} = 5800\,\text{MHz}$. To reduce the coupling effect at high frequencies between inter- and intra coated areas, insulating (decoated) lines denoted with i are arranged close enough to the coated areas. Their thickness is chosen to trade-off between the visibility disruption and RF degradation, i.e., permeability. In other words, the higher the thickness the worse the visibility through the window and possibly less RF degradation.

4.2.2. Measurement Track

The measurement campaign was conducted along the track from Vienna to Graz as illustrated in Fig. 4.3. This track has 209 km length, built mainly along rural environments as it is common for inter-city railways. The measurement campaign started from the train station Wien Matzleinsdorfer Platz and then led south towards city of Graz. Inter-city HST under test was Railjet (RJ) [71] that commutes between cities at maximum velocity 230 km/h. This type of operational train (see Fig. 4.4a) has social and economical impact and is typical for its inter-city as well as inter-country operation.

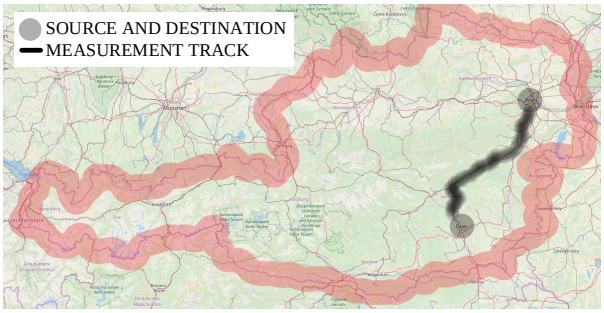

Fig. 4.3.: Measurement track: Vienna to Graz. To estimate and validate VPL were taken into consideration the observations from the track from Vienna to Salzburg as well. ©2019 IEEE [28]

(a) Train type: Railjet [71].

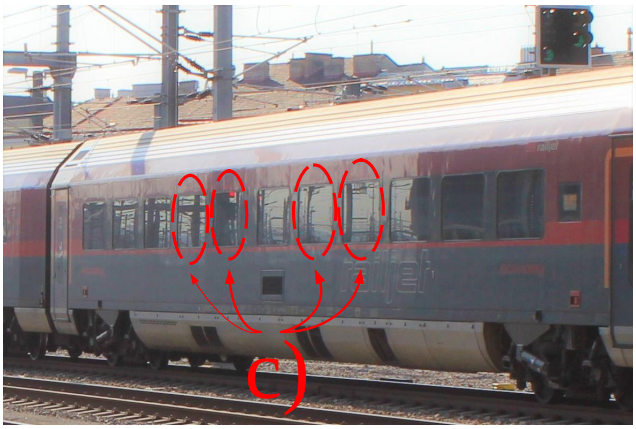

(b) Modified train wagon.

Fig. 4.4.: HST under test: FSS-free windows were replaced with FSS windows at positions c). ©2019 IEEE [28]

Tab. 4.1.: Descriptive statistics: sample mean, median, variance and skewness are denoted with $\mathbb{E}(\cdot)$, $\mathbb{M}(\cdot)$, $\mathbb{V}(\cdot)$ and $\mathbb{S}(\cdot)$, respectively.

	LTE 800						LTE 2600						UMTS 2100					
	E-UTRA RSSI			RSRP			E-UTRA RSSI			RSRP			UTRA RSSI			RSCP		
	$\{Y_1\}$	$\{Y_2\}$	$\{Y_3\}$	$\{Y_1\}$	$\{Y_2\}$	$\{Y_3\}$	$\{Y_1\}$	$\{Y_2\}$	$\{Y_3\}$	$\{Y_1\}$	$\{Y_2\}$	$\{Y_3\}$	$\{Y_1\}$	$\{Y_2\}$	$\{Y_3\}$	$\{Y_1\}$	$\{Y_2\}$	$\{Y_3\}$
	FSS-aided Railjet																	
$\mathbb{E}(\cdot)$	-74	-68.4	-65.2	-103.3	-97.7	-94.6	-72.1	-65.2	-62	-104.2	-95.5	-91.8	-73	-70.7	-65.7	-81.2	-78.5	-73.6
$\mathbb{M}(\cdot)$	-74.8	-68.9	-65.4	-104.1	-97.9	-94.4	-74.1	-66	-63.6	-105	-95.7	-92.7	-70	-67.8	-63.4	-77.4	-75.3	-71.2
$\mathbb{V}(\cdot)$	75	101.3	119.3	110.5	131.7	144.9	32.7	30.9	42.9	24.8	24.7	37.7	109.5	128.6	143.5	165.1	142.5	170
$\mathbb{S}(\cdot)$	0.3	0	0	-0.1	-0.3	-0.3	0.8	-0.1	1.2	2	-0.2	1.3	-0.9	-0.7	-0.8	-0.4	-0.7	-0.8

4.2.3. Smartphone Placements

The RJ windows are characterized with FSS-free properties, thus during measurements particular positions in RJ train (see Fig. 4.5a) were replaced with FSS windows. Fig. 4.5b illustrates the details. The FSSs were mounted in positions four, five, seven and eight on both sides of a modified train wagon. To evaluate the impact of FSS on Key Performance Indicators (KPIs), two UE were placed on passenger seat next to FSS window denoted with P_3. A UE was chosen to operate in GSM/UMTS/LTE and another one in GSM/UMTS based on network availability. Following the same logic, two other UE were placed next to a FSS-free window denoted with P_1. The reasons of not fully modifying the wagon are provided in the following: On one hand, since demounting and mounting process takes considerable amount of time it was more flexible to reduce the number of replacements. On the other hand, the aim was to target the robustness of FSSs and examine their impact on users positioned within the same wagon but situated next to FSS-free windows.

4.2.4. Smartphone Orientations and Relevant Entities

NEMO benchmarking system [73] was utilized to represent a UE on-board the FSS-aided RJ train. All the reasoning and the measurement details discussed in Section 3.2.4 hold here as well.

4.2.5. Measurement Configuration

The UE are configured with sequential tasks of voice and data as common end-user interactions that mimic *quasi-real* usage on-board the FSS-aided RJ train. Therefore, all the reasoning and the measurement details discussed in Section 3.2.5 hold here as well.

(a) UE placements.

(b) Modified train wagon: Two UE were placed next to FSS structures to represent the best scenario, i.e. position P_3. Two other UE were placed at the end of the modified wagon to represent the worst case scenario, i.e. position P_2. ©2019 IEEE [28]

Fig. 4.5.: FSS-aided RJ measurement setup.

4.3. Service Quality Improvements for Inter-city Train Passengers

4.3.1. Coverage Analysis

Being limited to investigate the improvements due to treatments solely on the observations at the user's side, this analysis points out two possibilities to analyze the coverage of a mobile operator. One one hand, it is expected that mobile users being in similar propagation conditions are served by the same Base Stations (BSs) within a particular amount of time. On the other hand, due to the FSS treatments on-board the railway vehicle, mobile users can be potentially served by BSs even placed far away from the railway track which compensates the absence of dedicated infrastructure, while mobile users unable to benefit from such a treatment are likely to fail to do so. Therefore, it is crucial to distinguish between two different service quality improvement scenarios associated with FSSs structures in RJ train: (1) the improvement observed over the entire railway track, and (2) the improvement observed over Cell IDs (CIDs). The former approach is discussed in this section by using empirical Quantile-Quantile (Q-Q).

Fig. 4.6 illustrates the coverage results by using descriptive statistics. Here, the discussion focuses on the improvement in FSS-aided users in comparison to an FSS-free user. Overall, a significant peak-to-peak improvement varying from $2-12$ dB is observed. The collected descriptive statistics of coverage measurements shown in Table 4.1 support the hypothesis that the equipment of the RJ train with FSSs significantly improves the observed Received Signal Strength Indicator (RSSI), Reference Signal Code Power (RSCP), and Reference Signal Received Power (RSRP) measurements. This is valid for cellular mobile telecommunication technologies: UMTS 2100 MHz and LTE $800/2600$ MHz.

The shape of the resulting Q-Q plots which describe the measurements with FSS and with FSS-free is almost linear in behavior with 7 dB improvement for the FSS-aided user P_3 and 3 dB improvement for the FSS-aided user P_2, respectively. This linearity is particularly true for LTE 800 and UMTS 2100 as can be observed from slight difference in skewness in Table 4.1. Technically, the linearity stems from the fact that FSS hexagonal structure with conductive periodic grating shows linear frequency-selective characteristic in the range of mobile communications from $700-2700$ MHz, while the transfer function of FSSs depends on polarization, angle of incidence and frequency. Therefore, the transmission of EM waves through FSSs is linear over a large dynamic range of wave amplitudes. On the other hand, LTE 2600 does not follow this linearity behavior due to strong burstiness behavior in occurrence of LTE in this frequency band.

4.3.2. User Equipment Placement Analysis

In this section, the improvement observed over CIDs is elaborated. The purpose of this analysis is to analyze the trends of KPIs with respect to particular UE placements.

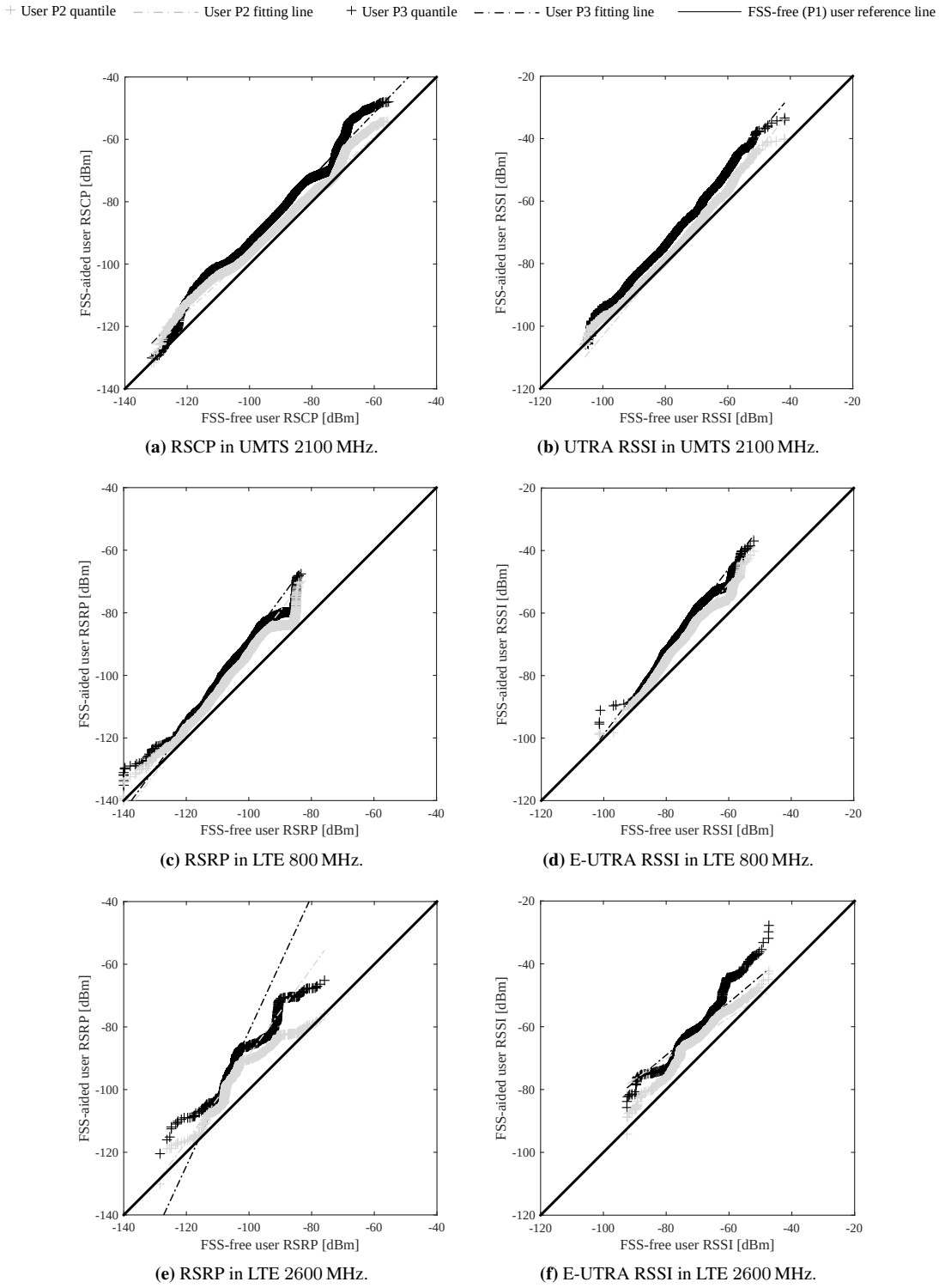

(a) RSCP in UMTS 2100 MHz.

(b) UTRA RSSI in UMTS 2100 MHz.

(c) RSRP in LTE 800 MHz.

(d) E-UTRA RSSI in LTE 800 MHz.

(e) RSRP in LTE 2600 MHz.

(f) E-UTRA RSSI in LTE 2600 MHz.

Fig. 4.6.: FSS-aided user quantile - FSS-free user quantile: RJ train case study.

Fig. 4.7 shows a few KPIs collected simultaneously in different vehicle's placements at LTE frequencies $800/2600$ MHz and UMTS 2100 MHz. As can be seen here, both wideband and narrowband received powers for FSS-aided users P_2 and P_3 show significant increase compared to FSS-free user P_1, i.e., see Figs. 4.7d and 5.4a to 5.4c. The measurement results suggest that UE P_2 still considerably benefits even though it was not located next to the FSS structure. The remarkable finding in this analysis strongly indicates the robust capability of low number of mounted FSSs in a wagon to efficiently serve all the users including those in poor propagation conditions.

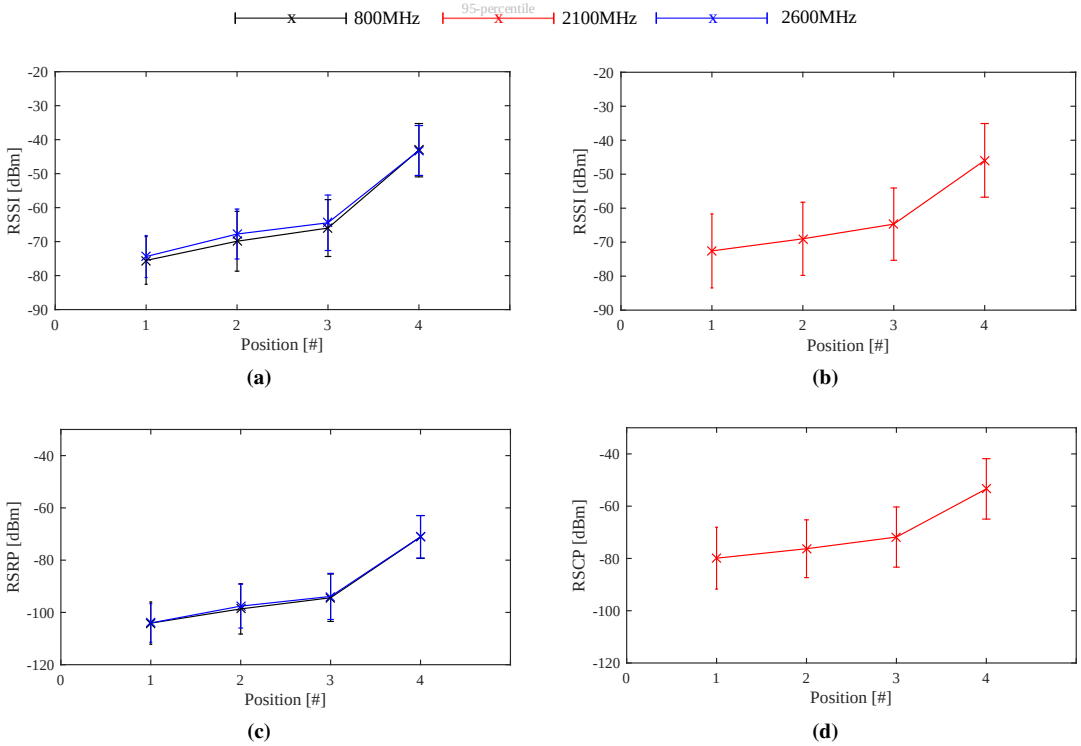

Fig. 4.7.: CID-based with respect to UE placements. ©2019 IEEE [28]

4.4. Service Quality Assessment

This approach distinguishes between two different assessment scenarios: (1) assessment observed along the whole track, and (2) assessment observed on specific data outage scenarios. While the former enables the assessment of service quality improvements independent from network availability, the latter enables the assessment over best- and worst case data outage scenarios by including intra- and inter-technology handovers. Both approaches are discussed in the following.

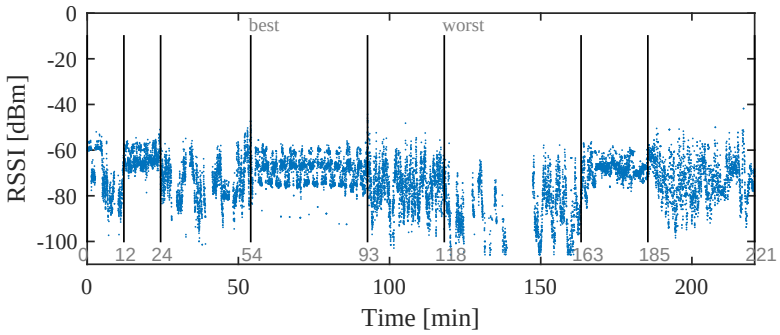

(a) Case study: FSS-aided RJ train

Fig. 4.8.: Illustration of outage-based assessment with RSSI. Vertical black lines represent intervals obtained with Agglomerative Information Bottleneck (aIB). Note that the data contain UMTS as well as LTE connections on served cells.

4.4.1. Trip-based Analysis

In the following, the desire is to assess possible improvements in KPIs as explained in Section 4.1.2. The motivation of trip-based assessment remains the same as in the case of Amplify-and-Forward Repeater (AFR)-aided RJ train, therefore no further discussion is conducted here. Table 4.2 provides the rejection ratio at significance level $\alpha = 0.05$ for the whole track denoted with $\tau_{i,j}$ derived over M number of hypothesis tests. The trip-based assessment is denoted with *overall* in Table 4.2.

On one hand, coverage parameters fully support the multiple hypothesis that a FSS-aided UE outperforms FSS-free UE. This is valid for both technologies UMTS and LTE as well as both pairs of users (P_1, P_3) and (P_1, P_2). On the other hand, link quality parameters do not support this for UMTS. The reason for this stems from the fact that Energy-per-Chip-over-Noise Ratio (EcN0) level is good enough averaging at -7 dB, while in Reference Signal Received Quality (RSRQ) for LTE this is not the case. This is accounted for the weak changes between pairs of comparisons, ranging in levels below 2 dB which results to be undetected by the procedure. Therefore, to verify this further analysis is required in Section 4.4.3. This however, does not truly imply no improvement in UMTS link quality parameters, it only indicates that there not sufficient evidence. Hence, it is necessary to verify this by applying a different approach of significance testing.

4.4.2. Outage-based Analysis

Outage-based assessment approach depends on level of received power by mutually taking into consideration LTE and UMTS availability. In opposite to trip-based assessment, the focus here is on outage-based assessment defined with *best* and *worst* scenarios according to their definition in Section 4.1.1. Table 4.2 summarizes the results of multiple hypothesis, while Fig. 4.8 demonstrates the RSSI over time for the FSS-free user.

Tab. 4.2.: Rejection ratios obtained from significance probability with adjustment at type I error $\alpha = 0.05$ and the number of hypotheses $M = 10^4$. The rejection ratio is denoted with $\tau_{i,j}$ which stands for pair of the users (i, j). While for voice the sub-sample size is kept the same over technologies and scenarios, to mimic the data sessions the following sub-sample sizes are applied: $n_{s,best}^{(UMTS)} = 75$, $n_{s,best}^{(LTE)} = 35$, $n_{s,worst}^{(UMTS)} = 320$, $n_{s,worst}^{(LTE)} = 160$.

	LTE 800/2600								UMTS 2100							
	E-UTRA RSSI		RSRP		RSRQ		T_x		UTRA RSSI		RSCP		E_c/N_0		T_x	
	τ_{Y_2,Y_1}	τ_{Y_3,Y_1}	τ_{Y_2,Y_1}	τ_{Y_3,Y_1}	τ_{Y_2,Y_1}	τ_{Y_3,Y_1}	τ_{Y_2,Y_1}	τ_{Y_3,Y_1}	τ_{Y_2,Y_1}	τ_{Y_3,Y_1}	τ_{Y_2,Y_1}	τ_{Y_3,Y_1}	τ_{Y_2,Y_1}	τ_{Y_3,Y_1}	τ_{Y_2,Y_1}	τ_{Y_3,Y_1}
best (voice)	1	1	1	1	1	1	1	1	1	1	0.99	1	0	0	0	0
best (data)	1	1	1	1	0.91	0.83	0.98	0.96	1	1	0.84	1	0	0	0	0
worst (voice)	0.96	1	0.57	0.99	0	0	0.04	0.12	0.99	1	0.98	0.99	0	10^{-4}	0	0
worst (data)	0.9	1	0.39	0.98	0	0	0.01	0.04	0.99	1	0.99	1	10^{-4}	0	0	0
overall	1	1	1	1	1	1	0.99	1	1	1	1	1	0	0	0	0

The results shown here strongly support the hypothesis that both technologies exhibit improvement in terms of E-UTRA RSSI, UTRA RSSI, RSRP and RSCP. This is valid for both FSS-aided users P_2 and P_3 as well as both scenarios with voice and data. The logic of UE placements in coverage parameters holds the relationship $\tau_{Y_3,Y_1} \geq \tau_{Y_2,Y_1}$ which supports the alternative against the null hypothesis with higher significance for user P_3.

While in LTE there is significant evidence in improvement in transmit power and signal quality in best scenario, in UMTS no improvement is evidenced at all. On one hand, this result indicates that LTE availability reveals a bursty nature being available only along areas with very good coverage, while UMTS is deployed continuously. This also impacts the transmit power as well. Similarly to trip-based, this approach again does not succeed to assess any improvement in terms of signal quality parameters. This is a good example why signal quality parameters need a different approach of significance testing which is demonstrated in Section 4.4.3.

4.4.3. Channel Quality Analysis

As persistently pointed out throughout this thesis, CQI is a crucial parameter which facilitates the performance evaluation for mobile users in operational networks. As solution, this section demonstrates the proposed assessment approach explained in Section 4.1.3. Having observed the scenario with AFRs on-board here the motivation is to investigate the link quality of FSS-aided and FSS-free UE on-board the RJ train.

The usual way to approach this problem is to find the cumulative distribution on each chunk separately, but this does not produce an aggregate distribution. The obtained results in Section 4.4.2 verify this. Hence, the goal is to evaluate the aggregate distribution of all the chunks grouped based on a particular hypothesis condition.

The results shown in Fig. 4.9 show CQI Empirical Cumulative Distribution Function (ECDF) for FSS-aided user P_3 and FSS-free user P_1 (defined in Fig. 4.5). In other words, the goal is to apply

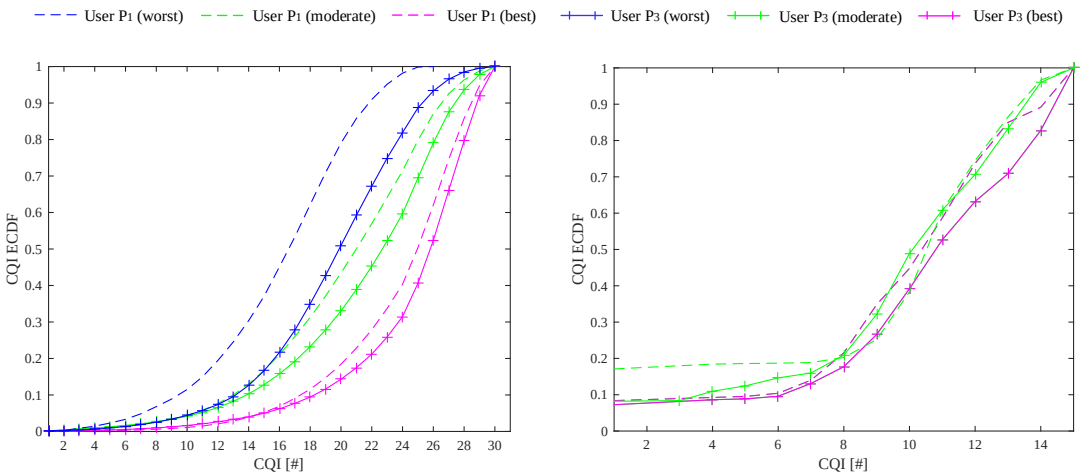

(a) UMTS 2100 MHz.

(b) LTE 800/2600 MHz.

Fig. 4.9.: Aggregate segmentation-based CQI assessment. ©2017 IEEE [25]

significance testing whether a UE placed next to FSSs outperforms a UE placed next to a FSS-free structure. As shown in Fig. 4.9a, CQI distribution strongly supports the hypothesis that FSSs boost the performance in terms of MIMO transmission. The situation tends to be the same for LTE UE. Though, it is difficult to clearly see the differences in Fig. 4.9b. This is a consequence of poor LTE coverage resulting in a low sample size which leads to a lack of evidence.

This brings up the comparing perspective between FSS- and AFR solution. On contrary to the solution with AFR-aided RJ train, the prototype FSS structures are different in behavior, because they conceptually support MIMO transmission. The FSSs show maximum gain of four indexes in CQI ECDF when compared to FSS-free scenario. In fact, the improvement is quite steady and vital over all hypothesis conditions, starting from the worst case scenario and then continuing being boosted for the moderate and best conditions.

4.5. Summary

In this chapter, descriptive and inferential statistics are applied to evaluate the improvements in coverage parameters for UMTS 2100 MHz and LTE 800/2600 MHz on-board FSS-aided RJ train. The results indicate that a maximum peak of 12 dB coverage improvement is achievable when a RJ is equipped with prototype FSS although the improvement gains are not as large as those with AFRs. Descriptive statistics support this over entire railway track as well as joint CIDs. Additionally, it is observed that the shape of empirical Q-Qs which describe the observations with FSS and FSS-free is almost linear in behavior. This result implies strong similarity of FSS-aided train to a road vehicle.

Supported by the fact of mobile users being dependent on network availability conditions the approach utilizes information bottleneck algorithm to characterize extreme coverage conditions. Coupled with the multiple hypothesis, this approach enables the assessment of various data-outage scenarios. The applied approach strongly supports the hypothesis that the equipment of RJ with FSSs improves the observed UTRA RSSI, E-UTRA RSSI, RSCP, and RSRP. The approach aims to serve as benchmarking baseline for data outage scenarios.

A combination of nonparametric hypothesis and segmentation of railway track is introduced. Small chunks of a track are fundamentally different from the entire track because they represent short-time observations during high velocities. Yet, they do not approximate a cumulative distribution. Therefore, sequential and composite hypotheses were applied to assess the improvement in link quality parameters. The FSS structures are different in behavior because, conceptually, they do support MIMO transmissions. It is observed that a RJ in a rich scattering environment, the FSSs show higher performance gains in terms of MIMO transmission.

Self-critically considering the contributions of this chapter, further ideas may be considered. First, the existing measurement configuration allows to investigate data-outage scenarios. Yet, it does not consider technology-concentric usage due to bursty nature of network availability in LTE. Hence, it would be interesting to analyze whether technology-concentric usage assessment leads to a higher coverage and link quality improvement gains than quasi-real usage. Second, the existing analysis considers the UE operating in a real-world cellular network while persistently being part of the operational traffic. As a consequence, channel conditions may change drastically for mobile users being considerably apart to each other in a long train of 210 m length. Therefore, it would be worth analyzing the performance gains of FSS-aided UE in a more controlled environment.

"The nonparametric tests are attractive because they do not require an assumption of the normal distribution. Even when the data do come from normal distributions, these nonparametric tests do not sacrifice much power in comparison to tests based on the normality assumption"

Ronald N. Forthofer (1944 – present)

5

Mobile Service Quality in Road Vehicles

Internet usage has become ubiquitous. The users today are a mix of humans and smart machines using the connectivity to exchange information of all kinds. The recent developments in vehicular industry towards smart, autonomous cars [87] have even driven further the need for low delay emergency [88] and high bandwidth data [89]. Combining these two elements, it becomes clear that today highways need to provide large capacity as well as signal coverage along the route.

To provide reliable connectivity and large capacity for in-vehicle LTE users, it is necessarily to determine the penetration loss caused by the vehicle. This is one of the main goals of wireless providers and field experiments are crucial to design the wireless networks. Independent from vehicle type, the increase of demand for high quality mobile communication services is tremendous [90–92]. Network performance of vehicular use cases, such as cars on highways and trains on railways, have technical challenges in common. First, both modern highways and railways are constructed along similar gentle curved tracks. In context of coverage, the network deployment is very similar, and cannot change drastically for future technologies, e.g. 5th generation of mobile networks (5G) or beyond. This leads to similar propagation conditions for mobile users moving on cars and trains. Second, the electric cars and current HSTs are being built with metal coated windows [62, 79, 81]. In terms of network performance, it is very important to observe whether VPL retains linear characteristic. Therefore, measurements are necessarily to find out how similar these problems are. Possible similar characteristics lead to apply the same technical solutions to both trains and cars.

Furthermore, it is required a theoretical approach to model all relevant variations of KPIs which are impacted by radio degradation considering the VPL. In this context, an important issue is to be able first to identify various nominal environments, i.e., urban, sub-urban, rural, in a statistical matter. This, due to the fact that any relation between various KPIs differs considerably, depending on whether

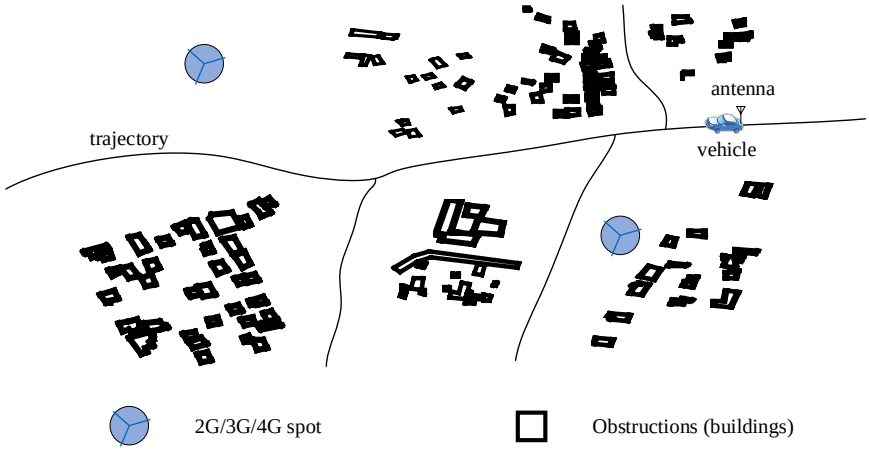

Figure 5.1.: Mobile networks GSM/UMTS/LTE on-board road vehicles.

a mobile user is in a noise- or interference limited environment. Next, an environment-specific assessment of KPI variations is necessary to facilitate the trade-off among vehicle's manufacturers and cellular operators. Furthermore, such approach needs to be compliant to all vehicular use cases and adaptable for future cellular technologies, such as 5G and beyond.

Another key aspect that simplifies the wireless designing and planning is to take into consideration a map-based approach [93]. The design of wireless links without prior knowledge of obstructions and base station locations is challenging. First, the information of the environment details, such as position, shape, size, and density of buildings, or trajectory of roads are very important in terms of modeling wireless communication systems known that obstructions add substantial penetration loss and affect the pathloss. Second, the lack of information of base station locations might lead to misinterpretation of measurement results, something crucial to avoid. Combining these two with drive test measurements simplifies the design of wireless links and network planning for vehicular use cases, particularly in urban environments (illustrated in Fig. 5.1).

Based on [29–31], the contributions of this chapter outline as in the following:

- A simple but effective approach to *characterize the VPL of road vehicles* is introduced. The idea is to collect samples of received power for two differently located users on-board a road vehicle while consistently moving along a trajectory. This is supported by measurements conducted in a live LTE 1800 network that covers a large-scale geographical area.
- A novel approach to *assess the service quality of vehicular use cases* is proposed. The key idea is to establish a common framework for service quality assessment which is independent from vehicular application. The proposed model serves

as a benchmarking baseline between road vehicle's manufacturers and cellular operators.

- An implementation of *2D Line of Sight (LOS)/Non Line of Sight (NLOS) urban maps* to evaluate LTE performance for vehicular use cases is introduced. The key idea is to correlate the RSSI-based coverage measurements to real-world geometry-based information of an urban environment. The LOS/NLOS links are derived from Open-StreetMap (OSM) [24] based on the distribution of obstacles in-between user-base station, while the exact locations of infrastructure are given from the provider. This approach supports the design of wireless links and simplify the network planning for vehicular use cases.

5.1. System Model

5.1.1. Nominal Environments

Commonly, it is not possible to perform drive tests over the same geographical area, e.g., highway tracks, that are covered by many frequency bands. In chapters Chapter 3 and Chapter 4 the discussion was based upon experiments for a mobile operator in Austria operating in two LTE bands, LTE 2600 and LTE 800. Typically, LTE 2600 is deployed in urban environments, while LTE 800 in rural environments. However, this configuration does not ensure continuity of observations over a long trajectory. Instead, here however the goal is to consider the whole range of nominal environments, i.e., urban, sub-urban, rural environments that are covered by a single frequency band. The continuity of collected observations in space and time enables the classification of nominal environments provided that in rural the coverage is the poorest compared to any other environment. This particularly is true for the best commercially available mobile cellular, i.e., LTE.

With this motivation the problem is formulated to finding strong changes of statistics of the parameter under investigation. Indeed, the coverage parameters E-UTRA RSSI or RSRP satisfy this requirement. Therefore, the problem formulates as a problem of partitioning *original time* t into m intervals (partitions). The ends of m intervals correspond to particular nominal environments identified with a subset $\mathcal{S}_i : s_{ii} \in \mathbb{R}$, where s_{ii} are its elements. The statistics of m-intervals are characterized with strong changes at the received signal denoted with r. It is worth noting, that variable t preserves the information of location, given that the vehicle moves along a trajectory. This problem motivates the usage of Information Bottleneck (IB) as discussed in Section 2.5.1. The task of aIB is to distinguish m-intervals such that

$$r \in \mathcal{S}_i, \quad \mathcal{S}_i \subseteq \mathcal{S}, \quad r \in \mathbb{R}, \quad t \in \mathbb{R}_+ \tag{5.1}$$

where $\mathcal{S}$ represents the set of all possible nominal environments. Then, the nominal environments i.e., urban, sub-urban, rural, are identified according to decreasing order of statistical average of each

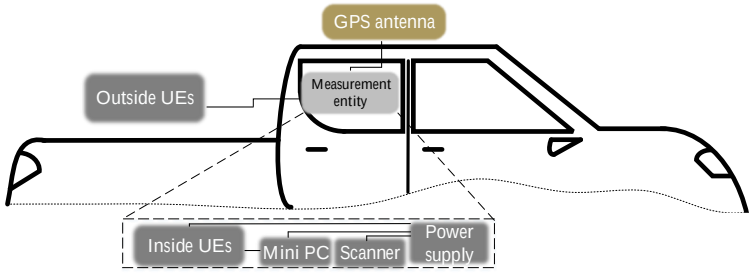

Figure 5.2.: Road vehicle under test. ©2017 IEEE [29]

interval under interest. That is to say, each unique nominal environment is identified with observed data distribution $Z^{(o)}(r)$, where $1 \leq o \leq m$, $o \in \mathbb{N}$. The procedure follows as in Section 3.1.1, where the function $\Psi(r,t) \equiv f_{JS,\pi_2}(p(r|\dot{t}_i), p(r|\dot{t}_j))$ enables the identification of the urban environment which formulates as

$$r_{MAX} = \max_{r \in Z}\{\mathbb{E}\{Z^{(1)}\}, \mathbb{E}\{Z^{(2)}\}, ..., \mathbb{E}\{Z^{(m-1)}\}, \mathbb{E}\{Z^{(m)}\}\}, \quad \forall m \in \mathbb{N} \tag{5.2}$$

and a rural environment which formulates as

$$r_{MIN} = \min_{r \in Z}\{\mathbb{E}\{Z^{(1)}\}, \mathbb{E}\{Z^{(2)}\}, ..., \mathbb{E}\{Z^{(m-1)}\}, \mathbb{E}\{Z^{(m)}\}\} \tag{5.3}$$

to represent the two most distinct environments under investigation.

5.1.2. Service Quality Assessment

Indeed, VPL is not as crucial for cars as it is for trains though. Despite this, the definition of nominal environments allows us to have a better estimation of VPL. This stems from the desire to place the vehicle in an environment with a number of multipaths as low as possible [62, 63], or inside an anechoic chamber [94] with random-LOS environment. The key problem of this chapter is demonstrated in Fig. 5.2 along with two differently located mobile users.

The goal is to compare the central tendencies of distributions of two observed data to test whether one distribution is greater or not (to answer e.g., "Is there any impairment in received power for a user outside the vehicle?", or "Is there any improvement in throughput if a user is placed outside the vehicle compared to the previous case?"). To do so, the users in Fig. 5.2 denoted as Inside User Equipment (IUE) and Outside User Equipment (OUE) which represent particular vehicular use cases.

In general, this problem is approached by using nonparametric inference where distributions and variances of both users are assumed to be unknown. Further motivation relates to various KPIs which may have very different distributions compared to the normal distribution. This restricts the

assessment and motivates the usage of nonparametric inference. Therefore, the improvement for OUE formulates by constructing binary hypothesis with WMW test as

$$\mathcal{I}_0 : \ F_{Z_I}(z) = F_{Z_O}(z) \quad \mathcal{I}_1 : \ F_{Z_I}(z) < F_{Z_O}(z) \tag{5.4}$$

where F_{Z_I} denotes CDF of the user placed inside the road vehicle, and F_{Z_O} represents CDF of the user placed outside the road vehicle. Similarly, the detect of a change for OUE formulates as

$$\mathcal{I}_0 : \ F_{Z_I}(z) = F_{Z_O}(z) \quad \mathcal{I}_1 : \ F_{Z_I}(z) \neq F_{Z_O}(z). \tag{5.5}$$

Similarly to Section 3.1.2 hold both fixed- and random treatment effect $\widehat{\Delta z}$. Therefore, no further discussion is done here. Let us now discuss explicitly the problem of assessing the improvements in received power. Transmission losses for IUE and OUE users can be estimated as in the following

$$\widehat{L_I} = -10 \log_{10} \Big(\frac{\widehat{P_{R_I}}}{\widehat{P_{T_I}}} \Big) (dB) \tag{5.6a}$$

$$\widehat{L_O} = -10 \log_{10} \Big(\frac{\widehat{P_{R_O}}}{\widehat{P_{T_O}}} \Big) (dB) \tag{5.6b}$$

where $\widehat{P_{R_O}} \in \mathbb{R}$ and $\widehat{P_{R_I}} \in \mathbb{R}$ denote the respective estimated received power and $\widehat{P_{T_O}} \in \mathbb{R}$ and $\widehat{P_{T_I}} \in \mathbb{R}$ denote the respective estimated transmitted power. Subtracting Eq. (5.6b) and Eq. (5.6a) implies an estimated power difference defined as

$$\widehat{\Delta L_{O,I}} = \widehat{L_O} - \widehat{L_I} \tag{5.7}$$

and if the below condition

$$\widehat{\Delta L_{O,I}} > 0 \Leftrightarrow \widehat{L_O} > \widehat{L_I} \tag{5.8}$$

is satisfied it indicates improvement in OUE. This further allows us the expression Eq. (5.7) to rewrite as

$$\widehat{P_{R_O}} = \widehat{P_{R_I}} + \tilde{\Delta} z \tag{5.9}$$

which exhibits a representation of the improved signal level, where $\widehat{P_{R_I}}$, $\widehat{P_{R_O}}$, and $\tilde{\Delta} z$ are estimates.

5.1.3. Small-scale Nominal Environment Measurements

The problem of small-scale nominal environment measurements, i.e., limited number of trips, arises due to observations gathered during only one measurement campaign. This is approached as an estimation problem of population distribution $Z_{I,j}$, denoted with $\tilde{Z}_{I,j}$. The idea here is to apply an estimation technique on the intervals specified from aIB instead of observations gathered over the entire highway track. Herein, let us denote with $Z_{I,j}$ and $Z_{O,j}$ the *original* sample distributions that

represent the OUE and IUE, respectively. Specifically, nonparamteric bootstrap estimators are applied to form respective bootstrap distributions denoted with $\tilde{Z}_{O,j}$, $\tilde{Z}_{I,j}$ for each nominal environment. The procedure is summarized as in the following:
(1) Let $Z_{I,j} = \{z_{j,I|1}, z_{j,I|2}, ..., z_{j,I|n_I}\}$ and $Z_{O,j} = \{z_{j,O|1}, z_{j,O|2}, ..., z_{j,O|n_O}\}$;
(2) The bootstrap sample distributions $\tilde{Z}_{I,j}$ and $\tilde{Z}_{O,j}$ are created with replacement of observations of $Z_{I,j}$ and $Z_{O,j}$, respectively. A sample (bootstrap distribution) size n_I is drawn with replacements from collection $\{z_{j,I|1}, z_{j,I|2}, ..., z_{j,I|n_I}\}$, and a sample size n_O is drawn with replacements from collection $\{z_{j,O|1}, z_{j,O|2}, ..., z_{j,O|n_O}\}$;
(3) Repeat step (2) L times to create L bootstrap resamples.
This allows us to asses the properties of the original ECDF $F_{Z_I}(z)$ and $F_{Z_O}(z)$ for each nominal environment without knowing the distributions of a particular environment. Let us denote with $\widetilde{F_{Z_I}(z)}$ and $\widetilde{F_{Z_O}(z)}$ bootstrap distributions. The sample of size n_O from $F_{Z_O}(z)$ is thus a sample of size n_O drawn with replacements from $\{z_{j,O|1}, z_{j,O|2}, ..., z_{j,O|n_O}\}$ and similarly the sample of size n_I from $F_{Z_I}(z)$ is thus a sample of size n_I drawn with replacements from $\{z_{j,I|1}, z_{j,I|2}, ..., z_{j,I|n_I}\}$. Herein, the bootstrap standard error Υ for $\tilde{\zeta_O}$ and $\tilde{\zeta_I}$ is estimated as

$$\Upsilon(\tilde{\zeta_O}) = \sqrt{\frac{1}{L}\sum_{a=1}^{L}(\tilde{\zeta_{a,O}} - \mathbb{E}(\zeta_O))^2} \tag{5.10a}$$

$$\Upsilon(\tilde{\zeta_I}) = \sqrt{\frac{1}{L}\sum_{a=1}^{L}(\tilde{\zeta_{a,I}} - \mathbb{E}(\zeta_I))^2} \tag{5.10b}$$

where

$$\mathbb{E}(\zeta_O) = \frac{1}{L}\sum_{a=1}^{L}\tilde{\zeta_{a,O}} \tag{5.11a}$$

$$\mathbb{E}(\zeta_I) = \frac{1}{L}\sum_{a=1}^{L}\tilde{\zeta_{a,I}} \tag{5.11b}$$

denotes the mean of the estimates across L bootstrap samples. Further, note that $\zeta_{1,O}, \zeta_{2,O}, ..., \zeta_{L,O}$ are produced from L sample of size n_O from the collection $\{z_{j,O|1}, z_{j,O|2}, ..., z_{j,O|n_O}\}$ and similarly $\zeta_{1,I}, \zeta_{2,I}, ..., \zeta_{L,I}$ are produced from L sample of size n_I from the collection $\{z_{j,I|1}, z_{j,I|2}, ..., z_{j,I|n_O}\}$. From this, the procedure follows the construction of multiple hypotheses $\ddot{\mathcal{I}}_{0,a,u}, \ddot{\mathcal{I}}_{1,a,u}$ as well as $\ddot{\mathcal{I}}_{0,a,r}, \ddot{\mathcal{I}}_{1,a,r}$ with $a = 1, 2, ..., L$. Thus, Eq. (5.5) combined with Eq. (5.2) now extends and for an

urban environment formulates

$$\ddot{\mathcal{I}}_{0,1,u}: \widetilde{F_{Z_{I,1,u}}}(z) = \widetilde{F_{Z_{O,1,u}}}(z) \quad \ddot{\mathcal{I}}_{1,1,u}: \widetilde{F_{Z_{I,1,u}}}(z) \neq \widetilde{F_{Z_{O,1,u}}}(z) \tag{5.12a}$$

$$\ddot{\mathcal{I}}_{0,2,u}: \widetilde{F_{Z_{I,2,u}}}(z) = \widetilde{F_{Z_{O,2,u}}}(z) \quad \ddot{\mathcal{I}}_{1,2,u}: \widetilde{F_{Z_{I,2,u}}}(z) \neq \widetilde{F_{Z_{O,2,u}}}(z) \tag{5.12b}$$

$$\vdots$$

$$\ddot{\mathcal{I}}_{0,L,u}: \widetilde{F_{Z_{I,L,u}}}(z) = \widetilde{F_{Z_{O,L,u}}}(z) \quad \ddot{\mathcal{I}}_{1,L,u}: \widetilde{F_{Z_{I,L,u}}}(z) \neq \widetilde{F_{Z_{O,L,u}}}(z) \tag{5.12c}$$

where index u stands for urban and similarly when combined with Eq. (5.3) formulates

$$\ddot{\mathcal{I}}_{0,1,r}: \widetilde{F_{Z_{I,1,r}}}(z) = \widetilde{F_{Z_{O,1,r}}}(z) \quad \ddot{\mathcal{I}}_{1,1,r}: \widetilde{F_{Z_{I,1,r}}}(z) \neq \widetilde{F_{Z_{O,1,r}}}(z) \tag{5.13a}$$

$$\ddot{\mathcal{I}}_{0,2,r}: \widetilde{F_{Z_{I,2,r}}}(z) = \widetilde{F_{Z_{O,2,r}}}(z) \quad \ddot{\mathcal{I}}_{1,2,r}: \widetilde{F_{Z_{I,2,r}}}(z) \neq \widetilde{F_{Z_{O,2,r}}}(z) \tag{5.13b}$$

$$\vdots$$

$$\ddot{\mathcal{I}}_{0,L,r}: \widetilde{F_{Z_{I,L,r}}}(z) = \widetilde{F_{Z_{O,L,r}}}(z) \quad \ddot{\mathcal{I}}_{1,L,r}: \widetilde{F_{Z_{I,L,r}}}(z) \neq \widetilde{F_{Z_{O,L,r}}}(z) \tag{5.13c}$$

where index r stands for rural environment. As next step, techniques of FDR [48, 52] to compensate for type II error are applied. Herein, as a performance metric is defined the rejection ratio for both environments as

$$\tau_u = \frac{\mathbb{P}(\text{accept } \ddot{\mathcal{I}}_{0,a,u}|z)}{\mathbb{P}(\text{accept } \ddot{\mathcal{I}}_{0,a,u}|z) + \mathbb{P}(\text{reject } \ddot{\mathcal{I}}_{0,a,u}|z)} \tag{5.14a}$$

$$\tau_r = \frac{\mathbb{P}(\text{accept } \ddot{\mathcal{I}}_{0,a,r}|z)}{\mathbb{P}(\text{accept } \ddot{\mathcal{I}}_{0,a,r}|z) + \mathbb{P}(\text{reject } \ddot{\mathcal{I}}_{0,a,r}|z)}. \tag{5.14b}$$

Rejection ratios τ_u and τ_r quantify the proportion of rejected $\ddot{\mathcal{I}}_{0,a}$s in a pool of L multiple hypotheses. The demonstrated framework allows to establish the assessment of KPIs in cellular networks on-board road vehicles.

5.2. Smartphone-based Measurement Setup

5.2.1. Measurement Track

The measurement campaign was performed in Kosovo along the route from Prishtina to Vërmica which covers approximately 100 km distance and has speed limitation of 120 km/h. The highway track is illustrated in Fig. 5.3. The campaign started from university campus in Prishtina and

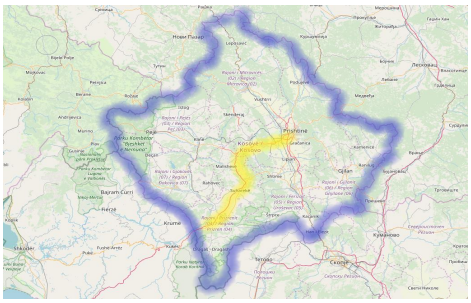

Figure 5.3.: Highlighted measurement track of the highway "Ibrahim Rugova" in Kosovo.

then led south-west along the newly constructed "Ibrahim Rugova" highway toward the Albanian border in Vërmica. This track includes several distinct areas such as cities, villages, mountains and highways. Since the LTE deployment is not fully established in this region, the changes among nominal environments are more severe, e.g., in rural areas there is poor coverage, and this satisfies our goal of modelling approximate intervals of nominal environments.

5.2.2. Smartphone Placements

Ideally, to measure the VPL is desired to compare a UE inside a vehicle to a measurement of a UE without a vehicle. However, this solution is not feasible as it is necessary to walk large distances on foot. As a trade-off solution, a OUE is mounted on the cargo area of a pickup truck as shown in Fig. 5.4a and Fig. 5.4c. This way, the approach still includes propagation effects on the vehicle, but excludes the loss from the cabin. It also allows us to measure both UE simultaneously along the same track. The IUE was placed on the passenger back-seat, i.e., within the vehicle as illustrated in Fig. 5.4b. This UE fully characterizes an indoor user, and because of additional scattering inside the vehicle's cabin, the propagation towards this user is very likely to be affected. Additionally, the inter-distance of 1 m between smartphone placements ensures both users to be highly correlated [95, 96]. Further measurement details are summarized in Table 5.1.

For some applications of drive tests, the use of omni-directional antennas is important. The authors in [98, 99] wanted to derive recommendations for operators on how to invest in infrastructure. However, the scope of this chapter aims to provide a common framework for service quality assessment which tends to serve as a benchmarking baseline for road vehicle's manufacturers and cellular operators. This is another reason why the measurement setup employs smartphones to reflect the best Quality of Experience (QoE).

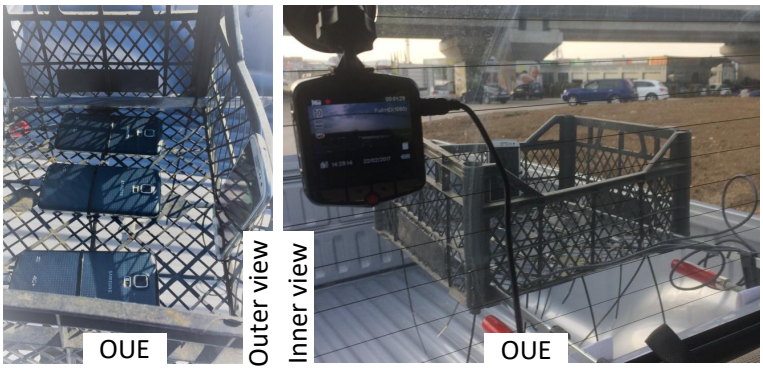

(a) Left/right: OUE, Right: Video recorder and other smartphones utilized for different purposes. ©2017 IEEE [29]

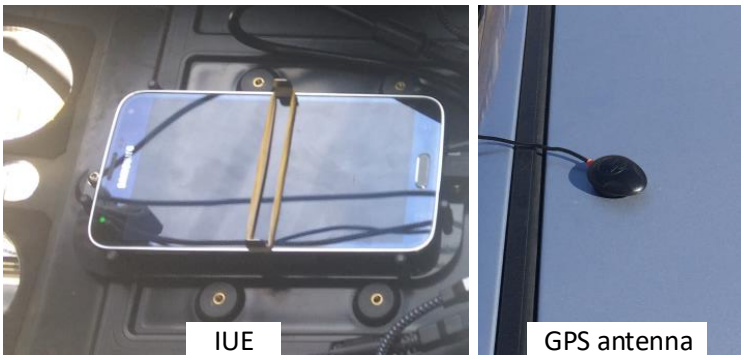

(b) Left: IUE located on passenger back-seat, Right: GPS antenna mounted on vehicle roof.

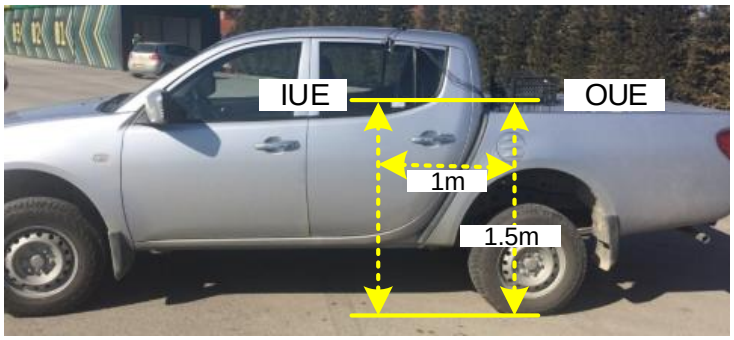

(c) Smartphone placements.

Figure 5.4.: Smartphone-based measurement setup.

Tab. 5.1.: Measurement parameters.

Parameter	Value
Location, measurement track	Kosovo, Prishtina—Vërmica
Date	22.02.2017
Frequency	1800 MHz LTE
Antenna configuration	2x2
Frequency band	15, 20 MHz
Transmitter antenna height	24, 30 m
Receiver antenna height	1.5 m
Vehicle model, Vehicle type	Mitsubishi KAOT L200, pickup truck
Average velocity	63 km/h
User equipment type	Rohde and Schwarz Swiss QualiPoc Freerider [97]
User equipment antenna pattern	omni-directional (assumed)
User equipment model	Samsung S5
GPS antenna model	NaviLOCK, Model No:NL-402U

5.2.3. Smartphone Orientations and Relevant Entities

The authors in [100–102] studied the effect of radiated performance of a smartphone device. They found that distribution of orientation angles concentrates around 0° on horizontal plane for the case of data service. This explains the reason of adjusting smartphones at this angle as it considers user's behavior to mimic *usage scenario with hands-free*.

The script-based configuration includes several user interactions such as video-streaming and file-transferring, and configured synchronous sequential tasks on both smartphones. In this way, the real-world user's behavior allows the assessment of service quality in different RF conditions on-board the vehicle. As the focus here is on scenario with hands-free, such a measurement setup mimics the *quasi-real passive usage* of end-users.

5.2.4. Measurement Configuration

The measurements are performed with Rohde and Schwarz SwissQual QualiPoc Freerider UE [97] which consists of six smartphones with measurement software, a performance logger, a mini PC, GPS positioning system, and power supply as depicted in Fig. 5.2. The number of UE is split up in two halves. Half of the UE are placed on the back-seat of the vehicle and the other half is mounted on the outside of the vehicle, in order to evaluate the penetration loss. Two UE are configured to measure UMTS voice services, two UE measure UMTS data services, and two UE measure LTE data services. KPI such as signal strength, data rate and quality of service indicators are measured and recorded. Data sessions were repeatable events carefully configured to approach a true usage scenario with File Transfer Protocol (FTP) file sizes 2 MB in uplink and 10 MB in downlink. Video-streaming sessions linked to youtube media servers were repeatably running too.

5.3. Power Difference Model

Power difference model supports the VPL characterization for the vehicle moving along the route for two different scenarios: inside the city, Prishtina (urban environment) and, outside the city, including CIDs all over the route till Vermica (suburban and rural environment). Fig. 5.5 shows the RSRP of OUE and IUE as well as for two different scenarios such as: urban environment, and suburban together with rural environment. That is to say, a deterministic model is utilized to define the borders of nominal environments. The results are provided for two different directions:
(1) Direction I – covers the route from Prishtina to Vermica;
(2) Direction II – covers the route from Vermica to Prishtina.

RSRP level in case of urban environment is largely different in terms of directions because it is not the exact same route since the goal was to cover different parts of the city. The power difference is calculated as the difference of the averaged received power in Resource Elements (REs) of OUE and IUE, $\widehat{P_{R_O}} - \widehat{P_{R_I}}$. Such a definition takes into account the VPL itself (caused mainly by vehicle glasses) as well as other propagation effects (e.g. shadowing, reflections, multipaths) that occur outside and inside of the vehicle. The power difference is expressed in terms of different cell IDs at 95-percentile Confidence Intervals (CIs). There are cases during drive test where UE are connected to different LTE CIDs depending on the direction of route. This is dependent on a large number of parameters, such as variation of cell load during the day, different time of measurements, different propagation conditions, different direction of vehicle and different vendors of LTE sites (15 MHz bandwidth of ALU and 20 MHz bandwidth of NOKIA sites). It is observed that the power difference has a peak-to-peak variation of 1.6 to 10.6 dB when estimated across the same CIDs.

As VPL is important in designing LTE networks in order to provide in-vehicle coverage, there are observed a significant number of CIDs, where the RSRP falls below -100 dBm. This is particularly severe in suburban and rural environments. Due to the impact of VPL the received power at IUE is decreased further and in some cases is similar to the cell edge conditions. This is noticeable in Fig. 5.5a-up, CID $\#14$ for suburban and rural environment.

The power differences at RSRP between directions occur due to vehicle orientation, i.e., shadowing of the antennas by the vehicle, and different propagation conditions, i.e., different time of measurements, different multipath environment. The penetration loss is defined to be a positive value according to its definition in Eq. (3.21). However, during the measurements there are some cases where the difference between sample instances yields a negative power difference.

Fig. 5.6 shows a different perspective by applying the descriptive statistics: empirical Q-Q plot of the RSRP. The 45° black solid-line is used as a reference to illustrate the difference of distributions between two users IUE and OUE. RSRP is up to 5 dB better for OUE. The Q-Q shows almost linear behavior as an indication that the pickup truck behaves linearly in terms of coverage.

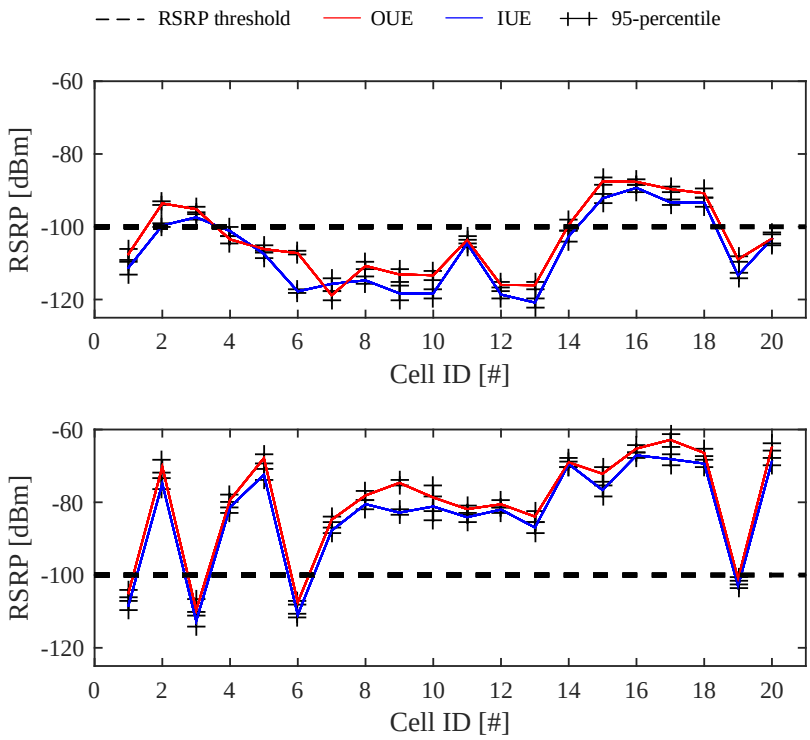

(a) Direction I: up: Sub-urban and rural, down: Urban.

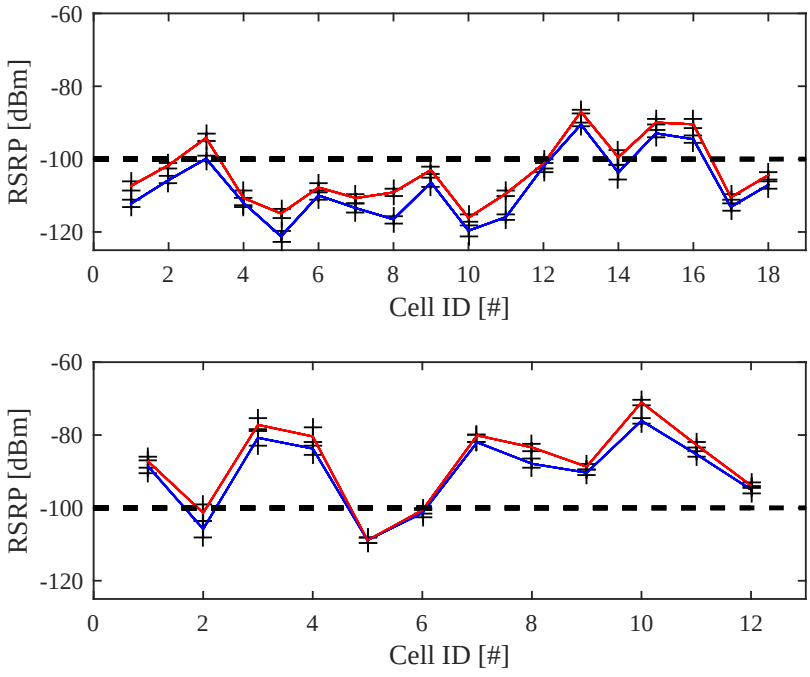

(b) Direction II: up: Sub-urban and rural, down: Urban.

Figure 5.5.: RSRP at IUE and OUE at 1800 MHz LTE. ©2017 IEEE [29]

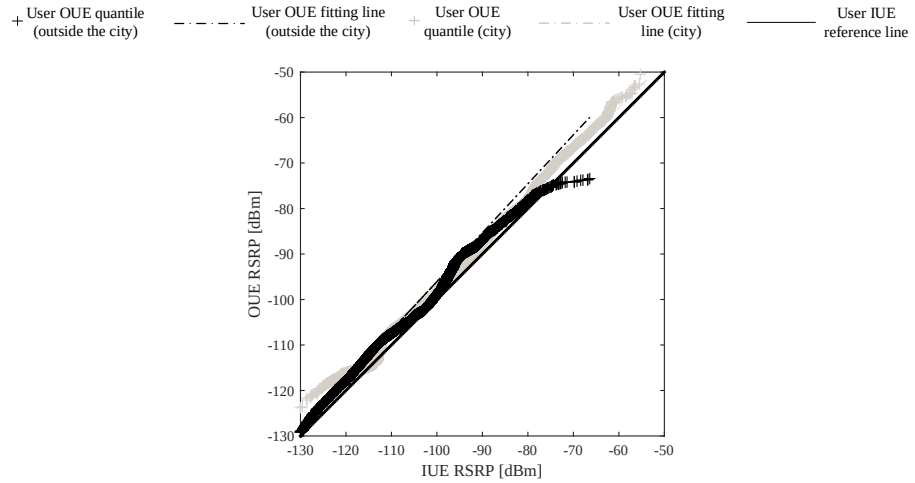

Figure 5.6.: Q-Q plot of LTE 1800 RSRP. ©2017 IEEE [29]

5.4. Service Quality Impairments for Pickup Truck Passengers

5.4.1. Trip-based Analysis

This section provides an overall evaluation of KPIs at 1800 MHz LTE. The main goal here is to show the amount of change in distributions of available KPIs by using descriptive statistics. The following KPIs are considered: RSRP, transmit power, RSRQ, and physical downlink throughput. Each Q-Q consists of a 45° straight line $f(z) = z$ which is artificially graphed to facilitate the graphical inspection. Therefore, if the points do lie above the reference line it suggests that the observations OUE come from the same distribution as observations IUE.

Fig. 5.7a exhibits a graphical representation of OUE RSRP quantile - IUE RSRP quantile. On one hand, there is slight difference in RSRP observations which implicates that the OUE distribution approximately comes from the same distribution as IUE and differ only in location, i.e., $f(z) \approx z + \Delta z$. On the other hand, the skewness slightly changes in high RSRP regime, i.e., along urban environments. This reveals the effect of VPL which impacts the IUE to receive lower RSRP values. Similarly, it is expected that the transmit power at IUE to be higher than at OUE. This is mainly impacted due to lower received power at IUE. Fig. 5.7b shows quantiles of transmit powers, which is discussed as in the following. As illustrated here, IUE quantiles are slightly higher than OUE quantiles with observations aligned over the $f(z) = z$ line with only a small location shift. Overall, this indicates similar distribution of transmit powers at both UE with only a shift in location. In high regime of transmit power above 15 dBm OUE quantiles tend to be higher or aligned over the reference line. In this regime, which is typical for rural environments, connection maintenance is desirable at both UE, thus they transmit at maximum power and attain the upper bound of transmit power.

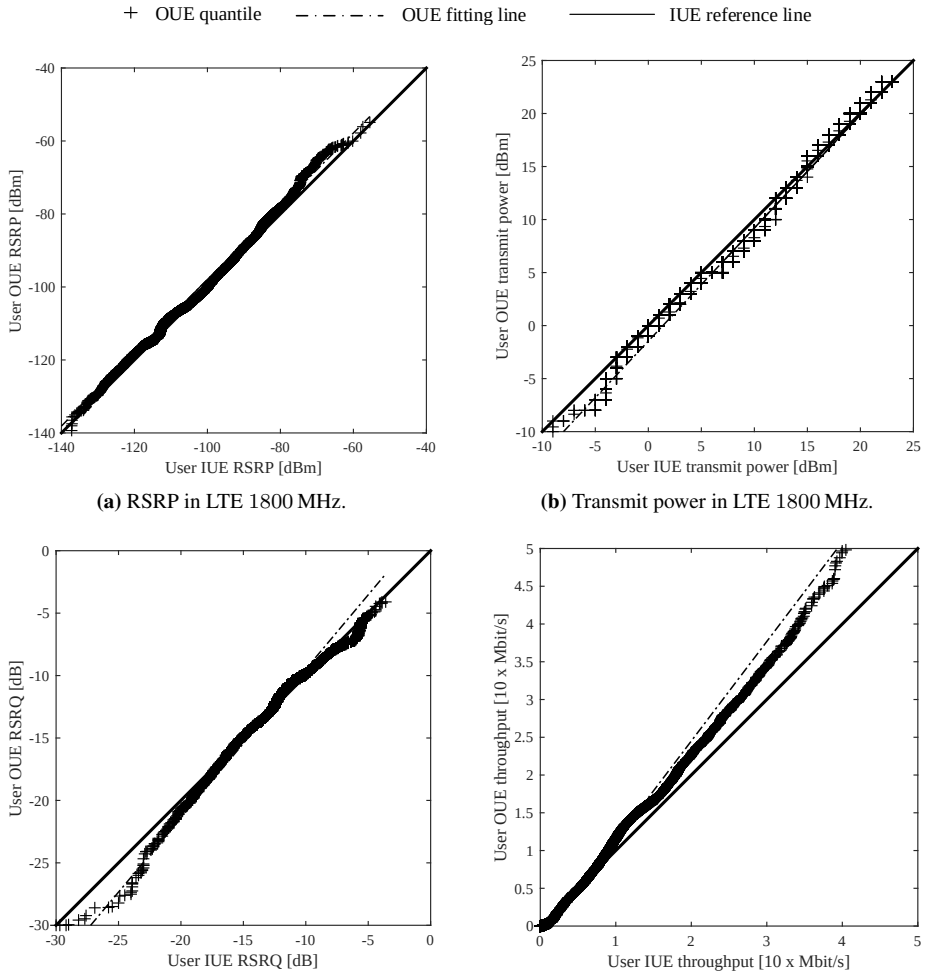

(a) RSRP in LTE 1800 MHz.

(b) Transmit power in LTE 1800 MHz.

(c) RSRQ in LTE 1800 MHz.

(d) Physical throughput in LTE 1800 MHz.

Fig. 5.7.: OUE quantile - IUE quantile: pickup truck case study.

Similar behavior is also shown in Fig. 5.7c representing RSRQ quantiles, where OUE quantiles tend to follow the $f(z) = z$ reference line. Additionally, there exist some outliers in low regime of RSRQ which are not taken into consideration known that according to 3GPP the parameter is defined up to -19.3 dB. In Fig. 5.7d are shown throughput quantiles where OUE quantiles show higher values over the whole trip. This difference starts expanding from around 20 Mbit/s and continues this trend along the quantiles collected in high regime. In this regime, the effect of rich multipath environment is further enhanced from vehicle's cabin and thus the overall physical throughput is also increased. Fitting line is not parallel compared to $f(z) = z$ reference line, and this reveals that the distributions differ both in location and skewness.

5.4.2. Map-based Analysis

2D LOS/NLOS Urban Maps

Peak-to-peak variation of power difference model along an urban environment was found to fluctuate from $1.9 - 3.9$ dB, according to Q-Q plot in Fig. 5.6. In this section, a map-based approach is applied to evaluate the LTE coverage, correlation between coverage and the density of buildings as well as wireless 2x2 MIMO transmission performance. Therefore, as a first step are implemented on Matlab 2D maps for an urban environment and then are calculated LOS/NLOS links from known measurement locations. To do so, the source map data are taken from OSM [24] and the exact location of transmitters was provided from the cellular operator. To decrease the complexity in calculating each LOS and NLOS link, the model ignores obstructions of detailed vegetation (e.g. trees, parks), specific objects on road (e.g. traffic lights), specific areas (e.g. parking lots), and considers only the obstructions caused by buildings. Large-scale analysis of 2D maps is also possible, but it is out of scope of this thesis due to the complexity issue.

Fig. 5.8 illustrates a real-world 2D map that represents the southern part of the city. The 2D map is then integrated with current base station locations of LTE live network. These are depicted with red and green circles. The campaign starts from university campus and runs towards south-west along suburbs of the city. On one hand, Fig. 5.8a shows the measured E-UTRA RSSI at IUE from field measurements. On the other hand, Fig. 5.8b shows the LOS/NLOS links derived per density of buildings, i.e. calculated number of outer walls of each building. A link is defined to be on LOS if the line that connects the mobile user and the serving base station is not intersected by more than one line, i.e. values 0 and 1. In cases where there is only one intersection, this is usually the case for urban environments when a base station is mounted on the roof of the building. Yet, this link is considered to be on LOS, whereas all other situations as NLOS links. Then, the links are paired with the measurement data for further evaluation.

The LOS links are mostly possible at the vicinity of base stations, thus, the measurement results shown in Fig. 5.8 are discussed as in the following: Mostly, the level of E-UTRA RSSI fits pretty well to the LOS/NLOS links. Overall, high levels of E-UTRA RSSI mainly correspond to LOS links. The higher the E-UTRA RSSI level on lower part of Fig. 5.8a illustrate a sub-urban environment which corresponds to LOS conditions. This stems from the fact of having less density of buildings in this area. There are cases where the matching between E-UTRA RSSI and LOS/NLOS links is not as expected. This mainly comes due to the fact that the city under analysis is partly a hilly terrain, thus the 2D geometry wrongly affects the distribution of LOS/NLOS links. Fig. 5.9 illustrates the E-UTRA RSSI with respect to outer wall distribution as well as the distance between base station and mobile user. Linear fit with a slope of -0.97 dBm/wall decrease is obtained. Additionally, high values of distances are concentrated on highest number of outer walls which also corresponds to low E-UTRA RSSI values.

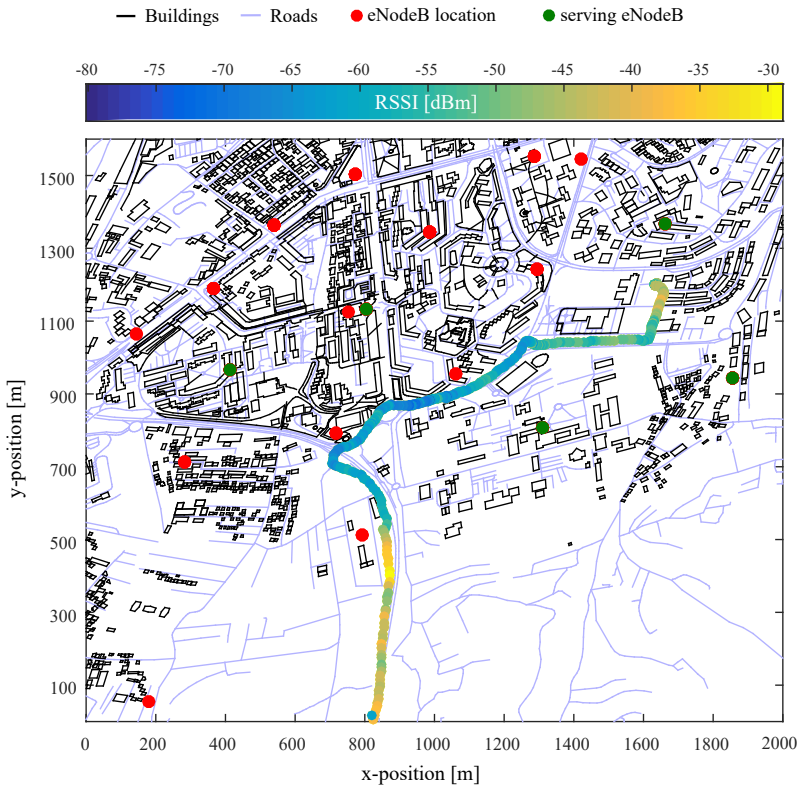

(a) E-UTRA RSSI with respect to serving eNodeB connections.

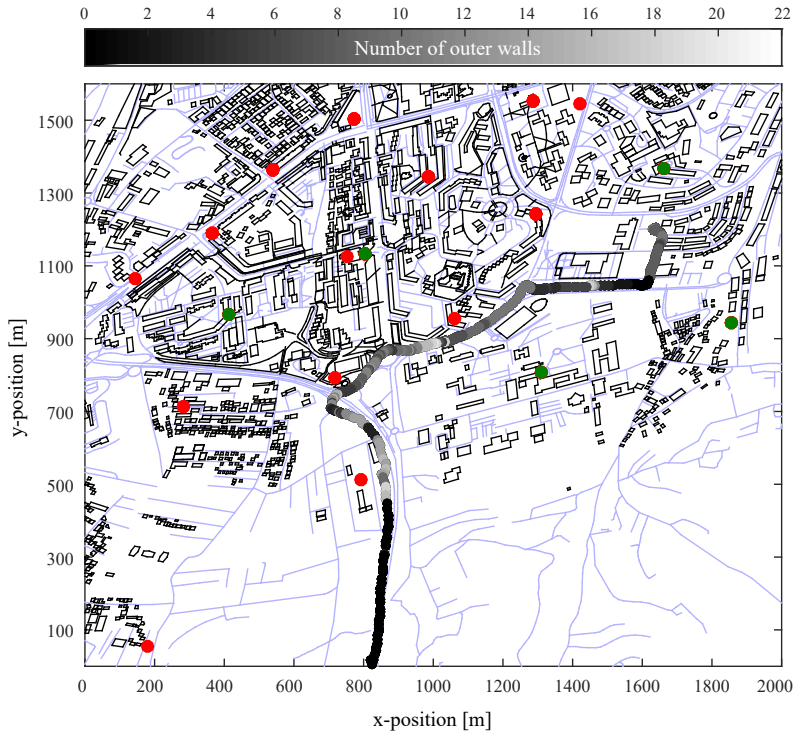

(b) Calculated LOS/NLOS links based on number of outer walls.

Fig. 5.8.: 2D LOS/NLOS urban maps. ©2017 IEEE [31]

Tab. 5.2.: The measured E-UTRA RSSI and LOS/NLOS links over distances at 95-percentile. ©2017 IEEE [31]

Parameter	LOS	NLOS
IUE E-UTRA RSSI [dBm]	-50 to -46	-58 to -56
OUE E-UTRA RSSI [dBm]	-46 to -42	-55 to -53
Distance [m]	$252 - 332$	$502 - 1010$

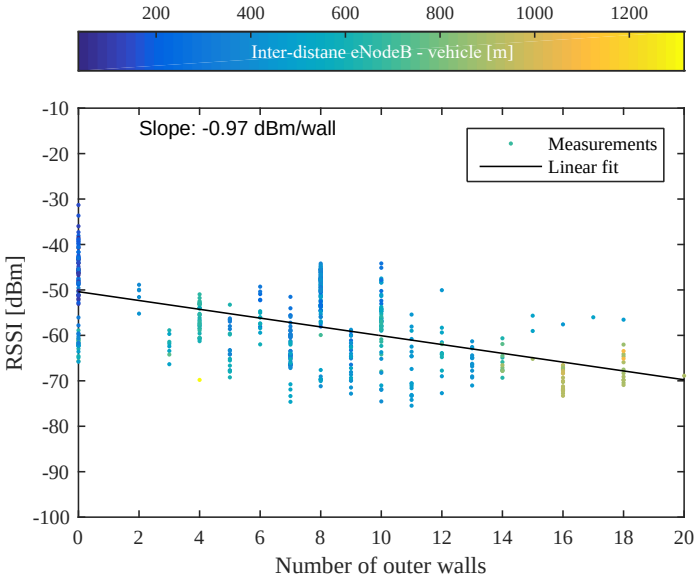

Fig. 5.9.: E-UTRA RSSI at IUE with respect to number of outer walls and inter-distance eNodeB - UE. ©2017 IEEE [31]

Table 5.2 summarizes some remarkable results: First, on one hand, the LOS links are concentrated on distances up to 332 m which is considered the vicinity of base stations. On the other hand, the NLOS links dominate statistics with 95-percentile ranging from $502 - 1010$ m. Second, the level of E-UTRA RSSI under LOS conditions is significantly stronger than NLOS. Therefore, the presented measurement results along with the implementation aim to serve the cellular operators for the purpose of planning and designing their networks. The LOS/NLOS maps are particularly very important on 2D/3D channel modelling as well as reducing the dependence on drive test measurements of 4th generation of mobile networks (4G) and next generation networks such as 5G and beyond.

MIMO Channel Rank

The knowledge of distribution of obstructions between a serving base station and a mobile user as well as LOS/NLOS conditions give rise to diversity-multiplexing trade-off. In this context, the channel rank analysis is crucial. This is elaborated in the following for both UE as depicted in Fig. 5.5. The maximum transmission rank of 2x2 MIMO system is two, thus multiplexing gains

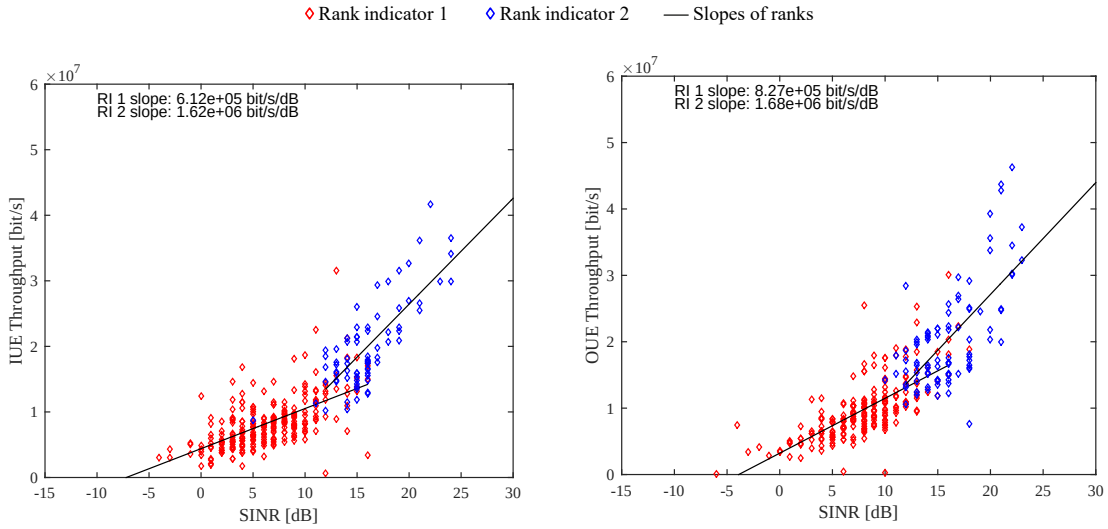

(a) IUE throughput.

(b) OUE throughput.

Fig. 5.10.: Throughput with respect to Signal-to-Interference-and-Noise Ratio (SINR) and Rank Indicator (RI). ©2017 IEEE [31]

are theoretically achievable. Fig. 5.10 illustrates the RI recorded every 500 ms. Herein, Fig. 5.10a shows the SINR distribution of IUE, whereas Fig. 5.10b the distribution of OUE. The RIs 1 and 2 provide slightly higher throughput at OUE. This way, OUE outperforms IUE in terms of diversity and multiplexing gains. This difference impacts the IUE to experience 1.4 Mbit/s average loss in achievable throughput.

5.4.3. Environment-based Analysis

In this section are presented the measurement results and the application of aIB algorithm to classify nominal environments, particularly urban and rural. Fig. 5.11 shows the measurement results of RSRP with respect to time for IUE and OUE. Herein, the number of m-intervals is set to 4 to classify nominal environments that show dissimilar statistics as discussed in Section 5.1.1. The reason of choosing such m is because the pattern of measurement track follows roughly this configuration. Among other, the pattern corresponds to urban and rural environments identified with subsets $\mathcal{S}_1$ and $\mathcal{S}_3$, respectively. The aIB algorithm is bottom-up approach, meaning that subsets $\{\mathcal{S}_3, \mathcal{S}_4\}$ are statistically closer than any other combination. The ordering is illustrated in Fig. 5.11 on top of *aIB classification line*. It can also be observed that the measurement results are in good agreement among IUE RSRP and OUE RSRP as can be noticed from values on bottom of aIB classification line.

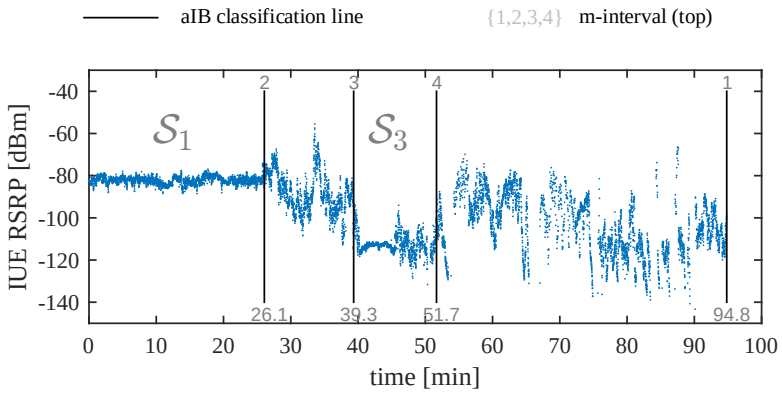

(a) IUE RSRP.

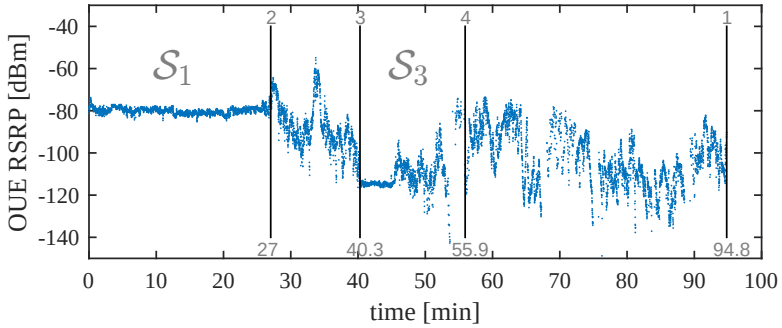

(b) OUE RSRP.

Fig. 5.11.: Nominal environment classification.

Service Quality Assessment

In Table 5.3 are provided the rejection ratios according to the definition in Eq. (5.14b). Each environment consists of $L = 10^4$ multiple hypotheses which corrsponds to L bootstrap samples. The focus here is on two most distinct environments, $\mathcal{S}_1$ and $\mathcal{S}_3$ representing urban and rural, respectively. Nondirectional hypothesis testing is applied for all KPIs. One one hand, the rejection ratio τ is maximum for all KPIs in urban environment according to the results summarized in Table 5.3. This result reflects the effect of VPL by fully rejecting all null hypotheses at significance level of $\alpha = 0.05$. On the other hand, no matter whether the uplink power is high or low, it is mostly on battery-saving state by triggering both UE to transmit at low power levels.

The rejection ratio for a rural environment starts to decrease for SINR, throughput as well as RSRP. Mostly, RSRQ and SINR show similar behaviors, however it is important to note that for OUE both KPIs are slightly worse than at IUE. To some extent, this results is counter-intuitive and most likely occurs due to higher interference level at OUE which does not affect similarly IUE along rural environments. Anyways, this is not too severe according to the obtained CIs in Table 5.4. Despite this, the CIs shall not be directly paired with rejection ratios. During situations with high variation in large-scale fading, e.g. rural environment, both UE tend to maintain good quality connection by transmitting at maximum power of around 22 dBm.

Fig. 5.12 illustrates the adjusted p-values as a function of the arranged hypotheses. The adjustment of p-values is controlled with Benjamini-Hochberg (BH) decision line denoted as BH threshold, where the rejection and acceptance regions are modeled with adjusted p-values located under and above this line, respectively.

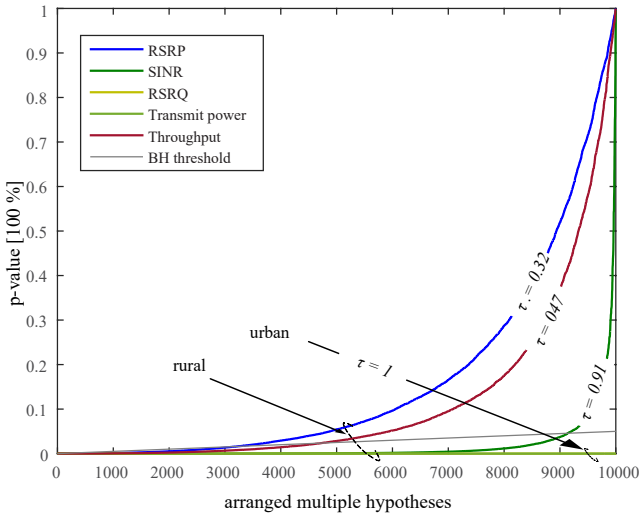

Fig. 5.12.: Rejection ratio.

Tab. 5.3.: Rejection ratios obtained from asymptotic p-values with adjustment at type I error $\alpha = 0.05$ and the number of hypotheses $M = 10^4$. The rejection ratio is denoted with τ_u and τ_r which stands for distributions of pair of the users (Z_O, Z_I) in urban and rural environments.

	LTE 1800				
	RSRP	SINR	RSRQ	T_x	R
τ_u	1	1	1	1	1
τ_r	0.32	0.91	1	1	0.47

Tab. 5.4.: Confidence intervals at mean for IUE and OUE denoted with ξ_I and ξ_O, respectively.

	LTE 1800									
	RSRP		SINR		RSRQ		T_x		R	
	ξ_I	ξ_O	ξ_I	ξ_O	ξ_I	ξ_O	ξ_I	ξ_O	ξ_I	ξ_O
$\mathcal{S}_1$	[-82.1,-82.02]	[-80.04,-79.94]	[3.35,3.51]	[7.1,7.25]	[-11.5,-11.4]	[-10.6,-10.5]	[7.4,7.8]	[6.6,7.1]	[10.8,11]	[13.35,13.65]
$\mathcal{S}_3$	[-111.68,-110.85]	[-110.77,-109.95]	[3.7,4.25]	[3.3,3.87]	[-12.55,-12.31]	[-13,-12.75]	[21.6,21.8]	[21.3,21.5]	[5.85,6.27]	[5.75,6.22]

5.5. Summary

In this chapter, a simple method of power-difference between two closely UE is introduced to characterize the VPL. The approach applies a CID-dependent model of two UE moving along deterministic trajectories that cover the entire range of nominal environments. Despite not claimed to be environment-related, the results suggest that overall peak-to-peak variation of power-difference fluctuates from $1.6 - 10.6$ dB. It is observed that KPIs tend to follow distributions that mostly change in statistical location being almost linearly correlated.

Supported by the fact of a network being not fully deployed and operating only in a single frequency band, it is applied an approach based on information theory to distinguish among nominal environments. This approach enables the environment-dependent assessment of service quality on-board road vehicles. Motivated by this classification, a combination of nonparametric- hypothesis testing and bootstrap is introduced to tackle the problem of assessment and small-scale measurements. The proposed theoretical approach aims to simplify the trade-off among road vehicle's manufacturers and cellular operators. Therefore, it aims to serve as benchmarking baseline for current and future cellular networks on-board road vehicles.

2D maps were implemented to extract the information of LOS/NLOS links. This is driven by real-world measurements and exact locations of infrastructure. Such a combination is a powerful tool to evaluate and estimate performance of vehicular use cases. It is observed that there exist high correlation between distribution of outer walls to coverage measurements. The aim of 2D LOS/NLOS urban maps is to facilitate modelling, planning and designing of wireless networks for dense scenarios.

Self-critically considering the contributions of this chapter, further ideas may be considered. First,

the existing VPL classical model is simplistic: concentrated on CID statistics, and evaluated on a particular road vehicle. However, the vehicle manufacturers design the road vehicles according to the needs and preferences of a driver. It is also expected that future road vehicles to be manufactured with metal coated windows to reduce the heat loss from leaking outside and increase thermal insulation to penetrate inside the vehicle. Consequently, these issues can possibly produce different descriptive statistics when a IUE is compared against a OUE. Although this issue is considered in Chapter 3, yet it analyses a fundamentally different type of vehicle, such as a train. Second, the implemented 2D LOS/NLOS urban maps can be mapped with drive tests and distribution of LOS/NLOS links. Yet, the problem becomes rather complex when cell load-related KPIs are analyzed. Operational mobile networks are a big impediment to this approach when cell load is unknown.

6

Conclusions

Within the last two decades, the rapid increase in speed of railway vehicles has largely closed the gap in competitiveness between trains and other transportation systems in regional travel. Today, on business or leisure, a tremendous large number of passengers no longer decide to travel by train or plane because of time spent to reach the destination, but rather their choices are influenced by the variety and quality of offered telecommunication services. On one hand, this has motivated the automotive industry and railway operators to closely collaborate with telecommunication providers, while on the other hand, has driven the research community to pursue efficient solutions to meet the increasing demands of mobile users.

Two promising solutions to increase the coverage and data rates for mobile users on-board High Speed Trains (HSTs) are either actively enhancing the signals at rooftop antennas or passively enhancing them by structural changes in the vehicle body. However, their benefits to the smartphone users in operational cellular networks and non-stationary scenarios have been little understood in literature. This has motivated this thesis to investigate the advantages of both solutions as well as establish methodologies to benchmark them.

The main contribution of this thesis is the development of new techniques in assessing improvements and impairments in service quality parameters represented by Key Performance Indicators (KPIs). While the practical concepts claim significant improvements in service quality, their applied theoretical concepts on real-world data sets with application of advanced statistical methods are of equal importance. In the following are highlighted the contributions of this thesis:

- Descriptive statistics reveal the nonlinear behavior of Amplify-and-Forward Repeater (AFR) due to RF circuit constraints and power transmission limits. This is valid for inter-city Railjet (RJ) train as well as regional Cityjet (CJ) train.
- Descriptive statistics reveal nearly the linear behavior of Frequency Selective Surfaces (FSSs) over a large dynamic range of wave amplitudes. This is valid for the RJ train.
- Inferential statistics evidence a strong significance that support the hypothesis for coverage improvements in KPIs when the RJ train is equipped with AFRs.
- Inferential statistics support the hypothesis that equipping RJ trains with FSSs improves coverage for the observed KPIs.

- Coverage improvements are lower for FSS-aided RJ train compared to the AFR-aided RJ train.
- The AFR fundamentally influences Multiple-Input Multiple-Output (MIMO) achievable data rates which leads to improved low data rates only.
- The FSSs do support MIMO transmissions exhibiting higher performance gains in a rich scattering environment.
- The AFR-aided CJ is not seen as a long-term solution knowing that dedicated infrastructure is expected to be deployed along regional railway tracks.
- The CJ train shows lower Vehicle Penetration Loss (VPL) than the RJ train.
- 2D Line of Sight (LOS)/Non Line of Sight (NLOS) maps facilitate the investigation of service quality impairments for mobile users inside a pickup truck. They convert into a powerful analytical tool when coupled with exact infrastructure locations and drive tests.
- A common assessment method composed of rank-based nonparametric inference and nonparametric bootstrap is proposed. The method allows to mimic small-scale measurements, such as regional travel, and short-time experiments, such as voice- or data sessions.

The applied theoretical framework in this dissertation along with measurement campaigns conducted in high mobility scenarios provide new concepts for the analysis of mobile user performance in operational cellular networks. Nonparametric inference promotes an estimation method of statistical treatment effect, which is a robust solution to challenges influenced by operational networks and measurement limitations. I am therefore confident that this dissertation provides a valuable contribution towards investigating, evaluating, and estimating improvements and impairments of Key Performance Indicators. This enables the assessment of Amplify-and-Forward Repeater and Frequency Selective Surface behaviors on-board railway vehicles as well as related issues on-board road vehicles.

Despite the careful statistical design along with descriptive evaluation applied in this dissertation, further ideas may be considered to promote investigations on the behavior of AFR and FSS. For instance, stationary traffic conditions do not dominate statistics when analyzed over a predefined regional travel. However, such scenarios are likely to support investigation on various use cases, e.g., planned stops in train stations, emergency stops, or unplanned stops in random locations of a railway track. Other optimal solutions could potentially be considered on-board HSTs as well. Nevertheless, it is crucial to develop network architectures that provide dependable connectivity for people on the move.

A

List of Abbreviations

3GPP	3rd Generation Partnership Project
4G	4th generation of mobile networks
5G	5th generation of mobile networks
AFR	Amplify-and-Forward Repeater
AoA	Angle of Arrival
BH	Benjamini-Hochberg
BS	Base Station
CCDF	Complementary Cumulative Distribution Function
CDF	Cumulative Distribution Function
CID	Cell ID
CI	Confidence Interval
CJ	Cityjet
CQI	Channel Quality Indicator
ECDF	Empirical Cumulative Distribution Function
ECSEN	European Committee for Standardization EN
ETSI	European Telecommunications Standard Institute
EcN0	Energy-per-Chip-over-Noise Ratio
FDD	Frequency Division Duplex
FDR	False Discovery Rate
FSS	Frequency Selective Surface
FTP	File Transfer Protocol
FWER	Family-wise Error Rate
GSM	Global System for Mobile Communications
HST	High Speed Train
HTTP	HyperText Transfer Protocol
IB	Information Bottleneck
IR	Infrared
ITS	Intelligent Transportation System
ITU	International Telecommunications Union
IUE	Inside User Equipment

KPI	Key Performance Indicator
LF	Logistic Function
LOS	Line of Sight
LTE	Long Term Evolution
MIMO	Multiple-Input Multiple-Output
MS	Mobile Station
NLOS	Non Line of Sight
OECD	Organisation for Economic Cooperation and Development
OSM	Open-StreetMap
OUE	Outside User Equipment
PDSCH	Physical Downlink Shared Channel
Q-Q	Quantile-Quantile
QoE	Quality of Experience
QoS	Quality of Service
R2R	Roll2Rail
RAU	Remote Antenna Unit
RC	Radiating Cable
RE	Resource Element
RI	Rank Indicator
RJ	Railjet
RSCP	Reference Signal Code Power
RSRP	Reference Signal Received Power
RSRQ	Reference Signal Received Quality
RSSI	Received Signal Strength Indicator
SINR	Signal-to-Interference-and-Noise Ratio
SISO	Single-Input Single-Output
TCS	Train Communication System
UE	User Equipment
UMTS	Universal Mobile Telecommunications System
UV	Ultraviolet
VPL	Vehicle Penetration Loss
WLAN	Wireless Local Area Network
WMW	Wilcoxon-Mann-Whitney
aIB	Agglomerative Information Bottleneck
gLF	Generalized Logistic Function
pdf	Probability Density Function
pmf	Probability Mass Function

Bibliography

[1] (2011). Interantional Transport Forum. [Online] http://www.itf-oecd.org/sites/default/files/docs/11outlook.pdf.

[2] *IEEE 802.11: Wireless LANs*, IEEE Standard Association, 2012.

[3] J. P. Conti, "Hot Spots on Rails", *IEEE Communications Engineer*, vol. 3, no. 5, pp. 18–21, Oct. 2005.

[4] H. Echensperger, "Railnet: High-Speed Internet on High-Speed train", in *Presented at the IET Seminar: Broadband on Trains*, Feb. 2007.

[5] (2019). [Online] https://www.oebb.at/en/reiseplanung-services/im-zug/wlan-im-zug.html.

[6] (2018). [Online] https://www.chroniclelive.co.uk/business/business-news/nomad-digital-strikes-deal-durhams-13727893.

[7] (2019). Acorde - broadband railway internet access on high speed trains via satellite links. [Online] https://www.acorde.com.

[8] B. Lannoo, D. Colle, M. Pickavet, and P. Demeester, "Radio-over-fiber-based solution to provide broadband internet access to train passengers [topics in optical communications]", *IEEE Communications Magazine*, vol. 45, no. 2, pp. 56–62, Feb. 2007.

[9] M. Müller, M. Taranetz, and M. Rupp, "Providing current and future cellular services to high speed trains", *IEEE Communications Magazine*, vol. 53, no. 10, pp. 96–101, Oct. 2015.

[10] M. Müller, M. Taranetz, and M. Rupp, "Performance of remote unit collaboration schemes in High Speed Train scenarios", in *82nd IEEE Vehicular Technology Conference (VTC-Fall)*, Sep. 2015.

[11] M. Aguado, O. Onandi, P. S. Agustin, M. Higuero, and E. Jacob Taquet, "Wimax on rails", *IEEE Vehicular Technology Magazine*, vol. 3, no. 3, pp. 47–56, Sep. 2008.

[12] B. Wilson. (2005). Rail internet access picks up speed. [Online] http://news.bbc.co.uk/2/hi/business/4363196.stm.

[13] G. P. White and Y. V. Zakharov, "Data communications to trains from high-altitude platforms", *IEEE Transactions on Vehicular Technology*, vol. 56, no. 4, pp. 2253–2266, Jul. 2007.

[14] D. J. Cree and L. J. Giles, "Practical Performance of Radiating Cables", *Radio and Electronic Engineer*, vol. 45, no. 5, pp. 215–223, May 1975.

[15] T. Y. and, "Train radio system using leaky coaxial cable", in *34th IEEE Vehicular Technology Conference*, vol. 34, May 1984, pp. 43–48.

[16] B. Kurt, E. Zeydan, U. Yabas, I. A. Karatepe, G. K. Kurt, and A. T. Cemgil, "A Network Monitoring System for High Speed Network Traffic", in *2016 13th Annual IEEE International Conference on Sensing, Communication, and Networking (SECON)*, Jun. 2016, pp. 1–3.

[17] A. Botha, K. Calteaux, M. Herselman, A. Grover, and E. Barnard, "Mobile User Experience for Voice Services: A Theoretical Framework", in *2012 3rd International Conference on Mobile Communication for Development*, Feb. 2012.

[18] C. Wang, A. Ghazal, B. Ai, Y. Liu, and P. Fan, "Channel measurements and models for high-speed train communication systems: A survey", *IEEE Communications Surveys Tutorials*, vol. 18, no. 2, pp. 974–987, Secondquarter 2016.

[19] Y. Wenn, Y. Ma, X. Zhang, X. Jin, and F. Wang, "Channel fading statistics in high-speed mobile environment", in *2012 IEEE-APS Topical Conference on Antennas and Propagation in Wireless Communications (APWC)*, Sep. 2012, pp. 1209–1212.

[20] J. Wu and P. Fan, "A survey on high mobility wireless communications: Challenges, opportunities and solutions", *IEEE Access*, vol. 4, pp. 450–476, 2016.

[21] F. J. Martin-Vega, I. M. Delgado-Luque, F. Blanquez-Casado, G. Gomez, M. C. Aguayo-Torres, and J. T. Entrambasaguas, "LTE Performance over High Speed Railway Channel", in *2013 IEEE 78th Vehicular Technology Conference (VTC Fall)*, Sep. 2013, pp. 1–5.

[22] P. A. Laplante and F. C. Woolsey, "IEEE 1472: An Open-source Communications Protocol for Railway Vehicles", *IT Professional*, vol. 5, no. 6, pp. 12–16, Nov. 2003.

[23] I. Beeby, "Demystifying Wireless Communications for Trains", in *Presented at the BWCS Train Communication Systems*, Jun. 2006.

[24] (2018), [Online]. Available: `https://www.openstreetmap.org/`.

[25] T. Berisha, P. Svoboda, S. Ojak, and C. F. Mecklenbräuker, "Seghyper: Segmentation- and Hypothesis based Network Performance Evaluation for High Speed Train Users", in *2017 IEEE International Conference on Communications (ICC)*, May 2017, Paris, France, pp. 1–6.

[26] T. Berisha, T. Blazek, and C. F. Mecklenbräuker, "Measurement and Analysis of Cellular Networks under Mobility: Investigation of Change Detection", in *VTC Fall 2018 - IEEE 88th Vehicular Technology Communications*, Sep. 2018, Chicago, IL, USA.

[27] T. Berisha and C. F. Mecklenbräuker, "Operational Service Quality Assessment on-board Railway Vehicles", in *IEEE ACCESS 5G and Beyond Mobile Wireless Communications Enabling Intelligent Mobility*, May 2019 (submitted).

[28] T. Berisha and C. F. Mecklenbräuker, "Smartphone-based Measurements on-board FSS-aided Railway Vehicles", in *13th European Conference on Antennas and Propagation (EuCAP)*, Mar. 2019, Krakow, Poland, pp. 1–5.

[29] T. Berisha, G. Artner, B. Kransiqi, B. Duriqi, M. Mucaj, S. Berisha, P. Svoboda, and C. F. Mecklenbräuker, “Measurement and Analysis of LTE Coverage for Vehicular Use Cases in Live Networks”, in *IEEE APWC - APS Topical Conference on Antennas and Propagation in Wireless Communications*, Sep. 2017, Verona, Italy.

[30] T. Berisha and C. F. Mecklenbräuker, “Modeling and Evaluation of Uplink and Downlink KPI variations using Information Bottleneck and Non-parametric Hypothesis”, in *BalcanCom 2018*, May 2018, Podgorica, Montenegro.

[31] T. Berisha and C. F. Mecklenbräuker, “2D LOS/NLOS Urban Maps and LTE MIMO Performance Evaluation for Vehicular Use Cases”, in *IEEE VNC - Vehicular Networking Conference*, Nov. 2017, Torino, Italy.

[32] M. Natrella, *Engineering Desing Handbook - Experimental Statistics (Section 4)*. Statistical Engineering Laboratory, National Bureau of Standards, 1969.

[33] W. Dixon and F. Massey, *Introduction to Statistical Analysis*. New York, McGraw-Hill, 1969.

[34] D. J. Sheskin, *Handbook of Parametric and Nonparametric Statistical Procedures*. A Chapman & Hall, 2011.

[35] G. W. Corder and D. I. Foreman, *Non-parametric Statistics for Non-Statisticians*. John Wiley and Sons, Inc, 20109.

[36] S. Bonnini, L. Corain, M. Marozzi, and L. Salmaso, *Non-parametric Hypothesis Testing*. Wiley Series in Probability and Statistics, 2014.

[37] M. Tate and R. Clelland, *Non-parametric and Shortcut Statistics*. Interstate Printers and Publishers, 1957.

[38] 3GPP TS 125.214, “Universal Mobile Telecommunications System (UMTS); Physical Layer Procedures (FDD)”, Tech. Rep. v8.2.0, Oct. 2008.

[39] 3GPP TS36.214, “E-UTRA Physical Layer Measurements”, Tech. Rep. v13.0.0, Dec. 2015.

[40] 3GPP TS 136.213, “LTE; Evolved Universal Terrestrial Radio Access (E-UTRA); Physical Layer Procedures”, Tech. Rep. v13.2.0, Dec. 2016.

[41] H. O. Hartley, “The Maximum F-ratio as a Short-cut Test for Heterogeneity of Variance”, *Biometrika*, vol. 37, no. 3/4, pp. 308–312, Dec. 1950.

[42] G. D. Ruxton, *Behavioral Ecology: The unequal Variance t-test is an underused alternative to Student’s t-test and the Mann-Whitney U test*. Oxford academic, 2006.

[43] C. Feng, H. Wang, N. Lu, and X. M. Tu, “Log transformation: Application and Interpretation in Biomedical Research”, 2012.

[44] E. L. Lehmann, “Nonparametrics: Statistical Methods based on Ranks”, *Springer*, 2006.

[45] F. Wilcoxon, “Individual Comparisons by Ranking Methods”, *Biometrics Bulletin*, vol. 1, no. 6, pp. 80–83, Dec. 1945.

[46] M. Hollander, D. Wolfe, and E. Chicken, *Nonparametric Statistical Methods*. John Wiley and Sons, 2014.

[47] J. D. Gibbons and S. Chakraborti, *Nonparametric Statistical Inference*. Marcel Dekker, 2003.

[48] Y. Hochberg and A. Tamhane, *Multiple Comparison Procedures*. John Wiley&Sons, 1987.

[49] D. Saville, "Multiple Comparison Procedures: The Practical Solution", *The American Statistician*, vol. 44, pp. 174–180, 1990.

[50] R. Simes, "An Improved Bonferroni Procedure for Multiple Tests of Significance", *Biometrika*, vol. 73, pp. 751–754, Dec. 1986.

[51] Y. Hochberg, "A sharper Bonferroni Procedure for Multiple Tests of Significance", *Biometrika*, vol. 75, pp. 800–803, 1988.

[52] Y. Benjamini and Y. Hochberg, "Controlling the False Discovery Rate: A Practical and Powerful Approach to Multiple Testing", *Journal of the Royal Statistical Society, Series B*, pp. 289–300, 1995.

[53] F. Pereira, N. Tishby, and L.Lee, "Distributional Clustering of English Words", *Annual Meeting of the Association for Computational Linguistics*, pp. 183–190, 1993.

[54] N. Tishby, F. C. Pereira, and W. Bialek, "The Information Bottleneck Method", in *Proc. 37th Allert. Conf. Commun. Control Comput.*, Apr. 1999, pp. 368–377. arXiv: `0004057 [physics]`.

[55] L. D. Baker and A.K.McCallum, "Distributional Clustering of Words for Text Classificaiton", 1998.

[56] T. Hofmann, J.Puzicha, and M. Jordan, "Learning from Dyadic Data".

[57] N. Slonim and N. Tishby, "Agglomerative Information Bottleneck", *Adv. Neural Inf. Process. Syst.*, pp. 617–623, 2000.

[58] J. Lin, "Divergence Measures based on the Shannon entropy", *IEEE Trans. Inf. Theory*, vol. 37, no. 1, pp. 145–151, 1991.

[59] (2018). Roll2rail. [Online] `http://roll2rail.eu`.

[60] *Railway Applications - Classification System for Railway Vehicles*, IEC EN 15380-4, 2013.

[61] D.J.Cichon and T. Kuerner, "Propagation Prediction Models", COST Telecom Secretariat, Brussels, Belgium, COST 231 Final Report, Tech. Rep., May 1999, pp. 1–5.

[62] M. Lerch, P. Svoboda, S. Ojak, M. Rupp, and C. Mecklenbraeuker, "Distributed Measurements of the Penetration Loss of Railroad Cars", in *2017 IEEE 86th Vehicular Technology Conference (VTC-Fall)*, Sep. 2017, pp. 1–5.

[63] U. T. Virk, K. Haneda, V. M. Kolmonen, P. Vainikainen, and Y. Kaipainen, "Characterization of Vehicle Penetration Loss at Wireless Communication Frequencies", in *The 8th European Conference on Antennas and Propagation (EuCAP 2014)*, Apr. 2014, pp. 234–238.

[64] E. Tanghe, W. Joseph, L. Verloock, and L. Martens, “Evaluation of Vehicle Penetration Loss at Wireless Communication Frequencies”, *IEEE Transactions on Vehicular Technology*, vol. 57, no. 4, pp. 2036–2041, Jul. 2008.

[65] R. Merz, A. Schumacher, N. Jamaly, D. Wenger, and S. Mauron, “A Measurement Study of MIMO Support with Radiating Cables in Passenger Rail Cars”, in *2015 IEEE 81st Vehicular Technology Conference (VTC Spring)*, May 2015, pp. 1–5.

[66] M. Tolstrup, *Indoor Radio Planning*. John Wiley&Sons, 2015.

[67] T. Berisha, P. Svoboda, S. Ojak, and C. F. Mecklenbräuker, “Cellular Network Quality Improvements for High Speed Train Passengers by on-board Amplify-and-Forward Relays”, in *13th International Symposium on Wireless Communication Systems (ISWCS)*, Sep. 2016, Poznan, Poland, pp. 325–329.

[68] T. Berisha, P. Svoboda, S. Ojak, and C. F. Mecklenbräuker, “Benchmarking In-Train Coverage Measurements of Mobile Cellular users”, in *VTC Fall 2017 - IEEE 86th Vehicular Technology Communications*, Sep. 2017, Toronto, Canada.

[69] J. Cohen, “Statistical Power Analysis for the Behavioral Sciences”, *Academic Press, New York*, 1988.

[70] M. Lerch, P. Svoboda, D. Maierhofer, J. Resch, A. Brantner, V. Raida, and M. Rupp, “Measurement based Modelling of In-Train Repeater Deployments”, in *2019 IEEE 89th Vehicular Technology Conference (VTC-Spring)*, 2019, pp. 1–5.

[71] (2018). [Online] `http://www.oebb.at/en/leistungen-und-services/railjet`.

[72] (2018). [Online] `http://www.oebb.at/en/leistungen-und-services/cityjet`.

[73] (2018). [Online] `https://www.keysight.com`.

[74] J. Garcia, S. Alfredsson, and A. Brunstrom, “Examining Cellular Access Systems on Trains: Measurements and Change Detection”, in *2017 Network Traffic Measurement and Analysis Conference (TMA)*, Jun. 2017, pp. 1–6.

[75] J. Garcia, S. Alfredsson, and A. Brunstrom, “Train Velocity and Data Throughput - A Large Scale LTE Cellular Measurement Study”, in *VTC Fall 2017 - IEEE 86th Vehicular Technology Communications*, 2017.

[76] P. Almers, F. Tufvesson, and A. F. Molisch, “Measurement of Keyhole effect in a Wireless Multiple-input Multiple-output (mimo) Channel”, *IEEE Communications Letters*, vol. 7, no. 8, pp. 373–375, Aug. 2003.

[77] F. Harell and C. Davis, “A new distribution-free quantile estimator”, *Biometrika*, vol. 69, pp. 635–640, Dec. 1982.

[78] ITU-R P.2040-1, “Effects of Building materials and structures on Radiowave Propagation above about 100 MHz”, Tech. Rep. 07/2015, 2015.

[79] S. u. Schollglass Holding GmbH, “Glasscheibe mit Strukturierter leitfaehigher Beschichtung”, 2018.

[80] N. Rousselet, S. Droste, M. Behmke, and B. Stelling, “Panel with High-frequency Transmission”, 2015.

[81] L. Mayer, A. Demmer, A. Hofmann, and M. Schiefer, “Metal-coated Windowpane, particularly for Rail Vehicles”, 2016.

[82] P. Ängskog, M. Bäckström, and B. Vallhagen, “Measurement of Radio Signal Propagation through Window Panes and Energy Saving Windows”, in *2015 IEEE International Symposium on Electromagnetic Compatibility (EMC)*, Aug. 2015, pp. 74–79.

[83] P. Ängskog, M. Bäckström, C. Samuelsson, and B. K. Vallhagen, “Shielding Effectiveness and HPM Vulnerability of Energy-Saving Windows and Window Panes”, *IEEE Transactions on Electromagnetic Compatibility*, pp. 1–8, 2018.

[84] I. Rodriguez, H. C. Nguyen, N. T. K. Jorgensen, T. B. Sorensen, and P. Mogensen, “Radio Propagation into Modern Buildings: Attenuation Measurements in the Range from 800 MHz to 18 GHz”, in *2014 IEEE 80th Vehicular Technology Conference (VTC2014-Fall)*, Sep. 2014, pp. 1–5.

[85] M. W. B. Silva and L. C. Kretly, “An Efficient Method based on Equivalent-circuit Modeling for Analysis of Frequency Selective Surfaces”, in *2013 SBMO/IEEE MTT-S International Microwave Optoelectronics Conference (IMOC)*, Aug. 2013, pp. 1–4.

[86] I. Ullah, D. Habibi, X. Zhao, and G. Kiani, “Design of RF/Microwave Efficient Buildings using Frequency Selective Surface”, in *2013 SBMO/IEEE MTT-S International Microwave Optoelectronics Conference (IMOC)*, 2011, pp. 2070–2074.

[87] B. Brown, “The Social Life of Autonomous Cars”, *Computer*, vol. 50, no. 2, pp. 92–96, Feb. 2017.

[88] F. Montori, M. Gramaglia, L. Bedogni, M. Fiore, F. Sheikh, L. Bononi, and A. Vesco, “Automotive Communications in LTE: A Simulation-based Performance Study”, in *2017 IEEE 86th Vehicular Technology Conference (VTC-Fall)*, Sep. 2017, pp. 1–6.

[89] M. Akselrod, N. Becker, M. Fidler, and R. Luebben, “4G LTE on the Road - What Impacts Download Speeds Most?”, in *2017 IEEE 86th Vehicular Technology Conference (VTC-Fall)*, Sep. 2017, pp. 1–6.

[90] European Commission, *Communication from the commission to the european parliament, the council, the european economic and social committee and the committee of the regions*. 2018, [Online] `https://eur-lex.europa.eu/homepage.html`.

[91] G. Araniti, C. Campolo, M. Condoluci, A. Iera, and A. Molinaro, “LTE for Vehicular Networking: A survey”, *IEEE Communications Magazine*, vol. 51, no. 5, pp. 148–157, May 2013.

[92] (2016). 5G empowering vertical industries. [Online] https://5g-ppp.eu/roadmaps/.

[93] S. Schwarz, I. Safiulin, T. Philosof, and M. Rupp, "Gaussian Modeling of Spatially Correlated LOS/NLOS Maps for Mobile Communications", in *2016 IEEE 84th Vehicular Technology Conference (VTC-Fall)*, Sep. 2016, pp. 1–5.

[94] A. A. Glazunov, "Test Zone Characterization in an Automotive Random-LOS OTA test Setup", in *2017 IEEE-APS Topical Conference on Antennas and Propagation in Wireless Communications (APWC)*, Sep. 2017, pp. 170–173.

[95] F. Ademaj, M. K. Mueller, S. Schwarz, and M. Rupp, "Modeling of Spatially Correlated Geometry-based Stochastic Channels", in *2017 IEEE 86th Vehicular Technology Conference (VTC-Fall)*, Sep. 2017, pp. 1–6.

[96] F. Ademaj, S. Schwarz, K. Guan, and M. Rupp, "Ray-tracing based Validation of Spatial Consistency for Geometry-based Stochastic Channels", in *2018 IEEE 88th Vehicular Technology Conference (VTC-Fall)*, Aug. 2018, pp. 1–6.

[97] (2018), [Online]. Available: https://www.rohde-schwarz.com/us/product/qualipoc_freerider3-productstartpage_63493-68867.html.

[98] C. Beckman, L. Eklund, B. Karlsson, B. Lindmark, D. Ribbenfjard, and P. Wirdemark, "Verifying 3G License Requirements when every dB is worth a billion", in *2006 First European Conference on Antennas and Propagation*, Nov. 2006, pp. 1–4.

[99] Ribbenfjard, Lindmark, Karlsson, and Eklund, "Omnidirectional Vehicle Antenna for Measurement of Radio Coverage at 2 GHz v.2.0", *IEEE Antennas and Wireless Propagation Letters*, vol. 3, pp. 269–272, 2004.

[100] P. H. Lehne, A. A. Glazunov, K. Mahmood, and P. S. Kildal, "Analyzing Smart phones' 3D Accelerometer Measurements to identify Typical Usage Positions in Voice Mode", in *2016 10th European Conference on Antennas and Propagation (EuCAP)*, Apr. 2016, pp. 1–5.

[101] P. H. Lehne, K. Mahmood, A. A. Glazunov, P. Gronsund, and P. S. Kildal, "Measuring User-induced Randomness to evaluate Smart phone Performance in Real Environments", in *2015 9th European Conference on Antennas and Propagation (EuCAP)*, May 2015, pp. 1–5.

[102] P. H. Lehne, A. A. Glazunov, and K. Karlsson, "Finding the Distribution of Users in a Cell from Smart phone based Measurements", in *2016 International Symposium on Wireless Communication Systems (ISWCS)*, Sep. 2016, pp. 538–542.